GEOMICROBIOLOGY OF IRON OXYHYDROXIDE MATS IN ACIDIC GEOTHERMAL SPRINGS OF YELLOWSTONE NATIONAL PARK, WYOMING, UNITED STATES OF AMERICA

by

Mark Andrew Kozubal

A dissertation submitted in partial fulfillment
of the requirements for the degree

of

Doctor of Philosophy

in

Ecology and Environmental Sciences

MONTANA STATE UNIVERSITY
Bozeman, Montana

July 2010

APPROVAL

of a dissertation submitted by

Mark Andrew Kozubal

This dissertation has been read by each member of the dissertation committee and has been found to be satisfactory regarding content, English usage, format, citations, bibliographic style and consistency, and is ready for submission to the Division of Graduate Education.

Dr. William P. Inskeep

Approved for the Department of Land Resources and Environmental Sciences

Dr. Tracy M. Sterling

Approved for the Division of Graduate Education

Dr. Carl A. Fox

STATEMENT OF PERMISSION TO USE

In presenting this dissertation in partial fulfillment of the requirements for a doctoral degree at Montana State University, I agree that the Library shall make it available to borrowers under rules of the Library. I further agree that copying of this dissertation is allowable only for scholarly purposes, consistent with "fair use" as prescribed in the U.S. Copyright Law. Requests for extensive copying or reproduction of this dissertation should be referred to ProQuest Information and Learning, 300 North Zeeb Road, Ann Arbor, Michigan 48106, to whom I have granted "the exclusive right to reproduce and distribute my dissertation in and from microform along with the non-exclusive right to reproduce and distribute my abstract in any format in whole or in part."

Mark Andrew Kozubal

July 2010

ACKNOWLEDGEMENTS

First, I would like to thank Dr. William Inskeep who has been a supported my research, education and personal growth with enthusiasm. Equally, I would like to thank Kaylee who has always had faith and support in my life's direction with much love and sacrifice. I also thank the members of my committee: Dr. Richard Macur for his tireless efforts with guiding research activities and teaching invaluable techniques; Dr. Gill Geesey for reminding me of the importance of applied research; and Dr. Mark Skidmore for teaching geomicrobiology in a fun and inspirational manner. I would also like to thank my family and friends for their encouragement, support and patience through the process of attaining my education. I thank foremost Yellowstone National Park (Center for Resources staff Mr. John Varley, Mr. Tom Oliff and Ms. Christie Hendrix) for allowing this research to take place. I appreciate funding from the NSF Microbial Observatory Program, the Inland Northwest Research Alliance, and the Big Sky Institute NSF GK-12 Program, which provided an exceptional opportunity to disseminate my research to high school students in the Gallatin Valley. I would like to specifically thank the following people for their friendship, advice, and assistance with my research in and out of the lab: Sarah Korf, Deanne Masur, Amanda Nagy, Zack Jay, Jake Beam, Ryan Jennings, Galena Ackerman, Seth D'Imperio, Katie Schultz, Yusuke Odake, Stuart Baker, Mensur Dlakic, Kimberly Popham, Lisa Rew and Erica Miller. Finally, I would like to dedicate this dissertation to my dear friend David Luck, who taught me how to live life to the fullest.

TABLE OF CONTENTS

TABLE OF CONTENTS CONTINUED

TABLE OF CONTENTS CONTINUED

LIST OF TABLES

LIST OF FIGURES

LIST OF FIGURES CONTINUED

LIST OF FIGURES CONTINUED

Figure Page

LIST OF FIGURES CONTINUED

LIST OF FIGURES CONTINUED

Figure Page

ABSTRACT

The microbial community structure and function in acidic, high-temperature iron-oxidizing geothermal springs of Yellowstone National Park was investigated utilizing a variety of complementary approaches including microbial cultivation and characterization, geochemical analysis of aqueous and solid phases, phylogenetic and functional gene analysis, comparative genomics, and protein sequence modeling. Cultivation efforts resulted in the isolation of an Fe(II)-oxidizing chemolithotroph *Metallosphaera yellowstonii* MK1^T. The distribution and relative abundance of MK1-like 16S rRNA gene sequences was evaluated in 14 acidic geothermal springs containing Fe(III)-oxide microbial mats. Highly related MK1-like sequences (>99% sequence similarity) were consistently observed in Fe(III)-oxide mats across a temperature range of 55 to 80 ^oC. Quantitative PCR confirmed that organisms highly similar to strain MK1 comprised up to 40% of the total archaeal community of selected sites. Four additional isolates were obtained from thermophilic Fe(III) microbial mats including *Sulfobacillus* sp. MK2, *Sulfolobus* sp. MK3, *Acidicaldus* sp. MK5 and Crenarchaeota sp. MK4, which represents a new taxonomical lineage at the class level or higher.

A draft genome has been assembled for *M. yellowstonii* strain MK1 and comparative studies indicate significant similarity to *Metallosphaera sedula* in regards to putative genes involved in iron and sulfur oxidation, carbon fixation, oxygen reduction and heavy metal resistance. Analysis of gene sequences reveal 7 heme copper oxidases (subunit I) and a variety of genes with possible importance in Fe(II) oxidation including the *fox*A-J gene cluster, a *cbs*A cytochrome $b_{558/566}$, and a novel sequence coding for a putative blue multi-copper protein (*mco*). Expression screens and reverse transcriptase-qPCR on samples from three ASC environments and in cultures grown autotrophically show that the *fox* gene cluster and *mco* are important when Fe(II) serves as the electron donor. Protein sequence analysis of *fox*C indicates a novel lysine-lysine or lysine-arginine heme *b* binding domain and is likely the cytochrome component of a heterodimer complex with *fox*G as a ferredoxin subunit. Analysis of *mco* indicates a novel multi-copper blue protein with two plastocyanin type I copper domains with only three homologous sequences found in Genbank. Both putative proteins likely play an important role in electron transport from Fe(II) to oxygen through Fox Proteins.

CHAPTER 1

THE SCOPE OF THESIS

The goal of this dissertation was to study microbial community structure and function in acidic, high-temperature iron-oxidizing geothermal springs of Yellowstone National Park (YNP) using multidisciplinary approaches including microbial cultivation and characterization, geochemical analysis of aqueous and solid phases, phylogenetic and functional gene analysis, comparative genomics, and protein sequence modeling. Specifically, this work focuses on ferric iron microbial mats found in numerous acid-sulfate-chloride (ASC) geothermal springs of Norris Geyser Basin, and acid-sulfate (AS) geothermal springs located in the Joseph's Coat and Rainbow Springs regions of YNP. The microbial populations and physiologies present in these high-temperature environments have not been studied, and the role of iron cycling in these communities is not well-understood. The thesis begins (Chapter 2) with a review of iron geochemistry and mechanisms of Fe(II) and sulfide mineral oxidation by mesophilic and thermophilic microorganisms. The chapter also reviews past work on the geomicrobiology of acidic, high-temperature environments.

The next chapter (Chapter 3) describes results on the isolation and characterization of *Metallosphaera* sp. strain MK1, a novel Fe(II)-oxidizing isolate obtained from *Beowulf Spring* in Norris Geyser Basin (also referred to as *Metallosphaera yellowstonii* strain MK1^{T}). This chapter, which has been published in *Applied and Environmental Microbiology* (Kozubal et al., 2008), reports on both growth

characteristics (e.g., pH, temperature, salt tolerance) and habitat distribution of *M. yellowstonii* across 14 different geothermal springs.

After isolating *M. yellowstonii* and obtaining draft genome sequence, a separate study (Chapter 4) was conducted to investigate the differential expression of genes involved in electron transport among cultures grown on Fe(II)-ferrihydrite, elemental S, pyrite and yeast extract (YE). This study evaluated the role of different heme copper terminal oxidases, as well as other functional genes that may be important in coding for proteins important in the oxidation of Fe(II). The expression of the same set of genes was also studied in samples obtained from three different Fe-oxyhydroxide microbial mats in Norris Geyser Basin (NGB), YNP. Detailed structural analysis and protein modeling were performed on two hypothetical proteins with possible roles in iron oxidation.

Chapter 5 is a detailed comparative genetic study of all acidophilic iron oxidizing prokaryotes with genomes available including *M. yellowstonii*, *Sulfolobus tokodaii*, *Acidithiobacillus ferrooxidans*, *Ferroplasma acidarmanus* and *Leptospirillum* group II. The chapter introduces a draft genome of *M. yellowstonii* with emphasis on the diversity of heme copper terminal oxidases and describes possible genes involved in iron and sulfur oxidation. The goal of this chapter was to (i) describe genes found in the draft *M. yellowstonii* genome with putative functions in iron oxidation, dissimilatory sulfur oxidation, CO_2 fixation, oxygen reduction, N_2 fixation and heavy metal resistance; (ii) compare these putative genes to those found in *M. sedula*, *A. ferrooxidans*, *Leptospirillum* group II, *F. acidarmanus* , and *S. tokodaii*; (iii) and compare terminal oxidase genes of the HCO and *bd*-type to sequences found in natural environments: three

hydrous ferric oxide (HFO) mat sampling locations from two acidic geothermal springs in YNP.

Several appendices are included in this thesis to provide supplemental information supporting the primary contributions of this work. Appendix 1reports on (i) detailed aqueous and solid phase geochemistry in acid-sulfate-chloride (ASC) and acid-sulfate (AS) geothermal springs including analysis of ferric iron solid phases collected from *M. yellowstonii* culture-vessels; (ii) results from a survey of microbial populations detected in 10 different geothermal springs using PCR amplification (16S rRNA gene), cloning and subsequent phylogenetic analysis; (iii) a summary of additional isolates cultivated from these environments (both bacteria and archaea) with possible relevance to iron redox cycling, and for which a full-characterization is beyond the scope of the current thesis; and (iv) results of an iron oxidation and reduction rate study of two isolates compared to abiotic controls performed to link specific organisms with observed geochemical processes.

Appendix 2 was submitted to the *International Journal of Systematic and Evolutionary Microbiology* (IJSEM) and is currently awaiting publication. The article introduces the name *Metallosphaera yellowstonii* strain MK1^{T} as the type strain, further characterizes the range in growth substrates, provides brief genome comparisons to other species within the Sulfolobales, which together provide evidence for classification as a new species in the *Metallosphaera* genus. *Metallosphaera yellowstonii* strain MK1^{T} is now available at the American Type Culture Collection (ATCC reference BAA-1887), as well as the RIKEN BioResource Japan Collection of Microorganisms.

In addition to the work presented in this dissertation, contributions were made to the following projects during the course of the PhD program :

Hamamura N., R. E. Macur, S. Korf, G. Ackerman, W. P. Taylor, M. Kozubal, A. L. Reysenbach and W. P. Inskeep. 2008. Linking microbial oxidation of arsenic with detection and phylogenetic analysis of arsenite oxidase genes in diverse geothermal environments. *Environmental Microbiology*. **11**:421-431.

Inskeep W.P., Ackerman G.G., Taylor W.P., Kozubal M., Korf S, and Macur R.E. 2005. On the energetics of chemolithotrophy in nonequilibrium systems: case studies of geothermal springs in Yellowstone National Park. *Geobiology*. **3**: 297-320.

Inskeep, W.P., D. Rusch, Z. Jay, M.J. Herrgard, M.A. Kozubal, T.H. Richardson, R.E. Macur, N. Hamamura, B. Fouke, A-L. Reysenbach, F. Roberto, M. Young, R. Jennings, A. Schwartz, S. Korf, E. Boyd, J. Badger, M. Bateson, G. Geesey, E. Mathur and M. Frazier. 2010. Metagenomes from High-Temperature Chemotrophic Systems Reveal Geochemical Controls on Microbial Community Structure and Function. *PLoS One*. 5: e9773.

Macur, R.E., W.P. Taylor, S. Korf, G. Ackerman, M. Kozubal, B.D. Kocar, T. Borch and W.P. Inskeep. 2010. Microbial Community Structure and Sulfur Biogeochemistry in Sulfidic Hyperthermophilic Geothermal Environments. *Geobiology.* In Review.

CHAPTER 2

ACID-SULFATE CHLORIDE AND ACID-SULFATE GEOTHERMAL SPRINGS IN YELLOWSTONE NATIONAL PARK: CASE STUDIES ON THE GEOMICROBIOLOGY OF IRON AND SULFUR

Introduction

Microorganisms inhabit nearly every niche on Earth including extreme environments such as the dry valleys of Antarctica (Mikucki and Priscu 2007), acid mine drainage (AMD; Baker and Banfield 2003; Johnson and Hallberg, 2003), glacier ice (Skidmore et al., 2005; Lanoil et al., 2009), geothermal springs (Ward et al., 1998; Reysenbach et al., 2003; Johnson et al., 2003; Inskeep et al., 2004; Macur et al., 2004; Donahoe-Christiansen et al., 2004; Boyd et al., 2007; Kozubal et al., 2008), and deep-sea vents (Reysenbach et al., 1994; Stetter et al., 1999; Miroshnichenko et al., 2004). Many of these organisms utilize reduced inorganic compounds, such as H_2, H_2S, S^0, $S_2O_3^{2-}$, CH_4, As(III) or Fe(II) as energy sources for metabolism (Johnson et al., 2003; Inskeep et al., 2004; Macur et al., 2004; Kozubal et al., 2008). Additionally, many YNP environments contain high concentrations of toxic trace elements including arsenic and mercury. Two major types of geothermal environments were involved in the current study: acid-sulfate-chloride (ASC) and acid-sulfate (AS) springs. A general review of the geomicrobiology of iron and sulfur and an introduction to AS and ASC geothermal systems is necessary prior to presenting results focused on microbial mechanisms of ferrous iron oxidation in high-temperature geothermal systems.

Iron and Sulfur Chemistry

Iron comprises 7.5% of the earth's lithosphere and is a required element for growth in all domains of life (Kappler and Straub, 2005; Essington 2004). Under current earth-surface conditions (T=25 ^{o}C, 1 atm), iron cycles between two oxidation states (+2, +3) and can be present in a variety of aqueous species or complexes, reduced (e.g., $FeCO_3$ (siderite) and FeS_2 (pyrite)) or oxidized minerals (e.g., Fe_2O_3(hematite)) , and adsorbed to solid surfaces such as other oxide minerals, layer silicates and natural organic matter (NOM).

Iron oxidizing microorganisms are found in numerous natural environments, but are often prominent in geothermal or hydrothermal springs, AMD, or sediment-water interfaces where high levels of aqueous Fe(II) and reduced iron minerals (often various sulfides of iron) provide a source of electrons for microbial metabolism (Inskeep et al. 2004; Konhauser 1998; Miroshnichenko 2004; Prieur et al. 2004). At pH values less than 4.5, the chemical (abiotic) rate of Fe(II) oxidation is very slow (Kappler and Straub 2005; Singer and Stumm 1970) and at pH < 4.5 has been found to follow the rate expression:

$$-d[\mathrm{Fe(II)}]/dt = k[\mathrm{Fe(II)}][O_2] \qquad k = 1 \times 10^{-7}\ \mathrm{min^{-1}\ atm^{-1}\ mol^{-2}\ L^{-2}}$$

Consequently, under acidic conditions, the oxidation of Fe(II) is performed primarily by a few genera of acidophilic chemolithotrophic microorganisms that thrive at pH levels as low as 0.5 (Blake and Johnson 2000;Hallberg and Johnson 2001). In contrast, the

chemical rates of Fe(II) oxidation above pH 4.5 are 20 orders of magnitude faster and follow the rate expression:(Konhauser, 2007):

$$-d[Fe(II)]/dt = k[Fe(II)][OH^-]^2[O_2] \quad k = 8(\pm 2.5) \times 10^{13}\ min^{-1}\ atm^{-1}\ mol^{-2}\ L^{-2}$$

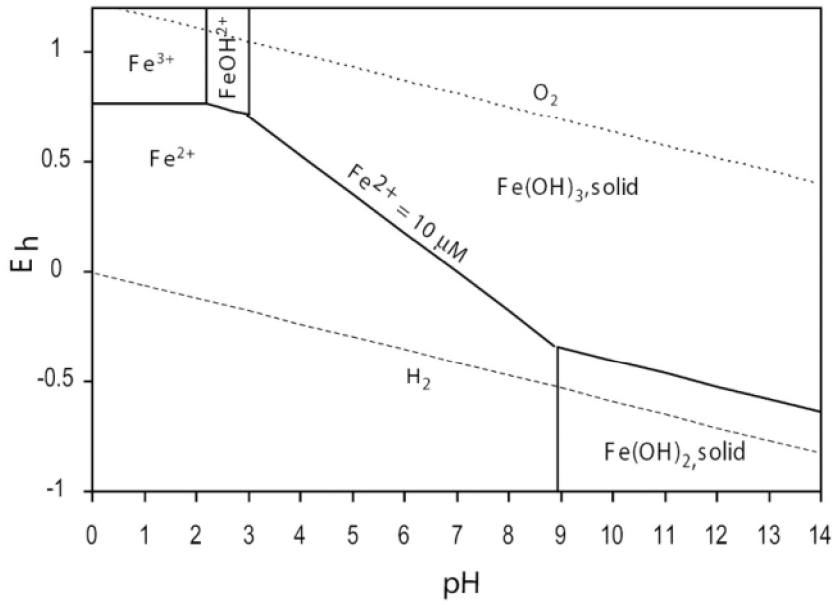

Figure 2.1. Eh-pH diagram for Fe(II), Fe(III), O_2 and H_2 calculated with a Fe^{2+} concentration of 10^{-3}M. For simplicity $Fe(OH)_3$ is used as approximation for the Fe(III) precipitates that are formed. (Reproduced from Kappler and Straub 2005)

The Fe^{2+}/Fe^{3+} redox potential is 0.77 Volts(V) at pH 2 (Figure 2.1), which is close to the O_2/H_2O potential of 0.85 V at pH 6.5 (oxygen reduction takes place in the near neutral cytoplasm of the cell; Konhauser 2007). Approximately 120 moles of Fe^{2+} must be oxidized for the formation of 1 mole of glucose, consequently, low cell numbers are associated with the oxidation of significant amounts of iron. Due in large part to the insolubility of ferric iron minerals, the biological oxidization of iron in AS and ASC

springs of YNP often results in the deposition of ferric oxyhydroxides and or jarosite ($KFe_3(SO_4)_2(OH)_6$). In geothermal systems of YNP, iron oxide microbial mats and or sediments may range in thickness and hardness depending on the geochemistry, flow rate and microbial populations present (Inskeep et al. 2004; Inskeep et al., 2005; Ackermann, 2006). For example, ferric iron mats in acidic geothermal springs of YNP range in thickness from 0.1 to 4 cm and can contain different solid phases such as amorphous Fe(III)-hydroxides, hematite, or jarosite, depending on spring conditions (Macur et al., 2004; Inskeep et al. 2004; Inskeep et al. 2005; Ackermann, 2006). At circumneutral pH, the abiotic oxidation of Fe(II) can occur on seconds time-scale, however, some neutrophilic Fe(II)-oxidizing microorganisms are able to compete with this rapid abiotic rate including species from the *Gallionella* and *Lepthothrix* genera (Blake and Johnson 2000). Under aerobic conditions, the potential energy yield from Fe(II)-oxidation is much greater at pH 7 than at pH 2. Using the redox couples involving $Fe(OH)_3/Fe^{2+}$ (-0.23 V) and O_2/H_20 (0.81 V), the oxidation of Fe(II) yields 1.04 V at pH 7 versus only 0.08 V at pH 2.0 (Konhauser 2007). Ironically, despite the favorable thermodynamics and higher energy yields of Fe(II)-oxidation at higher pH, slower rates of Fe(II)-oxidation at low pH provide opportunities for microbial utilization of Fe(II) as a primary energy source.

Sulfur has five common oxidation states (-2, -1, 0, 4 and 6) and can be found in natural systems in a wide variety of minerals or aqueous species (Stumm and Morgan 1996). Sulfide minerals (e.g., FeS_2 – pyrite; CuS – covellite; ZnS – sphalerite; HgS – cinnabar; PbS – galena; CuFeS - chalcopyrite) are common in reduced systems, whereas

oxidized forms of sulfur (sulfites and sulfates) are considerably more soluble and accumulate primarily in evaporate basins or under extremely acidic conditions (Essington 2004). Thiosulfate, tetrathionate and polysulfides are aqueous sulfur species of intermediate oxidation state and important in the biogeochemical cycling of sulfur. Organic sulfur compounds found in natural environments include thiols, thioesters, sulfoxides and sulfones (Schippers et al. 2003; Stumm and Morgan 1996), as well as the essential amino acids, cysteine and methionine. Iron and other metal sulfides are commonly associated with precious metal deposits, and hard-rock mining results in the potential for environmental impact associated with acid mine drainage (AMD) originating from exposed sulfidic ores during mining operations (Johnson and Hallberg 2003). Inorganic sulfur species serve as important electron donors for microorganisms in a variety of environments, and the reaction of reduced sulfur with oxygen yields considerably more energy than the oxidation of Fe(II) (Kletzin et al. 2004; Stumm and Morgan 1996). Species of sulfur known to be utilized by chemolithotrophic microorganisms for a primary energy source include H_2S, polysulfides, elemental S, tetrathionate, and thiosulfate.

Mechanisms of Sulfide Mineral Oxidation

Sulfide minerals serve as an energy source for a variety of chemolithotrophic microorganisms that utilize free energy available from mineral dissolution and oxidation to yield oxidized sulfur (usually sulfate) and metal cations. The two accepted models for oxidation of sulfide minerals (Rohwerder et al. 2003) include the *acid independent*

thiosulfate mechanism and the *acid dependent polysulfide mechanism* (Figure 2.2). Sulfur bonding in the mineral determines the mechanism of dissolution. Both models show the importance of the oxidation of aqueous Fe^{2+} by microorganisms and the subsequent abiotic attack of the sulfide-metal bond by Fe^{3+}, which is then recycled for microbial oxidation. The direct oxidation of sulfide minerals is a proton generating reaction only in the thiosulfate mechanism, but both mechanisms create acidity if the products are fully oxidized. Acidic aqueous aerated conditions and a continuous supply of Fe^{3+} are optimum for the rapid dissolution of pyrite, thus iron-oxidizing organisms play an important role in accelerating this process through the recycling of Fe(II).

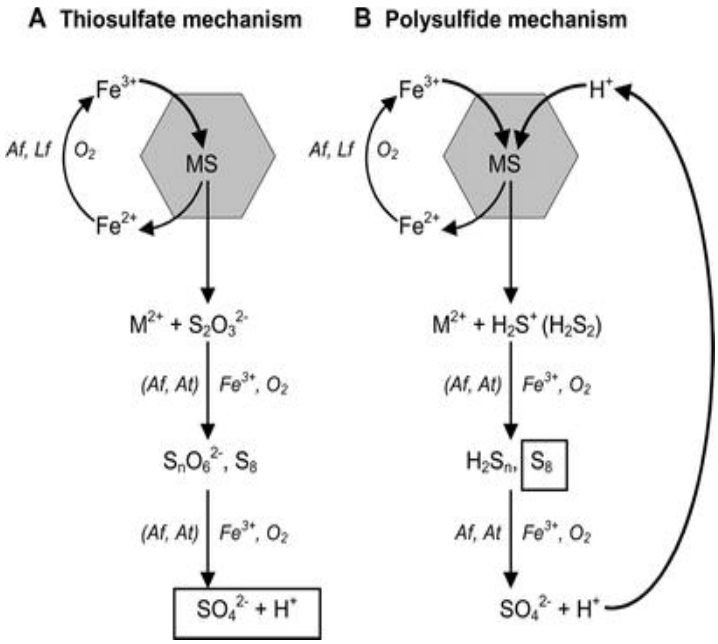

Figure 2.2. Mechanisms of sulfide mineral dissolution. **(A)** Fe^{3+} ions attack metal sulfides (MS) by electron extraction and are subsequently reduced. Metal cations (M^{2+}) and water-soluble intermediary sulfur compounds are released. Fe^{2+} oxidizing bacteria such as *A. ferrooxidans* (Af) and *L. ferrooxidans* (Lf) recycle Fe^{3+}. In the polysulfide mechanism **(B)**, an additional attack is performed by protons. Sulfur species are oxidized abiotically (bracketed reactions) and by sulfur-compound oxidizing bacteria such as *At. ferrooxidans* and *At. thiooxidans* (At). (Reproduced from Rohwerder et al., 2003)

$FeS_2 + 6Fe^{3+} + 3H_2O \rightarrow S_2O_3^{2-} + 7Fe^{2+} + 6H^+$

$S_2O_3^{2-} + 8Fe^{3+} + 5H_2O \rightarrow 2SO_4^{2-} + 8\ Fe^{2+} + 10\ H^+$

Thiosulfate mechanism (FeS_2, MoS_2 and WS_2)

$MS + Fe^{3+} + H^+ \rightarrow M^{2+} + 0.5H_2S_n + Fe^{2+}$ $(n \geq 2)$

$0.5H_2S_n + Fe^{3+} \rightarrow 0.125S_8 + Fe^{2+} + H^+$

$0.125S_8 + 1.5O_2 + H_20 \rightarrow SO_4^{2-} + 2H^+$

Polysulfide mechanism (e.g., ZnS, $CuFeS_2$, or PbS)

The rate-limiting step in sulfide mineral dissolution is thought to be cleavage of the sulfur-metal bond by Fe^{3+} and studies indicate that attachment to the mineral surface by some iron oxidizing microorganisms may increase the kinetics of dissolution by favorably altering local redox conditions and Fe^{3+} solubility by organic ligands (Kozubal et al. 2008; Rohwerder et al. 2003). Thus, proteins involved in attachment likely play an important role in enhancing the oxidation of sulfide minerals. In addition, temperatures above 60 °C greatly increase reaction kinetics if thermophilic iron-oxidizing microorganisms are present (Olson et al. 2003; Rohwerder et al. 2003), and if iron concentrations are high (i.e. during heap leaching), these temperatures may be maintained directly by microbial metabolism (Olson et al. 2003). In fact, there is similarity in environmental conditions between high-temperature heap-leach piles and acidic geothermal systems of YNP, and in some cases, similar iron and or sulfur-oxidizing thermophiles are found in both environments.

Iron Oxidation by Mesophilic Microorganisms

The oxidation of Fe(II) and/or reduced sulfur by mesophilic microorganisms is an important process in mining environments (Rawlings 2002) creating acidic conditions

necessary for acid rock drainage (ARD) and or acid mine drainage (AMD). The mechanism of Fe(II)-oxidation has been studied extensively in a number of mesophilic and moderately thermophilic bacteria including *Acidithiobacillus ferrooxidans, Leptospirillum ferrooxidans, Leptospirillum ferriphilum* and *Sulfobacillus spp.* (Yarzábal et al., 2002a and 2002b; Dopson et al. 2005; Rawlings 2005; Rohwerder and Sand 2003; Singer et al. 2008). The Fe(II) oxidation pathway in *Acidithiobacillus ferrooxidans* is believed to involve three cytochromes c (Cyc2, Cyc1 and CycA1) and a blue-copper protein (rusticyanin), which may act as an electron buffer after direct oxidation of Fe^{2+} by Cyc2 (Rawlings 2005).

L. ferrooxidans can oxidize Fe(II) at concentrations up to 42.8 mM, and thus has a niche in iron-rich environments such as the Richmond mine at Iron Mountain, CA. A novel Cyt_{572} is believed to oxidize Fe(II) directly, and then transfer electrons to a cytochrome Cyt_{579} in the periplasm (Jeans et al., 2008; Singer et al. 2008). The redox potential of Cyt_{572} is closer to the O_2/H_2O couple than Cyc2 and, therefore, *L. ferrooxidans* does not grow as robustly as *A. ferrooxidans* in environments where both species are present (Rohwerder et al. 2003). The mechanism of Fe(II)-oxidation in the Euryarchaeota *Ferroplasma acidarmanus* has also been studied and a complete pathway has been proposed (Dopson et al., 2005). A blue copper protein is believed to be linked directly to Fe^{2+} oxidation and may interact with the subunit I oxygen reductase of a aa_3 type heme copper terminal oxidase complex.

Iron and Sulfur Oxidation by Thermophilic Microorganisms

The Sulfolobales contain the highest temperature iron oxidizing microorganisms known (Konhauser 2007), but little is understood about the pathways involved. There is a great deal of interest in deciphering Fe^{2+} chemolithotrophic respiratory chain pathways in these unique microorganisms because of their extreme thermo-tolerance and their suitability for biomining applications (Olson et al. 2003; Rawlings 2002; Rohwerder et al. 2003). Of the described Sulfolobales, only *Metallosphaera* spp., *Acidianus brierleyi, Sulfolobus metallicus* and *Sulfolobus tokodaii* are capable of chemolithoautotrophic growth on Fe^{2+} with limited growth reported for *S. tokodaii* (Bathe and Norris 2007). However, all known *Sulfolobus* and *Metallosphaera* spp. are capable of oxidizing S^0 and other reduced forms of sulfur (Fuchs et al. 1995; Huber et al. 1989; Huber and Stetter 1991; Kozubal et al. 2008; Kurosawa et al. 2003; Suzuki et al. 2002; Takayanagi 1996).

Pathways involved in the oxidation of sulfur in the Sulfolobales have been reviewed (Kletzin et al., 2004) and are confined to only one organism: *Acidianus ambivalens*. The putative pathway in *A. ambivalens* involves a number of proteins with activities for specific sulfur species including a sulfide oxido-reductase (SQR), a sulfur oxygenase reductase (SOR), a thiosulfate oxidase (TQO) and two mechanisms for sulfite oxidation (adenylsulfate (APS)-reductase and a sulfite oxidase molybdopterin (SOM). In addition, expression and protein activity studies (Purschke et al. 1997) ultimately link the *A. ambivalens* model of sulfur oxidation to oxygen reduction by the DoxBCEF terminal oxidase complex. The sulfur oxidation pathways in *Sulfolobus* and *Metallosphaera* spp. contain similar deduced proteins of Tqo, Som, and APS reductase found in *A.*

ambivalens, but genes similar to the SOR are only found in *S. tokodaii* and *S. metallicus* (Bathe and Norris 2007; Kozubal et al. 2008). The comparative genome chapter of this dissertation describes a novel *hdr* gene cluster which may be involved in sulfur oxidation in a variety of acidophilic microorganisms.

The Sulfolobales can utilize additional electron donors besides Fe(II) and reduced sulfur substrates including H_2 and organic compounds. The electron transport mechanism varies, depending on the electron donor, especially between two substrates with vastly different redox potentials such as Fe(II) and elemental sulfur. The complete electron transport chain in these thermophilic microorganisms is complex (Gomes et al., 2001; Lemos et al., 2001; Iwasaki et al., 2002; Bandeiras et al., 2003; Pereira 2004) and key enzymes in the well-described complex I, II, III and IV of the aerobic respiratory chain are undoubtedly involved.

AS and ASC Springs of YNP

Yellowstone National Park has greater than 10,000 geothermal features which are located along the margins of a 0.6 million year old caldera. Magma (or partially molten rock) is located approximately 3 km beneath the caldera (Fournier, 2005). The myriad of geochemical conditions found in YNP originate from complex subsurface interactions of meteoric water (from precipitation and recharge) mixing with hydrothermal fluids, magmatic gases, and superheated subsurface rocks. Sub-surface geothermal waters may then acquire ions from the dissolution and or ion exchange with mineral phases (Fournier, 2005). Three classes of geothermal springs are observed in YNP: (i) *Acid-Sulfate-*

Chloride (ASC) springs that are characterized by low pH (< 4) and high concentrations of dissolved SO_4^{2-} (~ 1 mM), and Cl^- (~ 13 mM), (ii) *Acid-Sulfate* (AS) springs that have low pH (< 4) and high dissolved concentrations of SO_4^{2-} (~ 6 mM), and (iii) *Alkaline-Chloride-Carbonate* (ACC) springs that exhibit higher pH (> 6), and mM concentrations of Cl^- (~ 10 - 20 mM) and dissolved inorganic carbon (DIC; ~ 0.5 mM) (Ball et al., 2002; Inskeep et al., 2005; McCleskey et al., 2005; Inskeep and McDermott, 2005; Nordstrom et al., 2005). The aqueous geochemical signature of geothermal springs discussed in the current study can be summarized using a piper plot (Figure 2.3), showing the major separation that occurs between AS springs (such as those found at Rainbow Springs or Joseph's Coat Hot Springs) and ASC springs (such as those found in Norris Geyser Basin (Figure 2.4)).

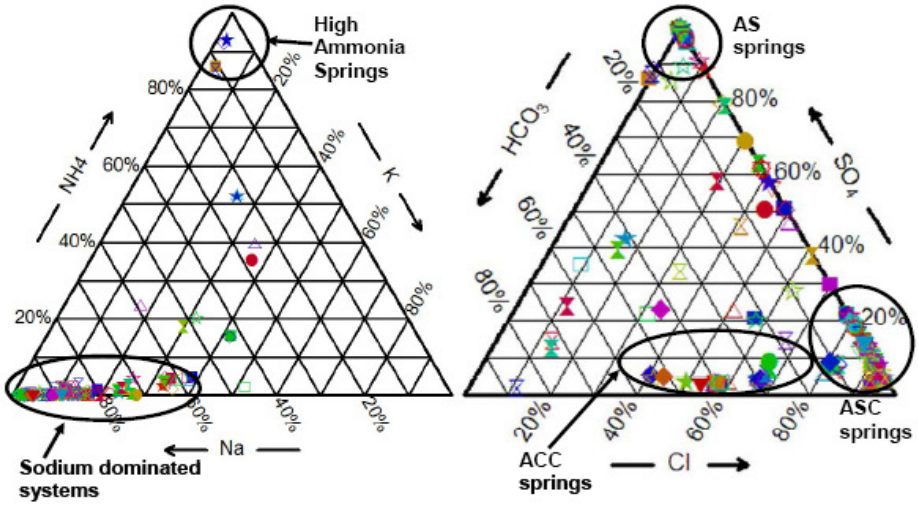

Figure 2.3. Piper plots of major dissolved cations (left) and anions (right) in geothermal source waters of YNP. Triangular graph displays the importance of a particular ion as a percent compared to other ions on opposing axis. Symbols represent sampling points from 166 locations within YNP showing the broad diversity in chemical makeup of geothermal fluids.

The low pH of AS and ASC springs originates from sulfuric acid likely generated as a result of the oxidation of reduced sulfur compounds (i.e. H_2S and S^0) and/or from hydrolysis of dissolved SO_2 from magma gasses (Nordstrom and McClesky 2005; Xu et al., 1998). The high chloride in ASC springs is likely due to chloride-rich subsurface waters mixing with the acidic waters from thermal regions (Nordstrom and McClesky 2005). Source water temperatures from both ASC and AS springs are often greater than 75 °C, contain reduced chemical species such as H_2, CH_4, H_2S, NH_4, Fe(II), and As(III), are typically supersaturated with respect to atmospheric CO_2, and contain little dissolved O_2 (Jackson et al., 2001; Langner et al., 2001; Inskeep et al., 2004; Macur et al., 2004). Previous energetic calculations indicate that all these reduced compounds are favorable for chemolithotrophic growth (Inskeep et al., 2005).

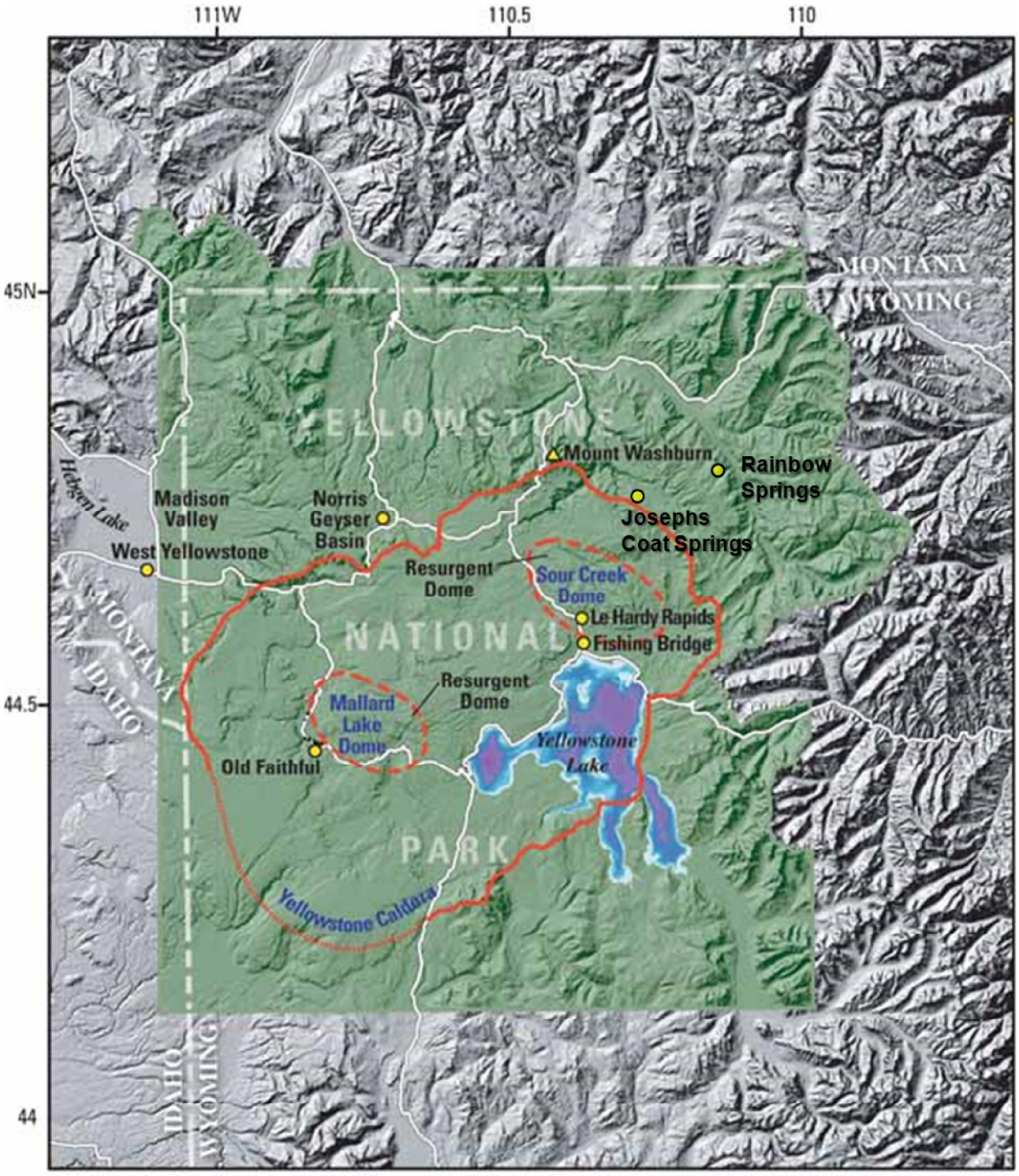

Figure 2.4. Map of Yellowstone National Park showing locations of Norris Geyser Basin, Rainbow Springs and Joseph's Coat Springs. Orange lines represent the caldera margin. (Source: USGS website)

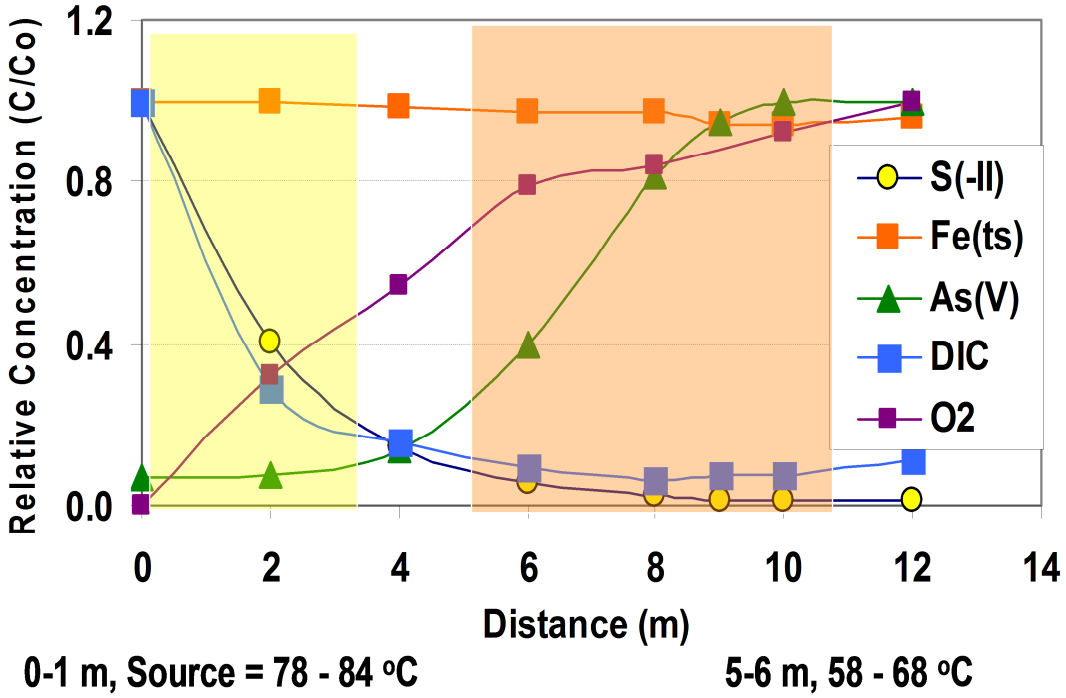

Figure 2.5. Geochemistry profile for an ASC spring (*Beowulf*) of dissolved chemical species as a function of distance from the spring source for sulfide (S^{2-}), total Fe, As(V), dissolved inorganic carbon (DIC) and O_2. Dissolved O_2 increases downstream, DIC decreases, and total Fe is constant. As(III) oxidation to As(V) is too fast to be abiotic (Langner et. al., 2001). Yellow represents the S^0 deposition zone followed by an AsV-rich HFO zone (Inskeep et. al., 2004).

Acid-sulfate-chloride and acid-sulfate geothermal springs exhibit changes in gas composition, aqueous chemical species and temperature as discharge water flows downstream from the source (Figure 2.5). Concentrations of CO_2, H_2 and H_2S are highest at the spring source and decrease as a function of both mass transfer across the air-water interface and via microbial transformations (e.g., H_2S to solid S^0). Conversely, the concentration of dissolved O_2 increases gradually with increasing distance from spring discharge, eventually reaching equilibrium with atmospheric O_2. Typically, elemental S is deposited immediately downstream from the source and is likely a result of microbial

H_2S oxidation (D'Imperio et al., 2007). A zone of ferric iron biomineralization is found downstream of the deposition of elemental S in regions where H_2S levels have dropped significantly and O_2 levels are beginning to increase. Ferric iron is usually biomineralized as an amorphous hydrous ferric oxyhydroxide (HFO) in ASC springs, and contains arsenate (As:Fe mole ratio =0.6-0.7) adsorbed to small octahedral Fe(III)-oxide clusters (Inskeep et al., 2004). to 0.62 mol percent (Inskeep et al., 2004). In AS springs, potassium jarosite ($KFe_3(SO_4)_2(OH)_6$), and/or a variety of ferric oxides including hematite, goethite or amorphous Fe-oxyhydroxides (Inskeep et al., 2005). At temperatures below 50 ºC, a "green zone" appears with *Cyanidia* algae as the primary biomass (Jackson et al., 2001; Lehr et al., 2007).

A variety of electron donors are available to thermoacidophilic microorganisms for chemolithotrophic growth, as indicated by free energy ($\Delta G°_{rxn}$) calculations for different redox pairs, including H_2, CH_4, H_2S, S^0, NH_4 (mainly in AS springs), Fe(II), and As(III) (Inskeep et al., 2005). These electron donors are exergonic with a variety of electron acceptors including O_2, Fe^{3+}, SO_4^{2-}, As^{5+}, NO_3^{2-}, and S^0. However, Fe^{2+} is only exergonic with NO_3^{2-} and O_2. Electron flux calculations are more informative than $\Delta G°_{rxn}$ in regards to total energy available for microorganisms. For instance, the theoretical energetic flux was calculated in *Beowulf* Spring and ranged from 0.007 to 0.02 KJ m^{-2} min^{-1} for all reactions with H_2 as the donor; 30–500 KJ m^{-2} min^{-1} for H_2S reactions; 5–15 KJ m^{-2} min^{-1} for reactions with As(III); 0.4–7 KJ m^{-2} min^{-1} for reactions with Fe(II); and 0.7–3 KJ m^{-2} min^{-1} for reactions with CH_4. Microbial community structure is defined, in part, by available energy flux but pH, temperature, O_2 concentration, flow rate and other

ecological factors (i.e. mutualism, predation, and competition) are also important parameters.

References

1. Ackerman, G.G. 2006. Biogeochemical Gradients and Energetics in Geothermal Systems of Yellowstone National Park. Masters Thesis. Montana State University. Bozeman, MT.

2. Baker, B.J. and J. F. Banfield. 2003. Microbial communities in acid mine drainage. FEMS Microbiology Ecology. 44: 139-152.

3. Ball, J. W., R. B. McCleskey, D.K. Nordstrom, J.M. Holloway, P.L. Verplanck. 2002. Water-chemistry data for selected springs, geysers, and streams in Yellowstone National Park, Wyoming 1999-2000. Boulder, CO, USGS.

4. Bandeiras, T. M., C. A. Salgueiro, H. Huber, C. M. Gomes, and M. Teixeira. 2003. The respiratory chain of the thermophilic archaeon *Sulfolobus metallicus*: studies on the type-II NADH dehydrogenase. Biochim. Biophys. Acta. 1557:13-19.

5. Bathe, S. and P. R. Norris. 2007. Ferrous Iron- and Sulfur-Induced Genes in *Sulfolobus metallicus.* Appl. Environ. Microbiol. 73: 2491-2497

6. Boyd E. S., R. A. Jackson, G. Encarnacion, J. A. Zahn, T. Beard, W. D. Leavitt, Y. Pi, C. L. Zhang, A. Pearson, and G. G. Geesey. 2007. Isolation, Characterization, and Ecology of Sulfur-Respiring Crenarchaea Inhabiting Acid-Sulfate-Chloride-Containing Geothermal Springs in Yellowstone National Park. Appl. Envir. Microbiol. 73: 6669-6677

7. Dahl, C., S. Engels, A. S. Pott-Sperling, A. Schulte, J. Sander, Y. Lübbe, O. Deuster, and D. C. Brune. 2005. Novel genes of the dsr gene cluster and evidence for close interaction of Dsr proteins during sulfur oxidation in the phototrophic sulfur bacterium *Allochromatium vinosum*. J Bacteriol.187: 1392-404

8. D'Imperio, S., C. R. Lehr, H. Oduro, G. Druschel, M. Kühl, and T.R. McDermott. 2007. The Relative Importance of H_2 and H_2S as Energy Sources for Primary Production in Geothermal Springs. Appl. Environ. Microbiol. AEM.00852-08v1

9. Donahoe-Christiansen, J., S. D'Imperio, C.R. Jackson, W.P Inskeep and T.R. McDermott. 2004. Arsenite-oxidizing *Hydrogenobaculum* strain isolated from and acid-sulfate-chloride spring in Yellowstone National Park. Appl. Environ. Microbiol. 70: 1865-1868

10. Dopson, M., C. Baker-Austin and P. L. Bond. 2005. Analysis of differential protein expression during growth states of *Ferroplasma* strains and insights into electron transport for iron oxidation. Microbiology 151: 4127–4137

11. Essington, M. E. 2004. Soil and Water Chemistry: An Integrative Approach. CRC Press. 552 pp. ISBN 978-0849312588

12. Friedrich C. G., F. Bardischewsky, D. Rother, A. Quentmeier, and J. Fischer. 2005. Prokaryotic Sulfur Oxidation. Curr Opin Microbiol. 8: 253-9

13. Fournier, R.O. 2005. Geochemistry and Dynamics of the Yellowstone National Park Hydrothermal System. *in* Geothermal Biology and Geochemistry in Yellowstone. National Park. *eds* W.P Inskeep and T.R. McDermott.

14. Fuchs T., H. Huber, K. Teiner, S. Burggraf, and K.O Stetter. 1995. *Metallosphaera prunae*, sp. nov., a novel metal-mobilizing, thermoacidophilic Archaeum, isolated from a uranium mine in Germany. Syst. Appl. Microbiol. 18: 560-566.

15. Gomes, C. M., T. M. Bandeiras, and M. Teixeira. 2001. A new type-II NADH dehydrogenase from the archaeon *Acidianus ambivalens*: characterization and in vitro reconstitution of the respiratory chain. J. Bioenerg. Biomembr. 33:1-8.

16. Huber, G., C. Spinnler, A. Gambacorta, and K. O. Stetter. 1989. *Metallosphaera sedula* gen. nov. and sp. nov. represents a new genus of aerobic, metal-mobilizing, thermoacidophilic archaebacteria. Syst. Appl. Microbiol. 12: 38-47

17. Huber G. and K.O. Stetter. 1991. *Sulfolobus metallicus*, sp. nov., a novel strictly chemolithoautotrophic thermophilic archaeal species of metal-mobilizers. Syst. Appl. Microbiol. 14: 372-378.

18. Inskeep W.P., R.E. Macur, G. Harrison, B.C. Bostick, S. Fendorf. 2004. Biomineralization of As(V)-hydrous ferric oxyhydroxide in microbial mats of an acid-sulfate-chloride geothermal spring, Yellowstone National Park. Geochimica et Cosmochimica Acta. 68: 3141–3155.

19. Inskeep W.P., G.G. Ackerman, W.P. Taylor, M. Kozubal, S. Korf, and R.E. Macur. 2005. On the energetics of chemolithotrophy in nonequilibrium systems: case studies of geothermal springs in Yellowstone National Park. Geobiology. 3: 297-320.

20. Inskeep, W. P., and T. R. McDermott. 2005. Geothermal biology and geochemistryin Yellowstone Montana State University Publication, Bozeman, MT.

21. Inskeep, W.P., D. Rusch, Z. Jay, M.J. Herrgard, M.A. Kozubal, T.H. Richardson, R.E. Macur, N. Hamamura, B. Fouke, A-L. Reysenbach, F. Roberto, M. Young, R. Jennings, A. Schwartz, S. Korf, E. Boyd, J. Badger, M. Bateson, G. Geesey, E. Mathur and M. Frazier. 2009. Geochemistry underpins metagenome composition (phylogeny and function) in high temperature geothermal springs in Yellowstone National Park. *PLoS One*. 5: e9773.

22. Iwasaki, T., A. Kounosu, M. Aoshima, D. Ohmori, T. Imai, A. Urushiyama, N. J. Cosper, and R. A. Scott. 2002. Novel [2Fe-2S]-type redox center C in SdhC of archaeal respiratory complex II from *Sulfolobus tokodaii* strain 7. J. Biol. Chem. 277:39642-39648.

23. Jackson, C.R., H.W. Langner, J. Donahoe-Christiansen, W. P. Inskeep and T. R. McDermott. 2001. Molecular analysis of microbial community structure in an arsenite-oxidizing acidic thermal spring. Environ. Microbiol. 3: 532-542

24. Johnson, D.B., and K.B. Hallberg. 2003. The microbiology of acidic mine waters. Research in Microbiology .154: 466-73.

25. Johnson D.B., Okibe N., and Roberto F.F. 2003. Novel thermo-acidophilic bacteria isolated from geothermal sites in Yellowstone National Park: physiological and phylogenetic characteristics. Arch Microbiol. 180: 60-8.

26. Kappler A., and K. L. Straub. 2005. Geomicrobiological Cycling of Iron. Reviews in Mineralogy and Geochemistry. 59: 85-108

27. Kappler, U., L.I. Sly, and A.G. McEwan. 2005. Respiratory gene clusters of *Metallosphaera sedula* – differential expression and transcriptional organization. Microbiology. 151: 35-43

28. Kletzin A., Urich T., Müller F., Bandeiras T.M., and C.M. Gomes. 2004. Dissimilatory Oxidation and Reduction of Elemental sulfur in thermophilic archaea. Journal of bioenergetics and biomembranes. 36: 77-91.

29. Konhauser, K. O. 2007. Introduction to Geomicrobiology. Blackwell Science. 425 pp. ISBN 978-0-632-05454-1

30. Kozubal M., Macur R.E., Korf S., Taylor W.P., Ackerman G.G., Nagy A., and W.P. Inskeep. 2008. Isolation and Distribution of a Novel Iron-Oxidizing Crenarchaeon from Acidic Geothermal Springs in Yellowstone National Park. Appl. Environ. Microbiol. 74: 942-949.

31. Kurosawa, N., Y.H. Itoh, and T. Itoh. 2003. Reclassification of *Sulfolobus hakonensis* Takayanagi et al. 1996 as *Metallosphaera hakonensis* comb. Nov.

based on phylogenetic evidence and DNA G+C content. Int. J. Syst. Evol. Microbiol. 53: 1607–1608

32. Langner, H.W., C.R. Jackson, T.R. McDermott and W.P. Inskeep. 2001. Rapid Oxidation of arsenite in a hot spring ecosystem, Yellowstone National Park. Environ. Sci. Tech. 35: 3302-3309

33. Lanoil B., Skidmore M, Priscu JC, Han S, Foo W, Vogel SW, Tulaczyk S, Engelhardt H. 2009. Bacteria beneath the West Antarctic ice sheet. Environ Microbiol. Mar;11(3):609-15

34. Lehr, C. R., S. D. Frank, T. B. Norris, S. D'Imperio, A. V. Kalinin, J. A. Toplin, R. W. Castenholz, and T. R. McDermott. 2007. *Cyanidia*(*Cyanidiales*) population diversity and dynamics in an acid-sulfate-chloride spring in Yellowstone National Park. J. Phycol. 43:3-14.

35. Lemos, R. S., C. M. Gomes, and M. Teixeira. 2001. *Acidianus ambivalens* complex II typifies a novel family of succinate dehydrogenases. Biochem. Biophys. Res. Commun. 281:141-150.

36. Macur, R.E., H.W. Langner, B.D. Kocar, and W.P. Inskeep. 2004. Linking geochemical processes with microbial community analysis: successional dynamics in an arsenic-rich, acid-sulfate-chloride geothermal spring. Geobiology. 2: 163-177

37. McCleskey, R.B., J.W. Ball, D.K. Nordstrom, J.M. Holloway, and H.E. Taylor. 2005. Water-Chemistry Data for Selected Hot Springs, Geysers, and Streams in Yellowstone National Park, Wyoming, 2001-2001. Boulder, CO, USGS

38. Mikucki JA, Priscu JC. 2007. Appl Environ Microbiol. Bacterial diversity associated with Blood Falls, a subglacial outflow from the Taylor Glacier, Antarctica. Jun;73(12):4029-39. Epub 2007 Apr 27.

39. Miroshnichenko, M.L. 2004 Thermophilic microbial communities of deep-sea hydrothermal vents. Microbiology. 73: 1–13.

40. Nordstrom, D.K. and G. Southam. 1997. Geomicrobiology of sulfide mineral oxidation. Reviews in Mineralogy. 35: 361-390

41. Nordstrom, D.K., J.W. Ball, R. B. McClesky. 2005. Ground water to surface water: chemistry of thermal outflows in Yellowstone National Park. *in* Geothermal Biology and Geochemistry in Yellowstone National Park. *Eds* W.P Inskeep and T.R. McDermott

42. Olson, G.J., J.A. Brierley, C.L. Brierley. 2003. Bioleaching review part B: Applied Microbiology and Biotechnology. 63: 249 – 257

43. Pereira, M. M.,T. M. Bandeiras, A. S. Fernandes, R. S. Lemos, M. P. Melo, and M. Teixeira. 2004. Respiratory Chains From Aerobic Thermophilic Prokaryotes. Journal of Bioenergetics and Biomembranes. 36: 93-105

44. Prieur, D., M.A Voytek, C. Jeanthon and A.L. Reysenbach. 2001. Deep-Sea Thermophilic Prokaryotes. "Thermophiles: Biodiversity, Ecology and Evolution" pp 11-22. A-L. Reysenbach, M.A. Voytek and R. Mancinelli (eds.). Kluwer Academic/ Plenum Publishers. New York, NY.

45. Purschke, W.G., Schmidt, C.L., Petersen, A., and G Schäfer. 1997. The terminal quinol oxidase of the hyperthermophilic archaeon Acidianus ambivalens exhibits a novel subunit structure and gene organization. J Bacteriol. 179: 1344-53.

46. Rawlings, D.E. 2002. Heavy metal mining using microbes. Annual Review of Microbiology. 56: 65-91

47. Rawlings, D. E. 2005. Characteristics and adaptability of iron- and sulfur-oxidizing microorganisms used for the recovery of metals from minerals and their concentrates. Microbial Cell Factories. 4:13.

48. Reysenbach, A.L., G.S. Wickham, and N.R. Pace. 1994. Phylogenetic analysis of the hyperthermophilic pink filament community in Octopus Spring, Yellowstone National Park. Appl. Environ. Microbiol. 60: 2113–2119.

49. Reysenbach AL, Ehringer M, Hershberger K. 2000. Microbial diversity at 83 degrees C in Calcite Springs, Yellowstone National Park: another environment where the Aquificales and "Korarchaeota" coexist. Extremophiles. Feb;4(1):61-7.

50. Rohwerder, T., T. Gehrke, K. Kinzler, and W. Sand. 2003. Bioleaching review part A: progress in bioleaching: fundamentals and mechanisms of bacterial metal sulfide oxidation. Appl. Microbiol. Biotechnol. 63: 239-48.

51. Schippers, A., T. Rohwerder, and W. Sand. 1999. Intermediary sulfur compounds in pyrite oxidation: Implications for bioleaching and biodepyritization of coal. Appl. Microbiol. Biotechnology. 52: 104-110.

52. Schwertmann, U. and R.M. Cornell. 2000. Iron Oxides in the Laboratory. 2nd Ed., VCH, Weinheim, Germany. 105-107.

53. Singer, P.C., and M.W. Stumm. 1970. Acid mine drainage: The rate determining step. Science. 167: 1121–1123.

54. Skidmore M, Anderson SP, Sharp M, Foght J, Lanoil BD. 2005. Comparison of microbial community compositions of two subglacial environments reveals a possible role for microbes in chemical weathering processes. Appl Environ Microbiol. Nov;71(11):6986-97.

55. Spurr A. R. 1969. A low-viscosity epoxy resin embedding medium for electron microscopy. J. Ultrastructure Res. 26: 31–43.

56. Stetter, K. O. 1999. Extremophiles and their adaptation to hot environments. FEBS Lett. 452: 22–25.

57. Stumm, W. and J. J. Morgan. 1996. Aquatic Chemistry. Wiley-Interscience; 3rd edition. 1022 pp. ISBN 978-0471511854

58. Suzuki, T., Iwasaki, T. Uzawa, T. Hara, K. Nemoto, N. Kon, T. Ueki, T. Yamagishi, A. and T. Oshima. 2002. Sulfolobus tokodaii sp. nov. (f. Sulfolobus sp. strain 7), a new member of the genus Sulfolobus isolated from Beppu Hot Springs, Japan. Extremophiles. 6: 39-44.

59. Takayanagi, S., H. Kawasaki, K. Sugimori, T. Yamada, A. Sugai, T. Ito, K. Yamasato, and M. Shioda. 1996. *Sulfolobus hakonensis* sp. nov., a novel species of acidothermophilic archaeon Int. J. Syst. Bacteroil. 46: 377–382

60. Ward DM, Ferris MJ, Nold SC, Bateson MM. 1998. A natural view of microbial biodiversity within hot spring cyanobacterial mat communities. Microbiol Mol Biol Rev. Dec;62(4):1353-70

61. Xu, Y., M. A. A. Schoonen, D. K. Nordstrom, K. M. Cunningham, and J. W. Ball. 1998.Sulfur geochemistry of hydrothermal waters in Yellowstone National Park: I. The origin of thiosulfate in hot spring waters. Geochim. Cosmochim. Acta. 62: 3729-3743

62. Yarzábal A, Brasseur G, Bonnefoy V. 2002a. Cytochromes c of Acidithiobacillus ferrooxidans. FEMS Microbiol Lett 209:189–195

63. Yarzábal A, Brasseur G, Ratouchniak J, Lund K, Lemesle-Meunier D, DeMoss JA, Bonnefoy V. 2002b. The high-molecular-weight cytochrome c Cyc2 of Acidithiobacillus ferrooxidans is an outer membrane protein. J Bacteriol 184:313–317

CHAPTER 3

ISOLATION AND DISTRIBUTION OF A NOVEL IRON-OXIDIZING CRENARCHAEON FROM ACIDIC GEOTHERMAL SPRINGS IN YELLOWSTONE NATIONAL PARK

Abstract

Novel thermophilic Crenarchaea have been observed in Fe^{III}-oxide microbial mats of Yellowstone National Park (YNP); however, no definitive work has identified specific microorganisms responsible for the oxidation of Fe^{II}. The objectives of the current study were to isolate and characterize an Fe^{II}-oxidizing Sulfolobales observed in prior 16S rRNA gene surveys, and to determine the abundance and distribution of close relatives of this organism in acidic geothermal springs containing high concentrations of dissolved Fe^{II}. Here we report the isolation and characterization of a novel Fe^{II}-oxidizing thermophilic, acidophilic *Metallosphaera* sp. strain MK1 obtained from a well-characterized acid-sulfate-chloride geothermal spring in Norris Geyser Basin, YNP. Full-length 16S rRNA gene sequence analysis revealed that strain MK1 exhibits only 94.9-96.1% sequence similarity to other known *Metallosphaera* spp. and less than 89.1% similarity to known *Sulfolobus* spp. Strain MK1 is a facultative chemolithoautotroph with an optimum pH range of 2.0-3.0 and an optimum temperature range of 65-75 °C. Strain MK1 grows optimally on pyrite or Fe^{II} sorbed onto ferrihydrite, exhibiting doubling times between 10-11 hours under aerobic conditions (65 ^{o}C). The distribution and relative abundance of MK1-like 16S rRNA gene sequences was evaluated in 14 acidic

geothermal springs containing Fe^{III}-oxide microbial mats. Highly related MK1-like 16S rRNA gene sequences (>99% sequence similarity) were consistently observed in Fe^{III}-oxide mats across temperatures from 55-80 ^{o}C. Quantitative PCR using *Metallosphaera*-specific primers confirmed that organisms highly similar to strain MK1 comprised up to 40% of the total archaeal community of selected sites. The broad distribution of highly related MK1-like 16S rRNA gene sequences in acidic Fe^{III}-oxide microbial mats is consistent with the observed characteristics and growth optima of *Metallosphaera*-like strain MK1, and emphasizes the importance of this newly described taxon in Fe^{II} chemolithotrophy in acidic high-temperature environments of YNP.

Introduction

Thermophilic, acidophilic, chemolithoautotrophs are thought to be important microorganisms in the evolutionary history of Earth (37). Their ability to thrive in high-temperature environments with minimal requirements other than carbon dioxide and inorganic constituents suggests that these organisms serve as important primary producers in extreme environments. Acid-tolerant thermophiles have been found in a variety of geothermal springs, mud pots and deep-sea vents (25, 29, 37). Many of these organisms utilize reduced inorganic compounds such as hydrogen, sulfide, elemental sulfur, thiosulfate, methane or ferrous iron as energy sources for metabolism (1, 7). Although the 16S rRNA gene sequences detected in extreme thermophilic habitats (13, 15, 16, 31) provide important clues regarding microbial processes *in situ*, phylogenetic similarity to cultivated organisms is not sufficient for confirming the physiologies of

these novel microorganisms. Cultivation efforts, therefore, are of critical importance for implicating specific microorganisms in biogeochemical processes occurring *in situ* and for interpreting the role of these populations in community ecology.

Yellowstone National Park (YNP) is a pristine location for studying thermophilic acid-tolerant microorgansisms and their role in mediating geochemical processes. Recent studies have provided a foundation for understanding potential linkages between specific microbial populations and oxidation-reduction reactions controlling the behavior of As, S and Fe in acid-sulfate-chloride (ASC) springs of YNP (14, 15, 23, 24). Previous characterization of aqueous and solid phase geochemistry combined with analysis of 16S rRNA gene sequence distribution has provided data supporting the hypothesis that microbial oxidation of Fe^{II} results in the formation of extensive ferric oxide and or jarositic mats in acidic springs of YNP.

Hydrous ferric oxide (HFO) microbial mats are found in numerous environments including geothermal springs, hydrothermal vents, wetland seeps and acid mine drainage (3, 5, 14, 19, 24). The mechanism of Fe^{II} oxidation may include both chemical and biological contributions (21), but it is widely recognized that the rate of aqueous Fe^{II} oxidation is considerably slow at pH values less than 4 (26, 35) and acidophilic microorganisms are often important in mediating the oxidation of Fe^{II} in these environments. The HFO phases found in ASC springs (pH~3) of Norris Geyser Basin, YNP, form as a result of microbial processes, where oxide phases often occur as 1-2 μm thick encrustations around rod-shaped and filamentous microorganisms (14, 24). Several novel microorganisms (based on 16S rRNA gene phylogeny) have been identified in

these HFO mats and may contribute to Fe^{II} oxidation and subsequent formation of arsenate-rich HFO phases (14, 24). These organisms are represented by bacterial 16S rRNA gene sequences related to *Hydrogenobaculum acidophilum* (98-99 %), *Thermaerobacter subterraneus* (91%), *Acidimicrobium ferrooxidans* (98%), and *Meiothermus silvanus* (92%), as well as archaeal sequences related to *Metallosphaera prunae* (96%), *Sulfolobus solfataricus* (97%), *Vulcanisaeta distributa* (98%) and *Sulfolobus islandicus* (99%). Additional 16S rRNA gene sequences less than 90% similar to known cultivated organisms have also been consistently observed in these environments [e.g., sequences highly similar to clones YNPFFA85 (99%), YNPFFA108 (99%), SK305 (99%) and YNPFFA23 (99%); 14]. However, there is no direct evidence supporting the potential role of these organisms in Fe cycling in geothermal systems.

Efforts to cultivate relevant Fe^{II}-oxidizing microorganisms from acidic geothermal springs in YNP have been limited, yet the metabolisms of these thermophiles are responsible for an array of orange, red and maroon Fe^{III}-oxide phases in numerous geothermal outflow channels of YNP (Figure 3.1). Previous 16S rRNA gene sequence characterization of acidic Fe mats in Norris Geyser Basin suggested that *Metallosphaera*-like organisms are important in the oxidation of Fe^{II} and subsequent formation of copious amounts of Fe^{III}-oxides within geothermal outflow channels (14, 24). There are currently four characterized *Metallosphaera* spp., all isolated from high-temperature acidic environments (9, 11, 28). In most cases, these chemolithoautotrophs are capable of growth on sulfidic ores and or elemental sulfur. However, the importance of Fe^{II} as an electron donor in this understudied genus is not clear. Peeples and Kelly (28) have shown

that *M. prunae* may oxidize Fe^{II} as a sole energy source, and several studies have noted that *Metallosphaera* spp. are effective in accelerating the dissolution of pyrite and release of metals in biomining applications (27, 30, 32).

Given the potential importance of *Metallosphaera*-like organisms in geothermal environments and their possible utility in controlled bioleaching applications, the objectives of the current study were to (i) isolate and characterize an Fe^{II}-oxidizing *Metallosphaera*-like organism from acidic Fe mats in YNP, and (ii) determine the abundance and distribution of similar *Metallosphaera*-like 16S rRNA gene sequences across a variety of different Fe^{III} depositional mats common in acidic geothermal springs of YNP.

Materials and Methods

Initial Isolation Protocols

Approximately 2 grams of a hydrous ferric oxyhydroxide (HFO) microbial mat from the outflow channel of an ASC geothermal spring was placed in a sealed 60 ml serum bottle and filled with native spring water (62-63 °C). The site is unofficially named *Beowulf Spring* and is located in the One Hundred Springs Plain of Norris Geyser Basin, YNP (44°43’53.4’’N latitude, 110°42’40.9’’W longitude; YNP Thermal Inventory NHSP35). After 4 h, 1 ml of the slurry was transferred into each of three 20 ml serum bottles containing 15 ml of filtered (0.2 μm) spring water, 2% (w/w) pyrite-enriched mine tailings, and a 5 ml gas headspace composed of 25% O_2, 50% CO_2 and 25 % air. The pyrite-enriched mine tailings were obtained from a previous study using density

separation techniques and contain ~50 % pyrite (18). The cultures were incubated at 65 °C for 10 days, then subjected to several rounds of dilution to extinction. The progress of all cultures was monitored by extracting DNA from the serum bottles, followed by PCR amplification of 16S rRNA genes using universal bacterial and archaeal primers (14, 24), and separation and visualization of the PCR products using denaturing gradient gel electrophoresis (DGGE; 24). Pure cultures were also confirmed using cloning and sequencing of longer 16S rRNA gene fragments (discussed below). Pure cultures from serum bottles were centrifuged at 1000xg for 10 minutes and preserved in a 25% glycerol/ 75% synthetic growth medium. The glycerol stocks were stored at -80 °C after freezing in liquid nitrogen.

Growth Media, Conditions and Substrates

Pure cultures were maintained as described above, but spring water was substituted with a synthetic medium designed to match spring water aqueous geochemistry. The synthetic growth medium contained 11 mM Na^+, 10.1 mM Cl^-, 1.5 mM K^+, 1.2 mM SO_4^{2-}, 0.7 mM H_3BO_3, 0.4 mM NO_3^-, 0.25 mM Ca^{2+}, 0.1 mM PO_4^{3-}, 0.2 mM Al^{3+}, 0.1 mM NH_4^+, 0.1 mM H_4SiO_4, and 0.1 mM Mg^{2+}. Unless stated otherwise, 20 mM $FeSO_4$ (pH 2.5), vitamins, and trace metals (12) were added to the growth medium, and the pH was adjusted to 2.5 - 3.0 with H_2SO_4 followed by filter sterilization (0.2 µm). Medium specific for *Metallosphaera sedula* (11) containing 0.1% yeast extract was also used to check for growth enhancement on pyrite. Chemolithotrophic growth of the isolate was evaluated in 20 ml serum bottles containing 15 ml synthetic medium using a variety of possible electron donors including 0.5 and 10 mM Na-tetrathionate, 1 and 20 mM

$Fe^{II}SO_4$ (pH 2.5) as well as different solid phases including elemental S^0, Fe^{II} sorbed onto ferrihydrite and various sulfide minerals (Ward's Natural Science, Rochester NY).

Research-grade pyrite (FeS_2), chalcopyrite (FeCuS), sphalerite (ZnS), and covellite (CuS) were ground with an agate mortar and pestle, separated by sieving, and sonified in acetone for 15 min to remove fine particles created during grinding. The final mineral fractions were autoclaved 2 times at 132 °C prior to use in growth experiments. Two-line ferrihydrite was synthesized using the method outlined by Schwertmann and Cornell (35), then washed three times with 0.05 M $FeSO_4$ for 30 minutes in the dark followed by filtration (0.2 μm). This substrate, containing Fe^{II} sorbed to ferrihydrite, is referred to in this study as Fe^{II}-ferrihydrite. The mass of solid phase added to each of the serum bottles was 0.5 g of the < 0.15 mm size fraction. Anaerobic growth was tested with pyrite and Fe^{II} sorbed to ferrihydrite with 10 mM NO_3^- as the electron acceptor. Anaerobic growth was also tested in the presence of elemental sulfur and ferrihydrite. All anaerobic samples were purged for 30 minutes with N_2 gas, and anaerobic conditions verified using 1 mg/L resazurin.

Detailed growth curves were obtained under several geochemical conditions including: 1) pyrite and synthetic medium, 2) pyrite plus 0.005% yeast extract, 3) Fe^{II} sorbed to ferrihydrite with 0.005% yeast extract, and 4) elemental sulfur (S^0) with 0.005% yeast extract. Temperature and pH optima were determined in serum bottles containing pyrite and synthetic medium using 1 ml of diluted inoculum (500-1000 cells/ml). Cultures were grown in a solid Al-block incubator at 15 different temperatures ranging from 40 to 90 °C. The pH was adjusted by the addition of either HCl or NaOH

and the isolate was cultivated at pH values of 0.75, 1.0, 2.0, 2.5, 3.0, 3.5, 4.5, 5.0, 5.5, and 6.0. The pH of the growth medium was measured daily and adjusted with acid or base when necessary. Growth was quantified after 11 days using total DNA extracted from serum bottles in triplicate for each treatment after filtration of the contents onto 0.22 μm polycarbonate filters (FastDNA SPIN Kit for Soil, Q-Biogene, Irvine, CA, USA). DNA was measured on a NanoDrop® ND-1000 spectrophotometer (NanoDrop Technologies, Wilmington DE) after being blanked with a non-inoculated pyrite control sample. Additional pyrite containing serum bottles were spiked with 100 ng/ul DNA (100 bp DNA ladder by Promega, Cat # G2101) to evaluate extraction efficiency. Cell growth in selected treatments was also quantified directly using 0.2 ml samples treated with DAPI and counted in a Hausser Scientific counting chamber (Horsham, PA) using a Zeiss epifluorescent microscope (Zeiss Axioskop 2 plus, Oberkochen, Germany).

Chemical Analyses

Concentrations of SO_4^{2-}, $S_2O_3^{2-}$, NO_3^- and PO_4^{3-} in serum bottles were measured as a function of time using anion chromatography (Model DX500 with AS-16 4mm column, Dionex Corp., Sunnyvale, CA). Total soluble Fe and Fe^{II} were measured using the ferrozine method (40).

Electron Microscopy

Cultures were filtered through 0.22 μm polycarbonate filters after incubation for 10 days and the resulting pyrite suspensions were immediately fixed with 3% glutaraldehyde. Samples were then imbedded in 2% noble agar, refixed in

glutaraldehyde, dehydrated in an ethanol series, and treated with propylene oxide before infiltration with Spurr's epoxy resin (36). Thin sections were placed on 300 mesh copper grids and analyzed by transmission electron microscopy (TEM) using a LEO 912AB (LEO Electron Microscopy Inc., Thornwood, NY) equipped with an in-column OMEGA-type imaging spectrometer and controlled with Soft Imaging System software (Lakewood, CO).

Characterization of Geothermal Sites in Yellowstone National Park

Numerous acidic Fe mats from three geothermal basins in YNP (Norris Geyser Basin – NGB, Rainbow Springs- RS and Joseph's Coat Springs-JC) were sampled for aqueous and solid phase geochemical analysis, and for molecular characterization (16S rRNA gene sequencing). Fourteen distinct springs were analyzed in detail (Figure 3.1; Table 3.1) including nine sites in Norris Geyser Basin (NGB-BE [unofficially referred to as *Beowulf* –East], NGB-BW [*Beowulf* –West], NGB-DS [unofficially referred to as *Dragon Spring*], NGB-OSP [unnamed feature in the One Hundred Spring Plain], NGB-WG [*Whirlygig Geyser*], NGB-TC [unnamed spring along Tantalus Creek], NGB-EG [*Echinus Geyser*], NGB-PB [unnamed spring in *Porcelain Basin*], NGB-GAP [unnamed spring west of *Ragged Hills*]), two unnamed springs at Joseph's Coat (JC1, JC2), and three unnamed springs at Rainbow Springs (RS1, RS2, RS3). Each spring was sampled at multiple locations along a transect down the primary flow channel, including both S^0 and Fe-oxide depositional zones. Thorough geochemical characterization of spring water sampled directly above the Fe microbial mats was conducted for all sites (Table 3.1).

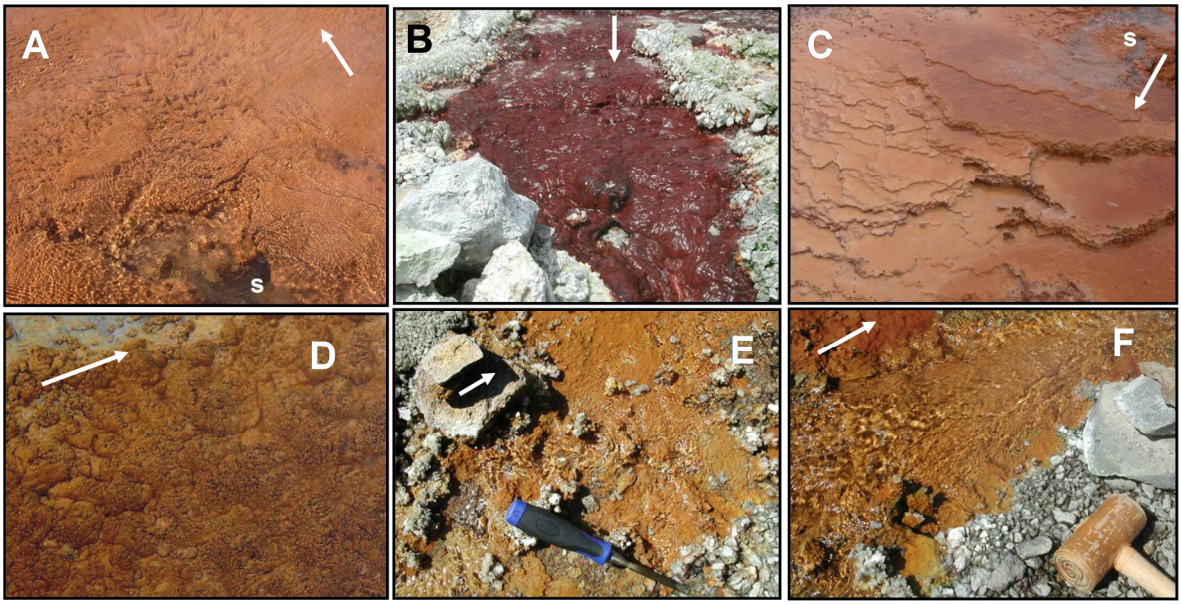

Figure 3.1. Acidic (pH 2.6 – 3.4), ferric hydroxide depositional environments in representative geothermal springs of Yellowstone National Park. (A) Norris Geyser Basin (NGB-OSP), (B) Joseph's Coat Springs (JC2) showing maroon Fe-oxide phases, (C) Norris Geyser Basin (NGB-GAP), (D) Norris Geyser Basin (NGB-DE), (E) Rainbow Springs (RS1), and (F) Rainbow Springs (RS2). These geochemical environments appear optimum for *Metallosphaera* sp. str. MK1-like organisms [white arrows indicate average flow direction, s = source discharge].

Table 3.1. Aqueous geochemistry[1] (total dissolved concentrations) of acidic geothermal sites in Yellowstone National Park containing *Metallosphaera*-like 16S rRNA gene sequences. All sites contain secondary ferric Fe mineralization products formed as a result of Fe^{II} oxidation. [1]All values are averages over multiple sampling trips and exhibit standard deviations < 10% for all constituents, with exception of dissolved gases; [2]Geothermal sampling sites are identified by site location (NGB – Norris Geyser Basin, JC – Josephs Coat, RS – Rainbow Springs), distance from geothermal source (m) and Lat-Long coordinates; [3] I=ionic strength, [4] nd = not determined.

Spring ID[2]	Position (m)	Lat-Long	T (C°)	pH	I[3] *mM*	Na *mM*	K *mM*
NGB-BE	**E (7.5)**	44°43'53.4'' N 110°42'41.0'' W	63	3.0	17.2	13.3	1.3
NGB-BW	**D (8.4)**	44°43'53.4'' N 110°42'40.9'' W	60	3.0	17.3	12.7	1.2
NGB-DE	**C (6)**	44° 43' 54.8" N 110° 42' 39.9" W	57	3.1	17.8	13.2	1.4
NGB-OSP	**A (0)** **B (2)**	44° 43' 58.8" N 110° 42' 32.1" W	74 63	3.4-3.6 3.4-3.6	15.1 15.8	12.1 12.1	1.5 1.5
NGB-WG	**A (0)**	44° 43' 43.3" N 110° 42' 11.29" W	66	3.4	19.1	14.8	1.9
NGB-TC	**B (2)**	44° 43' 35.7" N 110° 42' 32.5" W	64	2.7	13	7.1	1.8
NGB-EG	**A (0)** **C (10)**	44° 43' 19.4" N 110° 42' 7.58" W	76 70	3.5 3.4	13.4 13.4	8.2 8.4	1.5 1.5
NGB-PB	**A (0)**	44° 43' 43.3" N 110° 42' 11.32" W	85	3.4	18.6	14.4	1.9
NGB-GAP	**B (0.12)**	44° 43' 38.7" N 110° 42' 56.0" W	73	3.2	16.1	12.4	1.0
JC1	**B (1.3)**	44° 44' 19.8" N 110° 19' 33.5" W	65	2.7	10	1.1	1.0
JC2	**B (2.7)** **C (7.1)**	44° 44' 19.9" N 110° 19' 32.9" W	75 65	2.5 2.5	12.4 13.5	1.2 1.2	1.0 1.0
RS1	**B (1.6)**	44° 45' 59.1" N 110° 16' 03.9" W	75	2.6	15.5	3.8	2.2
RS2	**B (2.2)** **D (8.3)** **F (12.6)**	44° 45' 59.6" N 110° 16' 08.2" W	73 69 53	2.5 2.6 2.5	15.7 15.9 16.8	3.9 3.9 3.8	2.2 2.2 2.3
RS3	**A (0)** **B (0.9)**	44° 46' 07.2" N 110° 16' 14.9" W	54 54	3.3 3.3	16.1 16.0	4.2 4.2	2.1 2.1

Table 3.1 Continued.

Spring ID[2]	Fe_{TS} *μM*	Cl^- *mM*	SO_4^{2-} *mM*	As_{TS} *μM*	H_2S *μM*	H_2 *nM*	CH_4 *μM*	O_2 *μM*
NGB-BE	39	13.3	1.6	27.5	3.5	15.9	0.14	72
NGB-BW	33	12.4	1.6	25.6	2.4	10.8	0.3	87
NGB-DE	47	13.6	1.5	22.8	13.5	23.2	0.3	80
NGB-OSP	26 26	11.7 12.9	1 1.1	17.2 16.8	12.1 0.1	108 nd	0.35 nd	42 76
NGB-WG	7	15.8	1.2	29.2	< 0.3	20	0.36	nd
NGB-TC	96	7.6	2.5	11.5	nd	61	<0.01	85
NGB-EG	34 28	4.6 4.6	3.2 3.2	2.9 2.4	3.5 < 0.3	111 nd	0.37 nd	nd
NGB-PB	13	15.5	1.1	28.5	1.3	11	<0.01	nd
NGB-GAP	74	13.8	1.0	76.1	2.6	20.9	<0.01	32
JC1	132	0.02	5.1	0.97	0.12	4.5	<0.01	148
JC2	163 162	0.1 0.1	6.1 6.7	0.3 0.3	2 3.8	52.6 65.7	0.3 0.3	9 43
RS1	96	0.1	7.6	3.2	0.4	36.9	0.6	21
RS2	98 99 91	0.1 0.1 0.1	7.3 7.5 7.4	3.3 3.3 3.0	2.8 1.8 0.1	32 36.7 28.3	2.2 0.9 <0.01	22 44 102
RS3	231 230	0.15 0.15	6.6 6.6	2.8 3.0	< 0.3 < 0.3	11 nd	3.46 nd	< 1 14

DNA Extraction and 16S rRNA Gene Sequencing

The distribution and relative abundance of *Metallosphaera*-like 16S rRNA gene sequences was examined in all 14 geothermal sites described above. In the majority of cases, the sites were sampled several times over a three year period (2003-2005). Microbial mat samples were obtained using sterile tools and collection tubes, and immediately placed on dry-ice for transport to a -80 ^oC freezer. Total DNA was extracted from the samples (or the pure culture) using the FastDNA SPIN Kit for Soil (Q-Biogene, Irvine, CA). Near full-length PCR primers targeting 16S rRNA genes consisted of the

Bacteria-specific primer Bac8f (5'-AGAGTTTGATCCTGGCTCAG-3') coupled with the universal primer Univ1392r (5'-ACGGGCGGTGTGTAC-3'), and the *Archaea*-specific primer Arc2f (5'-TTCCGGTTGATCCYGCCGGA-3') also coupled with the universal primer Univ1392r. Briefly, The 50 µL PCR mixtures contained 10 mM Tris-HCl (pH 8), 50 mM KCl, 0.1 % Triton X-100, 4.0 mM $MgCl_2$, 800 µM dNTP's, 0.5 µL of each primer, 1.25 U *Taq* DNA polymerase (Promega, Madison, WI), and 1-5 µL template DNA (2-20 ng). Thermal cycler protocol was 94 ºC for 6 min, 25 - 35 cycles of 94 ºC and 54 ºC each for 45 sec followed by 72 ºC for 1 min 50 sec, and a final 7 min extension period at 72 ºC. Negative control reactions (no template) were routinely performed to ensure purity. The purified PCR products were cloned using the pGEM-T Vector System from Promega Corp. (Madison, WI) and the inserts were amplified and sequenced (TGEN, Phoenix, AZ, and the Ohio State Plant Genomics Facility, Columbus, OH). Eighty-six *Metallosphaera*-like 16S rRNA gene sequences (SK, EM and MK series) from Fe^{III}-oxide mats in YNP have been deposited in GenBank (see Table AC.1 in the Appendix Chapter AC for Accession Numbers and locations of the environmental clones). The near full-length 16S rRNA gene sequence for *Metallosphaera* sp. strain MK1 has been submitted to the GenBank database (Accession # DQ350777).

Isolate-specific 16S rRNA Primer

An 18 bp primer specific for MK1-like organisms was designed around 16S rRNA ribosomal class I and II sites (4) of strain MK1 as well as highly-related (>99%) sequences from Fe mats described in this study. The primer (5′-AGAAGGACTGCCGGTGTT-3′) had no homology to 16S rRNA gene sequences of

other organisms, and was further analyzed using the IDT ScitTools OligoAnalyzer 3.0 (Integrated DNA Technologies, Coralville, IA) for possible hairpins, dimers, and melting temperature. The MK1 primer was used as a reverse primer with the *Archaea*-specific primer Arc2f (total fragment length is ~ 1000 bp) to verify and test cultures and spring locations for MK1-1ike sequences. PCR conditions were as stated above with a modified annealing temperature of 55 ºC and a 1 min 30 sec extension at 72 ºC. Control reactions with no template were routinely performed to ensure purity. The specificity of the primer set was tested and confirmed by sequencing 25 clones after amplification of DNA extracts from ASC springs (NGB-BE, NGB-DS, NGB-OSP).

Quantitative-PCR and FISH

Quantitative(Q)-PCR analysis was performed with the Rotor-Gene RG-3000 (Corbett Life Science, Sydney Australia). Standards used for the calibration curve (e.g., initial DNA concentration versus cycle threshold number) were created using pooled DNA extracts from subject Fe mats of ASC springs. Extracted DNA was amplified with each of three primer sets: Arch931f/Univ1392r, Bac1070f/Univ1392r, and MET-MK1/Univ1392r according to the PCR protocol stated above. The resultant ~ 300 to 430 bp products (product size dependent on primer set) were purified with the QIAquick PCR cleanup kit (Qiagen, Valencia, CA) and quantified using UV spectroscopy (NanoDrop® ND-1000) and or agarose gel electrophoresis. Standards from each primer set were then serially diluted with master mix to create six Q-PCR working standards from $1{:}10^3$ to $1{:}10^8$. Reaction master mix was prepared as previously stated with the addition of 1X SYBR® Green I dye (Applied Biosystems, Foster City, CA). Environmental samples

were obtained from 55 ºC *Beowulf* HFO mat, 62.5 ºC *Beowulf* HFO mat, 55 ºC *Dragon Spring* HFO mat and DNA was extracted as previously stated. Extracted DNA was diluted 1:10 with master mix and analyzed along with the standards, a blank and a positive control consisting of extracted DNA from strain MK1.

The MK1 primer sequence (described above) was labeled with a 5'Cy5™ fluorescent tag by Integrated DNA Technologies (Coralville, IA) and probe hybridization was conducted according to Amann et al. (2). Fluorescent images were taken using a Zeiss epifluorescent microscope (Zeiss Axioskop 2 plus, Oberkochen, Germany) and a FITC filter.

Results

Initial enrichment cultures using Fe^{III}-oxide microbial mat inoculum contained 3 to 4 thermophilic populations based on DGGE analysis of culture complexity. Subsequent dilution to extinction resulted in the isolation of a pure culture, as determined using both DGGE analysis and full-length 16S rRNA gene sequence analysis with universal archaeal and bacterial primer sets. Sequencing results verified that the closest cultivated relatives of the pure culture obtained from this isolation protocol are *Metallosphaera* spp. within the order Sulfolobales (Figure 3.2). The 16S rRNA gene sequence (1331 bp fragment) of strain MK1 is only 95-96% similar to other *Metallosphaera* spp. and less than 89.1% similar to other *Sulfolobus* spp. Although this suggests that strain MK1 may be classified as a new genus within the Sulfolobales, we refer to this new taxon as *Metallosphaera* sp. strain MK1.

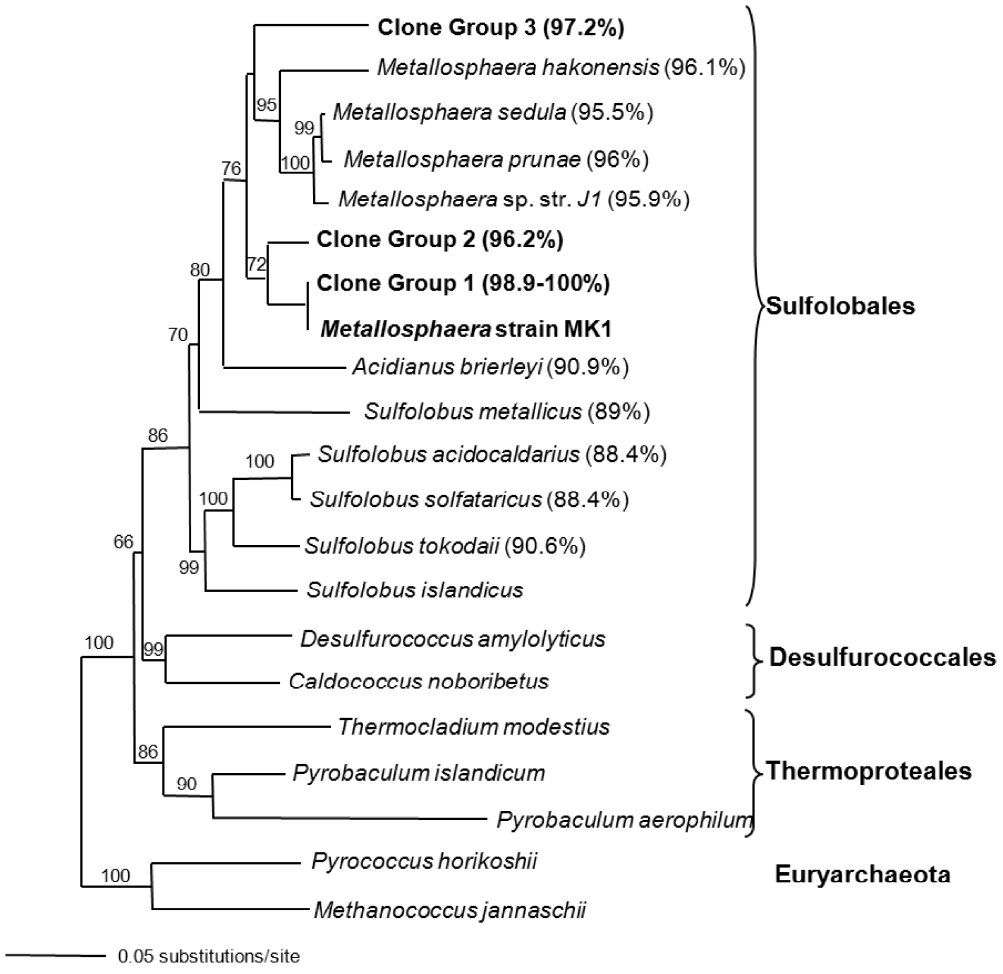

Figure 3.2. Phylogenetic (16S rRNA gene) tree showing the position of *Metallosphaera* sp. str. MK1 described in the current study, as well as three *Metallosphaera*-like clone groups obtained from 14 different acidic geothermal sites in YNP. A total of 421 *Metallosphaera*-like clones are represented in Clone Groups 1-3; however, the majority of clones (415) are contained in Group 1 and are > 98.9 % similar to strain MK1. Percent values given in parentheses indicate 16S rRNA gene sequence similarities to the isolate *Metallosphaera* str. MK1 (PAUP^{TM} Neighbour Joining tree with 1000 boot straps using *Aquifex pyrophilus* as the outgroup).

Growth Optima and Electron Donors

The growth of strain MK1 was evaluated in the presence of pyrite, S^0, and Fe^{II}-ferrihydrite. No significant statistical differences (α=0.05) in growth rates were noted in treatments containing pyrite, pyrite with 0.005% YE, or Fe^{II}-ferrihydrite (Fig. 2), and

under these conditions, maximum growth rates (2.1±0.5 x10^7 cells mL^{-1} hr^{-1}) were observed either in the presence of pyrite or Fe^{II}-ferrihydrite. Maximum growth rates observed at 65 ^oC corresponded to doubling times of 10.3±0.5 and 11.4±0.5 hours (± = standard errors) in the presence of Fe^{II}-ferrihydrite and pyrite, respectively. Strain MK1 did not exhibit measurable growth in the presence of 20 mM ferrous sulfate, suggesting that sorbed Fe^{II} or the presence of a mineral substrate are important prerequisites for the growth of this organism. The organism is also capable of growth on elemental S^0 (Figure 3.3), albeit at a reduced rate (doubling times = 16 ± 2 hours) compared to treatments containing Fe^{II}. The amount of sulfate produced (Figure 3.4) during growth in the presence of pyrite (~ 3 mM) or elemental sulfur (~ 1.3 mM) was consistent with the differential growth rates on these substrates and confirmed that strain MK1 is capable of oxidizing reduced forms of S.

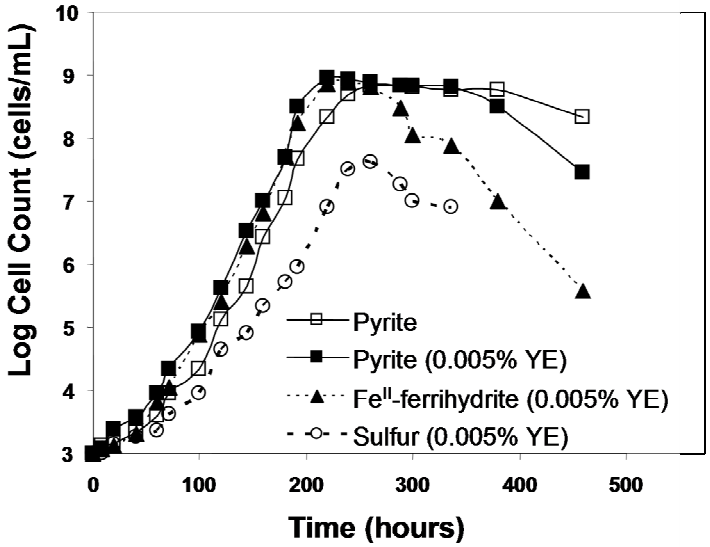

Figure 3.3. Growth curves (log base 10) of *Metallosphaera* sp. str. MK1 on specimen-grade pyrite (with and without added yeast extract), Fe^{II} sorbed to ferrihydrite, and elemental S. Maximum growth rates in the presence of pyrite or Fe^{II}-ferrihydrite correspond to 2.1±0.5 x10^7 cells mL^{-1} hr^{-1}.

The optimal pH and temperature for growth of strain MK1 were determined in the presence of 2% pyrite. The organism exhibited optimal growth over a pH range of 2-3 and temperatures of 65-75 ^{o}C (Figure 4.5); however, the organism can survive over a reasonably broad temperature range from 45 to 85 ^{o}C. The pH and temperature optima for strain MK1 are similar to the geothermal site conditions (pH=3.1, T=65 ^{o}C) of the Fe mat used as original inoculum.

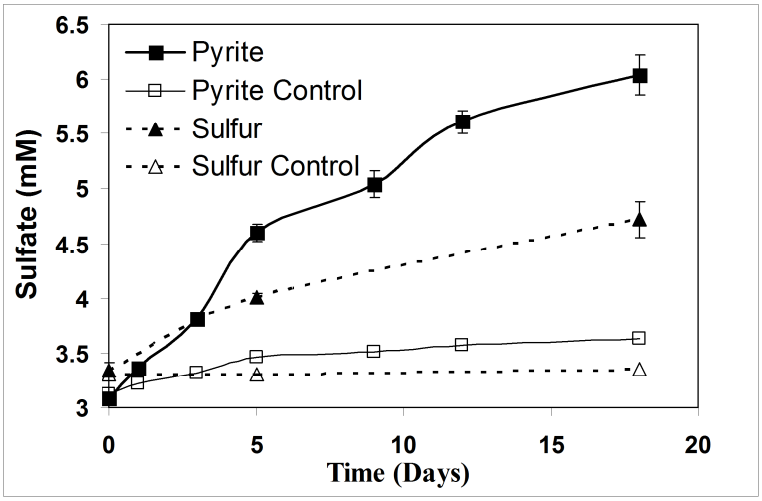

Figure 3.4. Production of sulfate during growth of *Metallosphaera* str. MK1 in the presence of pyrite and elemental S^0 (pH 3, T = 65 ^{o}C, 0.005% YE). The growth medium contained 3 mM initial aqueous sulfate, and controls reveal little change in sulfate in the absence of microbial growth (error bars are standard errors, n=3).

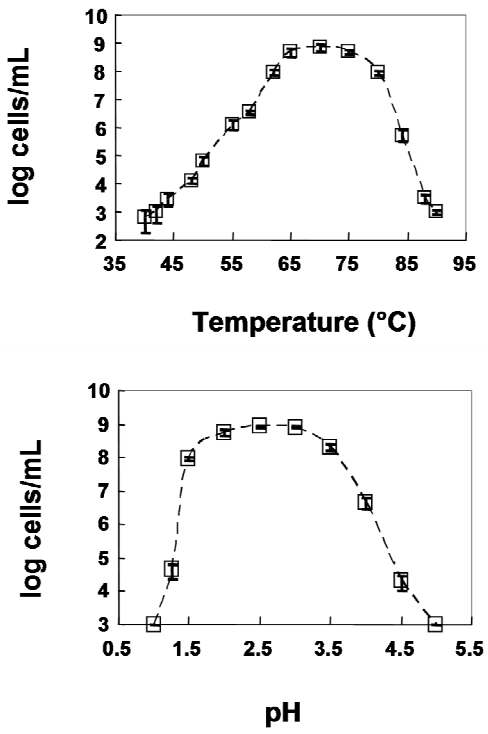

Figure 3.5. Temperature (A) and pH (B) growth optima of *Metallosphaera* sp. str. MK1 (grown on pyrite plus 0.005 % YE). The temperature series was performed at a constant pH = 3, while the pH series was performed at a constant temperature = 65 ^{o}C). Maximum growth rates were achieved at pH 2.5 and 75 ^{o}C (error bars are standard errors [n=3] and are generally within symbols; y-axis is log base 10).

Table 3.2. Growth of *Metallosphaera* sp. str. MK1 in the presence of different minerals, substrates or aqueous electron donors (pH = 3, T = 65 ^{o}C). Growth was assessed visually based on oxidation products ("+++" = substantial Fe^{III} oxide production; " - " = no growth) and quantitatively after 11 days using total extractable DNA from 20 ml growth vessels (n=3). [1] nd = not detected; [2] abiotic oxidation of aqueous Fe^{II} over time frames of >2 weeks resulted in the presence of Fe^{III}-oxide plus aqueous Fe^{II} which can support growth of strain MK1.

Culture Growth Conditions	Growth	Peak DNA, ng (std error)
Pyrite-enriched mine tailings	+++	3610 (255)
Fe^{II} sorbed to Ferrihydrite	+++	3277 (53)
Pyrite (FeS_2)+ Yeast Extract (DSMZ 485 Medium)	+++	3244 (110)
Pyrrhotite (FeS)	+++	2779 (280)
Pyrite(FeS_2) + 20mM Fe^{II}	+++	2592 (60)
Elemental Sulfur + 20 mM Fe^{II}	+++	2576 (313)
Chalcopyrite ($CuFeS_2$)	++	2140 (95)
Pyrite (FeS_2) - 20mM Fe^{II}	++	1807 (58)
Elemental Sulfur + 0.02% Yeast Extract	++	1609 (133)
Covellite (CuS)	+	1000 (92)
Sphalerite (ZnS)	+	335 (54)
Siderite ($FeCO_3$)	-	nd[1]
Magnetite (Fe_3O_4)	-	nd
20 mM $FeSO_4$	-	nd[2]
20 mM Tetrathionate	-	nd
5 µM Na_2S	-	nd
0.02% Yeast Extract in Synthetic Growth Medium	-	nd
Anaerobic: Sulfur /Ferrihydrite	-	nd
Anaerobic: Pyrite/10mM NO_3^-	-	nd
Anaerobic: Fe^{II}-Ferrihydrite/10mM NO_3^-	-	nd

Autotrophic growth was also significant in the presence of pyrite-enriched mine tailings, pyrrhotite (FeS), and chalcopyrite ($CuFeS_2$) as determined by evaluating DNA yields after 11 d of growth (Table 3.2). Growth was modest on S^0 plus 0.005% YE. Interestingly, growth on S^0 was enhanced considerably after the addition of 10 mM $Fe^{II}SO_4$, despite the fact that strain MK1 did not grow in media containing 20 mM aqueous $Fe^{II}SO_4$. Poor but modest growth was observed on other sulfide minerals including sphalerite (ZnS) and covellite (CuS), however, no growth was observed on aqueous sulfide, thiosulfate, tetrathionate, or on the reduced Fe minerals magnetite (Fe_3O_4) or siderite ($FeCO_3$). Anaerobic growth was not detected using S^0 as an electron donor and ferric iron (as ferrihydrite) as an electron acceptor. In addition, no growth was observed on pyrite, Fe^{II}-ferrihydrite or S^0 under anaerobic conditions where NO_3^- was present as a potential electron acceptor.

Isolate Morphology and Surface Association

Samples from actively growing pyrite cultures were examined using transmission electron microscopy (TEM). Strain MK1 cells are irregular lobed shaped (diameters ranging from 0.9 to 1.2 μm) and exhibits a plasma membrane and S-layer approximately 50 nm thick, typical of other members of the Sulfolobales (6, 17, 41). Optical, DAPI, FISH and TEM images also confirm that strain MK1 is closely associated with pyrite and or Fe^{III}-oxide particles formed as a result of Fe^{II}-oxidation (Figure 3.6).

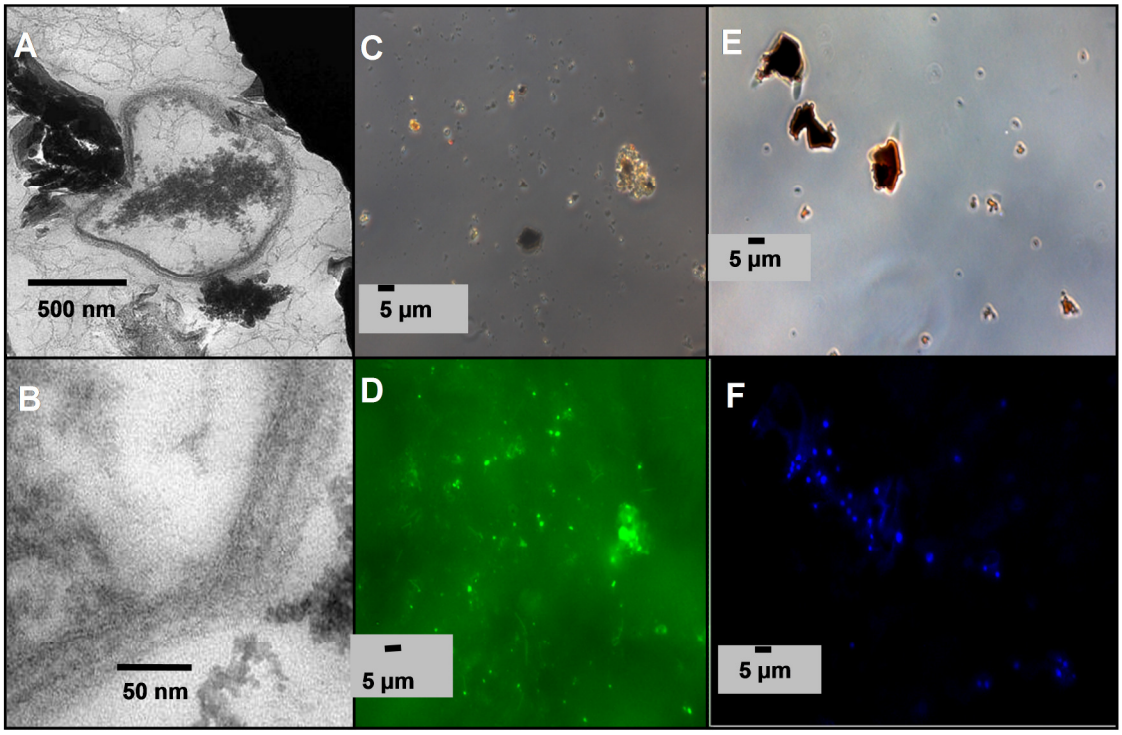

Figure 3.6**.** Transmission electron micrographs (TEM) of *Metallosphaera* sp. str. MK1 cultured in pyrite medium show irregular coccoid cells in close association with pyrite particles (A), and plasma membrane and S-layer typical of members of the order Sulfolobales (B). Optical phase contrast microscopy images of strain MK1 grown on pyrite (C,E) are shown with either a corresponding FISH (D) or DAPI image (F). Both probes confirm the close association of *Metallosphaera* sp. str. MK1 cells with pyrite and iron oxide particles.

Distribution of *Metallosphaera*-like 16S rRNA Gene Sequences

A total of 883 full-length 16S rRNA gene sequences were characterized from 14 different geothermal Fe mat samples, and 419 of these sequences (~46% of the total archaeal clones) are highly related (~99-100%) to *Metallosphaera* sp. str. MK1. The majority of *Metallosphaera*-like clones (404) were highly related to one another (> 99 % similarity) and are represented as a single entry in the phylogenetic tree entitled *Group 1* clones (Figure 3.1). This phylogenetic group also contains the 16S rRNA gene sequence of *Metallosphaera* sp. str. MK1, which exhibits from 98.9 to 100% sequence similarity to

Group 1 clones (Figure 3.1). Two additional *Metallosphaera*-like clone groups (*Group 2* and *3*) were identified in this study, each containing 2 entries from sites in Norris Geyser Basin (NGB-WG, NGB-OSP, NGB-EG). Relative to *Group 1* clones, these less frequent clones are more distantly related to strain MK1 ranging from 96-97% similarity (Figure 3.1). All *Metallosphaera*-like 16S rRNA gene sequences from these sites were less than 96% similar to previously cultured *Metallosphaera* spp. Finally, based on the 14 geothermal sites investigated in the current study, there was no obvious separation or grouping of *Metallosphaera*-like 16S rRNA sequences by location. For example, *Group 1* clones contained representatives from all of the 14 sites.

Semi-quantitative Estimates of Numerical Relevance

Quantitative PCR analysis was performed with universal bacterial, universal archaeal, and *Metallosphaera* sp. str. MK1-specific 16S rRNA gene primer sets on three Fe mats from Norris Geyser Basin (NGB-BEE, NGB-BWD and NGB-DC). Results indicate that sequences highly similar to *Metallosphaera* sp. str. MK1 represent a significant proportion of not only the archaeal species in ASC springs, but also the total microbial diversity (Figure 3.7A). For example, between 13-36 % of the total amplifiable archaeal sequences could be attributed to *Metallosphaera* sp. str. MK1-like sequences in ASC springs. Interestingly, results show a decrease in *Metallosphaera* str. MK1-like sequences from about 36% (of total archaeal sequences) at 65 °C (NGB-BEE) to 12% at 55 °C (NGB-BWD). Previous work on these springs had suggested that *Metallosphaera*-like sequences were more common at temperatures above 60 ^{o}C (14, 24) and this observation is consistent with the temperature optima of strain MK1 (range 65-75 ^{o}C). In

fact, HFO mats that form above 80 ^{o}C such as those found at the source of NGB-GAP (85 ^{o}C) do not contain clones related to *Metallosphaera* spp., further suggesting that strain MK1 is ecologically constrained to a temperature range of approximately 55-75 ^{o}C.

Estimates of the relative importance of MK1-like organisms obtained from Q-PCR agreed favorably with the relative abundance of *Metallosphaera*-like sequences identified in clone libraries from these three site positions (ASC Springs, Figure 3.7B). Further, environmental clones highly similar to strain MK1 were also obtained from acid-sulfate (AS) springs at Rainbow Springs (RS1, RS2) and Joseph's Coat Springs (JC1, JC2) (Figure 4.7B). These geothermal systems contain 1-2 mM NH_4^+, 5-8 mM SO_4^{2-} and very low Cl^- (Table 3.1, or www.rcn.montana.edu), which is quite different than the predominant cations and anions in springs of Norris Geyser Basin (e.g. Na^+ and Cl^-). Despite these differences, the high temperature (65-75 ^{o}C), low pH (2.5-2.6) and high ferrous Fe (~ 100 μM) of RS and JC sites appear optimum for *Metallosphaera* MK1-like organisms. In these habitats, MK1-like clones often dominated the archaeal clone libraries, ranging from 24 to 98 % of sequences detected at these sites.

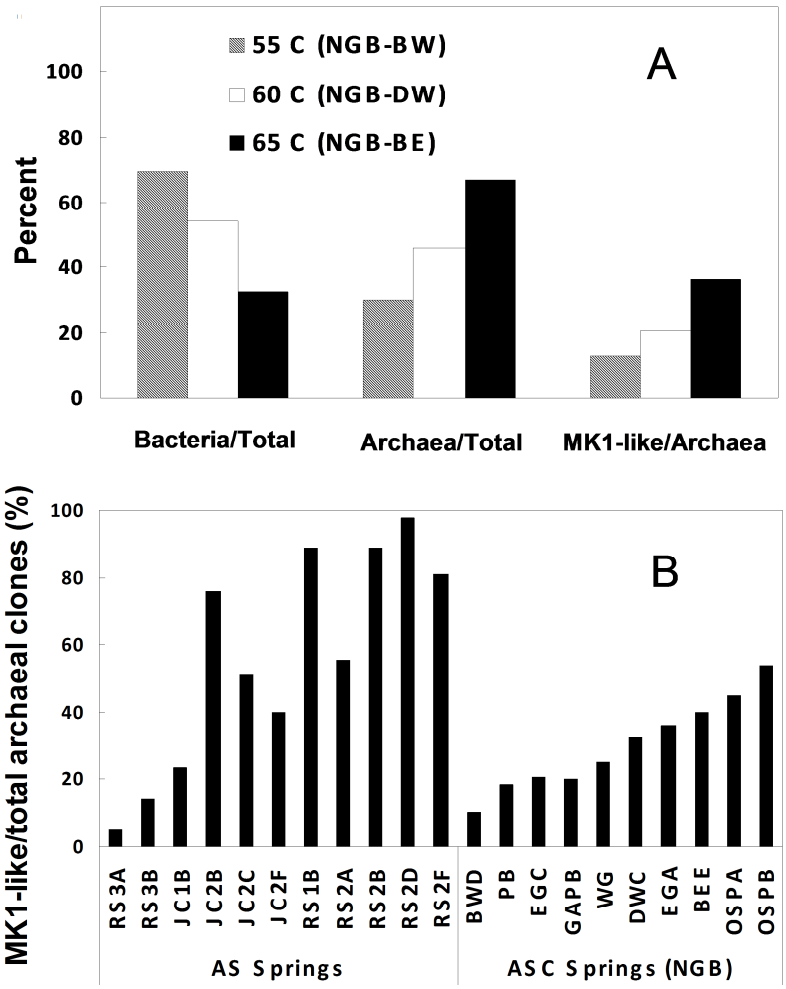

Figure 3.7. Distribution and abundance of *Metallosphaera*-like 16S rRNA gene sequences across acid-sulfate (AS) and acid-sulfate-chloride (ASC) geothermal springs in YNP. (A) Quantitative(Q)-PCR results from three ASC springs indicating percent of bacterial and archaeal 16S rRNA genes relative to total 16S rRNA gene, and percent of *Metallosphaera* str. MK1-like 16S rRNA genes relative to total archaeal 16S rRNA genes. (B) Relative abundance of *Metallosphaera*-like clones (421 total) expressed as a percent of total archaeal clones (883) across different sites.

Discussion

Two primary niche environments for Sulfolobales have been proposed, including aerobic geothermal springs and acidic soils usually exhibiting ferric Fe deposits, and

anaerobic habitats containing sulfide minerals (37). Strain MK1 exhibits growth and morphological characteristics that are generally similar to other members of the Sulfolobales; however, strain MK1 grows using Fe^{II} sorbed to ferrihydrite as a sole electron donor, in the absence of sulfide minerals, dissolved sulfide or elemental S. No measurable growth was observed on ferrous sulfate which may be explained by abiotic oxidation rates that out-compete biological oxidation at the relatively high pH values of the cultures (pH 2.5 to 3.0). Ferrous oxidation rates may slow significantly when Fe^{II} is sorbed to ferrihydrite allowing for growth of strain MK1 on this species. Although several *Sulfolobus*-like 16S rRNA gene sequences were observed in Fe^{III} mats of YNP acidic springs, sequences related to *Metallosphaera* str. MK1 were considerably more abundant. Based on the distribution patterns of MK1-like 16S rRNA gene sequences, as well as the characteristics of strain MK1, these organisms prefer Fe^{II} over reduced forms of S, and represent an important taxon responsible for Fe^{II} chemolithotrophy and biomineralization of Fe^{III} solid phases in geothermal systems of YNP (12, 38). This is an important finding because numerous low pH, high ferrous Fe geothermal habitats exist in YNP and elsewhere, which do not contain sufficient sulfide or elemental S to support robust growth of S-oxidizing Sulfolobales. Consequently, these environments constitute a separate niche for members of the Sulfolobales capable of Fe^{II} oxidization.

Gibbs free energy values (ΔG_{rxn}) calculated based on actual spring conditions reveal that the oxidation reactions of Fe^{2+} to form aqueous Fe^{3+} or Fe^{III} solid phases are exergonic in these systems ($\Delta G_{rxn} \sim$ -30 to -40 kJ mole electron^{-1}) when O_2 serves as the electron acceptor (1, 15). The rate of abiotic Fe^{2+} oxidation is highly pH dependent and

the abiotic rate is considerably slow at pH values < 4 (26, 35). Consequently, the deposition of Fe^{III} secondary minerals in high flow-rate environments (velocities range from 0.05-0.5 m/second) reflects the importance of microbial oxidation in mineral deposition (14, 24). An important geochemical attribute of these habitats is the combination of high dissolved ferrous Fe and the presence of Fe^{III} solid phases, such as Fe^{III} oxyhydroxides as well as jarosite (15). The interesting finding that strain MK1 grows robustly using Fe^{II} sorbed to ferrihydrite as an energy source is consistent with the geochemical conditions in these habitats.

During the course of the current study, we have inventoried a fairly extensive number of acidic springs in YNP including different Fe^{III}-oxide mats with variable geochemistry, and conclude that organisms highly related to *Metallosphaera* sp. strain MK1 are found primarily in low pH (2-4), high ferrous-Fe springs associated with the biomineralization of Fe^{III} solid phases across temperature ranges of 55-85 °C. Highly related organisms to strain MK1 were especially prevalent in aerobic outflow channel positions of the acid-sulfate (AS) systems at Rainbow Springs (RS1, RS2) and at Joseph's Coat Springs (JC2), and are important members of the archaeal community in the acid-sulfate-chloride (ASC) springs of Norris Geyser Basin (Figure 3.7). Conversely, strain MK1-like 16S rRNA sequences were not commonly observed in locations where dissolved sulfide (DS) concentrations were greater than approximately 10 μM or where dissolved oxygen concentrations are near or below detection (1-3 μM) (15, 28). In several of the acidic springs studied (e.g. NGB-BE, NGB-DW, RS2), concentrations of DS are significant at the point of discharge (10-150 μM) and *Metallosphaera*-like sequences are

generally not observed until DS values have dropped to ~ 5-10 μM, where Fe^{III}-oxide mats begin to form.

Future progress towards the characterization of regulatory mechanisms of Fe versus S oxidation in strain MK1 and other novel Sulfolobales will assist in developing more definitive linkages between habitat parameters (i.e. temperature, elemental S, Fe^{III} oxides, dissolved O_2) and the distribution of *Metallosphaera*-like organisms in geothermal habitats. Understanding microbial mechanisms of sulfide mineral oxidation under thermophilic conditions has important implications for bioleaching, metal recovery (20, 27, 30, 32), as well as coal desulfurization (6, 8, 33). Strain MK1 oxidizes pyrite, pyrite-enriched mine tailings, and other sulfide minerals (Fig. 3.4, Table 3.2) at significant rates under batch culture conditions. Given its broad temperature range from ~ 50-80 ^{o}C, strain MK1 and or closely related organisms from YNP may be suitable candidates for enhanced bioleaching under acidic, thermophilic conditions.

Acknowledgements

This work was supported by the National Science Foundation Microbial Observatory Program (MCB-0132022), the National Aeronautic and Space Administration (NASA) via funds provided to the Thermal Biology Institute at Montana State University (Project Numbers NAG5-8807, NNG04GR46G), and the Montana Agricultural Experiment Station (Project 911398). The authors appreciate assistance from S. Jennings for providing the pyrite-enriched mine tailing sample, Y. Odake and S. Brumfield for transmission electron microscopy, and from C. Hendrix and T. Olliff for permitting this work in Yellowstone National Park (Permit YELL-2007-SCI-5068).

References

1. Amend, J.P., and E.L. Shock. 2001. Energetics of overall metabolic reactions of thermophilic and hyperthermophilic Archaea and Bacteria. FEMS Microbiology Reviews. 25: 175-243.

2. Amann, R.I., B. Zarda, D.A. Stahl, and K.H. Schleifer. 1992. Identification of individual prokaryotic cells by using enzyme-labeled, rRNA-targeted oligonucleotide probes. Appl. Environ. Microbiol. 58: 3007-3011.

3. Baker, B.J. and J. F. Banfield. 2003. Microbial communities in acid mine drainage. FEMS Microbiology Ecology. 44: 139-152.

4. Behrens, S., C. Rühland, J. Inácio, H. Huber, A. Fonseca, I. Spencer-Martins, B. Fuchs, and R. Amann. 2003. In situ accessibility of small-subunit rRNA of members of the domains *Bacteria*, *Archaea*, and *Eucarya* to Cy3-labeled oligonucleotide probes. Appl. Environ. Microbiol. 69: 1748-1758.

5. Blake, R. and D.B Johnson. 2000. Phylogenetic and biochemical diversity among acidophilic bacteria that respire on iron. In: Environmental Microbe–Metal Interactions (Derek, L., Ed.). 53–78. ASM Press, Washington, DC.

6. Brierley, C. L., and J. A. Brierley. 1973. A chemoautotrophic and thermophilic microorganism isolated from an acid hot spring. Can. J. Microbiol. 19: 183–188.

7. Brock, T. D., K. M. Brock, R. T. Belly, and R. L. Weiss. 1972. Sulfolobus: a new genus of sulfur-oxidizing bacteria living at low pH and high temperature. Arch. Mikrobiol. 84: 54–68.

8. Clark, T. R., F. Baldi, and G. J. Olson. 1993. Coal depyritization by the thermophilic archaeon *Metallosphaera sedula*. Appl. Environ. Microbiol. 59: 2375–2379.

9. Fuchs T., H. Huber, K. Teiner, S. Burggraf, and K.O Stetter. 1995. Metallosphaera prunae, sp. nov., a novel metal-mobilizing, thermoacidophilic Archaeum, isolated from a uranium mine in Germany. Syst. Appl. Microbiol. 18: 560-566.

10. Hallberg K.B, D.B. Johnson. 2001. Biodiversity of acidophilic prokaryotes. Advances in Applied Microbiology. 49: 37-84.

11. Huber, G., C. Spinnler, A. Gambacorta, and K.O. Stetter. 1989. Metallosphaera sedula gen. nov. and sp. nov. represents a new genus of aerobic, metal-mobilizing, thermoacidophilic archaebacteria. Syst. Appl. Microbiol. 12: 38-47.

12. Huber G. and K.O. Stetter. 1991. Sulfolobus metallicus, sp. nov., a novel strictly chemolithoautotrophic thermophilic archaeal species of metal-mobilizers. Syst. Appl. Microbiol. 14: 372-378.

13. Hugenholtz P., C. Pitulle, K.L. Hershberger, and N.R. Pace. 1998. Novel division-level bacterial diversity in a Yellowstone hot spring. J Bacteriol. 180: 366-376.

14. Inskeep W.P., R.E. Macur, G. Harrison, B.C. Bostick, S. Fendorf. 2004. Biomineralization of As(V)-hydrous ferric oxyhydroxide in microbial mats of an acid-sulfate-chloride geothermal spring, Yellowstone National Park. Geochimica et Cosmochimica Acta. 68: 3141–3155.

15. Inskeep W.P., G.G. Ackerman, W.P. Taylor, M. Kozubal, S. Korf, and R.E. Macur. 2005. On the energetics of chemolithotrophy in nonequilibrium systems: case studies of geothermal springs in Yellowstone National Park. Geobiology. 3:297-320.

16. Jackson, C. R., H. W. Langner, J. Donahoe-Christiansen, W.P. Inskeep, and T.R. McDermott. 2001. Molecular analysis of microbial community structure in an arsenite-oxidizing acidic thermal spring. Environmental Microbiology. 3: 532-542.

17. Jan, R.L., J. Wu, S.M. Chaw, C.W. Tsai, and S.D. Tsen. 1999. A novel species of thermoacidophilic archaeon, *Sulfolobus yangmingensis* sp. nov. Int. J. Syst. Bacteriol. 49: 1809-1816.

18. Jennings, S. R. 1995. Geochemical characterization of sulfide mineral weathering for remediation of acid producing mine wastes. M.S. Thesis, Montana State University, Bozeman, MT. Publication No. 9502, 140 p.

19. Johnson, D.B., and K.B. Hallberg. 2003. The microbiology of acidic mine waters. Research in Microbiology .154: 466-73.

20. Kappler, U., L.I. Sly, and A.G. McEwan. 2005. Respiratory gene clusters of *Metallosphaera sedula* – differential expression and transcriptional organization. Microbiology. 151: 35-43.

21. Konhauser, K. O. 1998. Diversity of bacterial iron mineralization. Earth-Science Reviews. 43: 91-121.

22. Kurosawa, N., Y.H. Itoh, and T. Itoh. 2003. Reclassification of *Sulfolobus hakonensis* Takayanagi et al. 1996 as *Metallosphaera hakonensis* comb. nov. based on phylogenetic evidence and DNA G+C content. Int. J. Syst. Evol. Microbiol. 53: 1607–1608.

23. Langner, H.W., C.R. Jackson, T.R. McDermott, and W.P. Inskeep. 2001. Rapid oxidation of arsenite in a hot spring ecosystem, Yellowstone National Park. Environmental Science & Technology. 35: 3302-3309

24. Macur, R.E., H.W. Langner, B.D. Kocar, and W.P. Inskeep. 2004. Linking geochemical processes with microbial community analysis: successional dynamics in an arsenic-rich, acid-sulfate-chloride geothermal spring. Geobiology. 2: 163-177.

25. Miroshnichenko, M.L. 2004 Thermophilic microbial communities of deep-sea hydrothermal vents. Microbiology. 73: 1–13.

26. Nordstrom, D.K. and G. Southam. 1997. Geomicrobiology of sulfide mineral oxidation. Reviews in Mineralogy. 35: 361-390.

27. Olson, G.J., J.A. Brierley, C.L. Brierley. 2003. Bioleaching review part B: Applied Microbiology and Biotechnology. 63: 249 – 257.

28. Peeples, T.L. and R.M. Kelly. 1995. Bioenergetic response of the extreme thermoacidophile *Metallosphaera sedula* to thermal and nutritional stresses. Appl. Environ. Microbiol. 61: 2314-2321.

29. Prieur, D., M.A Voytek, C. Jeanthon and A.L. Reysenbach. 2001. Deep-Sea Thermophilic Prokaryotes. "Thermophiles: Biodiversity, Ecology and Evolution" pp 11-22. A-L. Reysenbach, M.A. Voytek and R. Mancinelli (eds.). Kluwer Academic/ Plenum Publishers. New York, NY.

30. Rawlings, D.E. 2002. Heavy metal mining using microbes. Annual Review of Microbiology. 56: 65-91.

31. Reysenbach, A.L., G.S. Wickham, and N.R. Pace. 1994. Phylogenetic analysis of the hyperthermophilic pink filament community in Octopus Spring, Yellowstone National Park. Appl. Environ. Microbiol. 60: 2113–2119.

32. Rohwerder, T., T. Gehrke, K. Kinzler, and W. Sand. 2003. Bioleaching review part A: progress in bioleaching: fundamentals and mechanisms of bacterial metal sulfide oxidation. Appl. Microbiol. Biotechnol. 63: 239-48.

33. Schippers, A., T. Rohwerder, and W. Sand. 1999. Intermediary sulfur compounds in pyrite oxidation: Implications for bioleaching and biodepyritization of coal. Appl. Microbiol. Biotechnology. 52: 104-110.

34. Schwertmann, U. and R.M. Cornell. 2000. Iron Oxides in the Laboratory. 2nd Ed., VCH, Weinheim, Germany. 105-107.

35. Singer, P.C., and M.W. Stumm. 1970. Acid mine drainage: The rate determining step. Science. 167: 1121–1123.

36. Spurr A. R. 1969. A low-viscosity epoxy resin embedding medium for electron microscopy. J. Ultrastructure Res. 26: 31–43.

37. Stetter, K. O. 1999. Extremophiles and their adaptation to hot environments. FEBS Lett. 452: 22–25.

38. Suzuki, T., Iwasaki, T. Uzawa, T. Hara, K. Nemoto, N. Kon, T. Ueki, T. Yamagishi, A. and T. Oshima. 2002. *Sulfolobus tokodaii* sp. nov. (f. Sulfolobus sp. strain 7), a new member of the genus Sulfolobus isolated from Beppu Hot Springs, Japan. Extremophiles. 6: 39-44.

39. Takayanagi, S., H. Kawasaki, K. Sugimori, T. Yamada, A. Sugai, T. Ito, K. Yamasato, and M. Shioda. 1996. *Sulfolobus hakonensis* sp. nov., a novel species of acidothermophilic archaeon Int. J. Syst. Bacteroil. 46: 377–382.

40. To, T.B., D.K. Nordstrom, K.M. Cunningham, J.W. Ball, R.B. McClesky. 1999. New method for the direct determination of dissolved Fe(III) concentration in acid mine waters. Environmental Science and Technology. 33: 807-813.

41. Trevisanato, S. I., N. Larsen, A. H. Segerer, K. O. Stetter, and R. A. Garrett. 1996. Phylogenetic analysis of the archaeal order of Sulfolobales based on sequences of 23S rRNA genes and 16S/23S rDNA spacers. Syst. Appl. Microbiol. 19: 61–65.

CHAPTER 4

TERMINAL OXIDASE DIVERSITY AND FUNCTION IN *METALLOSPHAERA YELLOWSTONII:* GENE EXPRESSION AND PROTEIN MODELING SUGGEST MECHANISMS OF FE(II) OXIDATION IN THE SULFOLOBALES

Abstract

Metallosphaera yellowstonii strain MK1 is a thermoacidophilic, chemotrophic crenarchaea isolated from Yellowstone National Park (YNP) and is capable of autotrophic growth on Fe(II), elemental S or pyrite (FeS_2). Analysis of gene sequence from a draft genome of *M. yellowstonii* strain MK1 reveals seven different copies of heme copper oxidases (subunit I) in a total of five different terminal oxidase complexes including *sox*ABC, *dox*BCEF, the *sox*M supercomplex, the *fox*A-J gene cluster, and a novel hypothetical two-protein *dox*B-like (*dox*B-2) polyferredoxin complex. Other genes with possible roles in S and or Fe cycling found in *M. yellowstonii* include a thiosulfate oxidase (*tqo*AB), a sulfite oxidase (*sox*), a *cbs*A cytochrome $b_{558/566}$, several sulfocyanin-like blue-copper proteins and a novel gene sequence coding for a putative multi-copper oxidase (Mco). Results from gene expression studies including reverse transciptase(RT) quantitative(q)PCR of cultures grown autotrophically on either elemental S, pyrite or Fe(II) show that the *fox* gene cluster and *mco* are highly expressed under conditions where Fe(II) is an electron donor. Results from gene expression studies under field conditions, as well as analysis of metagenome sequences from corresponding Fe(III) microbial mats confirm the importance of *fox* genes (e.g. *fox*A, *fox*C) and *mco* as highly

important under Fe(II)-oxidizing conditions. Protein sequence analysis of *fox*C indicates a novel lysine-lysine or lysine-arginine heme *b* binding domain and is likely the cytochrome component of a heterodimer complex with *fox*G as a ferredoxin subunit. Analysis of *mco* indicates that it encodes a novel multi-copper blue protein with two plastocyanin type I copper domains that may play a role in the transfer of electrons within the Fox protein complex. An understanding of metabolic pathways involved in aerobic iron and sulfur oxidation in the Sulfolobales has broad implications for understanding the evolution and niche diversification of these thermophiles as well as practical applications in fields such as bioleaching of trace metals from pyritic ores.

Introduction

Terminal oxidases, required for all aerobic organisms, perform the final step in electron transport, coupling the reduction of oxygen to proton translocation. There are two known types of terminal oxidases: the universal heme copper oxidases (HCOs) and the less ubiquitous, *bd*-type quinol oxidases found only in prokaryotes (García-Horsman et al., 1994; Pereira et al., 2004). Terminal oxidase complexes often contain three to four subunits in prokaryotes, compared to 13 in mitochondria. However, the HCO (Cu_B-Fe center) required for the reduction of O_2 is highly conserved across the three domains of life (consistently referred to as subunit I). Most prokaryotic terminal oxidase complexes also contain a conserved heme copper oxidase subunit II, responsible for binding and oxidation of either cytochrome *c* (with a Cu_A center) or ubiquinol (no Cu_A center), followed by electron transfer to subunit I (García-Horsman et al., 1994; Pereira et al.,

2004). Alternative mechanisms exist in some terminal oxidase complexes, such as the SoxM supercomplex, where a blue-copper sulfocyanin protein is thought to transfer electrons from subunit II to subunit I (Komorowski et al., 2001a and 2001b). Redox potential and oxygen affinity vary among different terminal oxidase complexes, consistent with the numerous electron donors used by aerobic microorganisms (García-Horsman et al., 1994; Pereira et al., 2004).

Reduced Fe and S species (e.g., Fe^{2+}, HS^-) are important electron donors in all natural environments, but are especially important in acid-mine drainage and hydrothermal systems (Hallberg and Johnson 2001; Baker and Banfield 2003; Johnson and Hallberg 2003). Metabolic pathways involved in the oxidation of ferrous iron (Fe(II)) have been studied extensively in the bacteria *Acidithiobacillus ferrooxidans* and *Leptospirillum ferrooxidans* (Blake and Johnson, 2000; Hallman et al., 1993; Appia-Ayme et al., 1999; Yarzábal et al., 2002a, 2002b; Rohwerder et al., 2003; Rawlings et al., 2005; Singer et al., 2008). The proposed pathway in *A. ferrooxidans* involves the blue-copper protein rusticyanin and various c-type cytochromes (Yarzábal et al., 2002a and 2002b). A novel c-type cytochrome c_{579} has been implicated in Fe(II)-oxidation in a *Leptospirillum*-dominated community at Iron Mountain, CA (Singer et al., 2008). In contrast, *Ferroplasma acidiphilum*, an archaeon present in the same community, is believed to oxidize Fe(II) directly via a small blue-copper protein (Dopson et al., 2005).

Several of the diverse HCOs from members of the order Sulfolobales (Phylum Crenarchaeota) have been characterized and include the aa_3 type quinol oxidase DoxBCEF complex from *Acidianus ambivalens* (Purshke et al., 1997), the aa_3 quinol

oxidase SoxABC complex, and the SoxM supercomplex of *Sulfolobus* spp. (Lübben et al., 1992; 1994a; 1994b; Komorowski et al., 2002). More recently, a novel terminal oxidase complex (*fox*A-J gene cluster) has been found in *S. metallicus*, S. *tokodaii and Metallosphaera sedula* and this complex has been associated with the oxidation of Fe(II) (Bathe and Norris, 2007; Auernik and Kelly, 2008). Several genes in the *fox* cluster code for hypothetical proteins whose role in electron transport via Fe(II) is unknown at the current time. In fact, only *fox*A and *fox*B are clearly defined as similar to subunit I and subunit II found in other terminal oxidase complexes, respectively. Previous gene expression studies in *M. sedula* and *S. metallicus* have shown up-expression of genes within the *fox* cluster as well as the *cbs*AB-*sox*LN cytochrome *ba* complex in cultures grown on Fe(II) or pyrite relative to S^0 (Kappler et al., 2005; Bathe and Norris, 2007; Auernik and Kelly, 2008; Bandeiras et al., 2009). However, no studies have been conducted in *Metallosphaera*-like organisms found in acidic geothermal habitats of Yellowstone National Park (YNP), where the oxidation of Fe(II) results in the deposition of numerous different types of Fe(III)-oxyhydroxide and or jarositic microbial mats, depending on other geochemical conditions (Inskeep et al., 2004; Kozubal et al., 2008).

Prior 16S rRNA gene surveys (Macur et al., 2004; Inskeep et al. 2005; Kozubal et al., 2008) and recent metagenome sequence (Inskeep et al., 2010) indicate that organisms highly similar (> 99 % identity to the 16S rRNA gene) to *Metallosphaera yellowstonii* (strain MK1) are consistently one of the dominant community members in thermophilic Fe(II)-oxidizing microbial mats of YNP. *Metallosphaera yellowstonii* is ideal for studying relationships among different terminal oxidases and electron donors

because the organism grows autotrophically on Fe(II), elemental S, or complex organic C (e.g., yeast extract) as a sole C and energy source (Kozubal et al., 2010). Moreover, the role of these Fe(II)-oxidizing chemoautotrophs in contemporary geothermal habitats provides clues regarding the importance of oxygen in the metabolism and evolutionary history of the Sulfolobales. The specific objectives of the current study were to (i) characterize the terminal oxidase genes found in draft genome sequence of *Metallosphaera yellowstonii* strain MK1 and in acidic, thermophilic Fe(III)-oxyhydroxide microbial mats of YNP, (ii) quantify the expression of terminal oxidase genes in field samples as well as cultures grown autotrophically on Fe(II), pyrite, or elemental S, , and heterotrophically on yeast extract (YE), and (iii) evaluate the potential function of genes within the *fox* cluster using bioinformatic approaches (e.g. protein modeling), with special focus on the putative blue-copper and cytochrome *b* proteins that appear to play an important role in the oxidation of Fe(II).

Material and Methods

DNA Extraction for Genomic Sequencing

Metallosphaera yellowstonii strain MK1 (Kozubal et al., 2008, 2010) was cultivated at 70 ºC in 2 L of growth medium , amended with 2% pyrite, 0.005% yeast extract and 15 mg/L vancomycin. Total DNA was extracted using the FastDNA SPIN Kit for Soil (Q-Biogene, Irvine, CA). Purity of the DNA sent for genomic sequencing was verified by DGGE with universal 931F and 1392GC primers and by sequencing 36 clones of PCR product amplified with near full length archaeal-specific primers as

described by Kozubal et al. (2008). DNA concentration and integrity was determined using gel electrophoresis, prior to construction of small insert libraries (2 kb), subsequent cloning and capillary sequencing (SymBio Corporation, Menlo Park, CA). Approximately 19 Mb of total sequence (~ 500 bp per sequence read) was assembled into 174 contigs larger than 5 kb, with an average coverage of 4.8X.

Genome Searches and Primer Design

Previously identified Fe(II) and S oxidation genes within the Sulfolobales were used as queries to search translated open reading frames (ORFs) from the draft sequence of *Metallosphaera yellowstonii* and included: the terminal oxidase complexes (*sox*ABCD, *sox*M, *dox*BCEF and *fox*A-J), blue copper proteins (Msed_0323 and Msed_1206), a rieske cytochrome *b* fusion protein (*rcbf*; Msed_1191), the *cbs*A-*sox*LN operons, thiosulfate oxidase (*tqo*AB), sulfite oxidase (*sox*; Msed_0362), sulfide quinone oxidoreductase (*sqr;* SSO2261), sulfur oxidoreductase (*sor*), and cytochromes thought to be important in the oxidation of Fe(II) in *A. ferrooxidans* and *Leptospirillum* group II. Deduced amino acid sequences of the subunit I HCOs (and additional selected proteins) were aligned, and used to develop Q-PCR primers (Supplemental Table 1), including those used for qPCR and for electrophoresis-based qualitative expression analysis. All qPCR primer pairs were designed to amplify approximately 200 bp fragments with melting temperatures of 58 °C. The primers were analyzed using the IDT SciTools OligoAnalyzer 3.0 (Integrated DNA Technologies, Coralville, IA) for hairpins, dimers, and melting temperature, and were tested on DNA from a *Metallosphaera* sp. strain MK1

culture and an HFO mat sample from an ASC geothermal spring, as well as negative controls.

Collection of Environmental Samples from YNP

Four acidic Fe-mat samples ranging from 54-72 ºC (ASC springs in the Norris Geyser Basin region of YNP) previously found to contain significant populations of *M. yellowstonii* str. MK1 (Inskeep et al., 2004; Kozubal et al., 2008), were chosen for analysis of mRNA:OSPA *(One Hundred Spring Plain Spring* 72 °C), OSPB (62 °C), BED *(Beowulf Spring,* 62 °C))and GAPB (*Gap Spring* (84 °C). Approximately 10 grams of Fe-oxide microbial mat were removed from the primary flow channel with heat sterilized spatulas and stored immediately in nuclease-free Falcon tubes on dry ice. RNA extraction took place within 8 hours of sampling. A negative control sample from a 75 °C sulfur deposition zone at the source of *Beowulf Spring (*previously shown not to contain 16S rRNA sequences related to *M. yellowstonii* strain MK1) did not result in amplification with primers used in this study.

Microorganism Growth Conditions

Pure cultures of *M. yellowstonii* strain MK1were maintained at 65 ºC in synthetic growth medium as described by Kozubal et al. (2008) using a pH of 3.0, adjusted with H_2SO_4. The cultures were grown in 20 ml serum bottles containing 15 ml synthetic medium with 0.5g (< 0.15 mm size fraction) of one of the following substrates, sterilized prior to use: Fe(II)-adsorbed to ferrihydrite, elemental S^0, and research grade pyrite (FeS_2, Wards Scientific) (Kozubal et al., 2008). Cultures of MK1 were also grown with

0.2% yeast extract (YE) with no mineral substrates. Cultures with no YE were grown autotrophically using a headspace composition of 25% O_2, 50% CO_2 and 25 % air.

RNA Extraction and DNase Treatment

Samples for RNA extraction were prepared from the > 0.2 µm fraction of cultures harvested at mid-log phase growth or from 0.5 g of Fe-oxide microbial mat sampled from YNP. All samples were washed with pH 3.0 rnase/dnase free water prior to RNA extraction. Total RNA was extracted with the FastRNA® Pro Blue Kit (Cat.# 6025-050; MP Biomedicals, Irvine CA) and treated with RQ1 RNase free DNase (Cat.# M6101; Promega, Madison WI) for one hour after extraction. Extracts were determined to be DNA-free using gel electrophoresis of PCR products with and without cDNA extension by reverse transcriptase for each primer used to obtain quantitative estimates of gene expression (Supplemental Table 1). Concentrations and purity of RNA were verified with a NanoDrop® ND-1000 spectrophotometer (NanoDrop Technologies, Wilmington DE) and by gel electrophoresis.

RT-PCR and Quantitative PCR [qPCR])

Reverse transcriptase PCR (RT-PCR) was performed with the Promega Access RT-PCR system (Cat.# A1260; Promega, Madison WI). RT-PCR was carried out with three controls for cultured cells: (1) RNA without reverse transcriptase to verify only RNA as the template, (2) nuclease free water as a negative control template, and (3) genomic DNA from *M. yellowstonii* strain MK1 as a positive control for amplification. For environmental samples, a negative control was used from the source of *Beowulf*

Spring, which does not contain sequences related to strain MK1. RNasin® Ribonuclease Inhibitor (Cat.# N2111; Promega, Madison WI) was added (8 µL) to 400 µL Promega GoTaq® master mix and 8 µL reverse transcriptase enzyme. Template RNA from specific culture treatments or from environmental samples was added to each master mix) to a final concentration of approximately 0.1 ng/µL RNA. Eight sets (one set for each culture treatment and spring site) of eight PCR tubes were prepared with 25 µmol of the RT-quant PCR primer pairs (one pair per tube) and 50 µL of master mix was added to each tube. The process was repeated with master mix containing no reverse transcriptase. Thermal cycler protocol was 45 ºC for 45 min, 94 ºC for 2 min; 35 cycles of 94 ºC (30 s) melting, 56 ºC (45 s) annealing, and 72 ºC (25 s) extension; and a final 5 min extension period at 72 ºC. qPCR analysis was performed with the Rotor-Gene RG-3000 (Corbett Life Science, Sydney Australia), and expression results normalized relative to the 16S rRNA gene according to the method described by Kappler et al. (2005). qPCR of total 16S rRNA was performed according to Kozubal et al. (2008) to verify that ribosome copies did not vary significantly across different culture treatments. Melt curve analysis was used to verify integrity of the qPCR product and to compare melting temperatures among pure cultures and spring sites.

Genome Sequence Analysis

Assembled contigs of *M. yellowstonii* were compared to the *M. sedula* genome for similarity of sequence content and synteny. Sequence gaps were filled by primer walking where possible. Additional protein sequences for tree construction were obtained from the GenBank database by conserved domain sequence searches across all taxonomical

lineages. Protein sequence alignments were performed using ClustalX (version 1.81); misalignments or gaps were edited with Se-Al v2.0a11. Distance analysis was performed using the Jukes and Cantor correction, followed by phylogenetic tree construction using the maximum likelihood method in PAUP*4.0 (Sinauer Associates, Sunderland, MA) with 1000 boot strap replicates. Several bioinformatic programs were used to verify putative functions of genes found in this study. Protein BLAST (blastp and PHI-BLAST) and conserved domain searches were used to identify obvious homology with characterized sequences in the NCBI databases. Multiple protein sequence analysis tools were used to determine structural relatives for less tractable sequences. These tools included the Pfam database, SMART, HHpred, and the BioInfoBank Metaserver. Structurally related sequences found with HHpred or the BioInfoBank metaserver were aligned with ClustalX and the DeepView (v. 3.7) and models were created with the SWISS-MODEL server (Arnold et al., 2006). Model quality was tested with ProQ (Wallner et al., 2003; Stockholm Bioinformatics Center), ProSA (Wiederstein and Sippl, 2007), MolProbity (Davis et al., 2007), and Verify3d (Lüthy et al., 1992). The protein and nucleotide sequences used in this study are available at the JGI IMG/M website.

Results

Terminal Oxidase Genes of *Metallosphaera yellowstonii* strain MK1

Genome sequence from *M. yellowstonii* strain MK1 contains coding regions for five putative terminal oxidase complexes (Figure 4.1): *sox*ABC*, dox*BCE, the *sox*M supercomplex, the *fox*A-J gene cluster, and a separate *dox*B-like subunit I transcribed as a

bicistronic mRNA with a polyferredoxin-like subunit (referred to as *dox*B-2/polyferredoxin in this study). The draft genome of *M. yellowstonii* strain MK1 contains three *fox*A heme Cu oxidases (subunit I)); two copies were found within separate *fox*A-J gene clusters (*fox*A-1, *fox*A-2), while a third (*fox*A-3) was associated with an insertion sequence elsewhere in the genome.

The gene arrangement of the *sox* and *dox* terminal oxidase complexes is conserved between *M. yellowstonii* str. MK1 and *M. sedula* DSM5348 (Figure 4.2). However, the *fox*A-J gene cluster exhibits more variation in both gene order and content between the two organisms. In *M. yellowstonii* strain MK1, *fox* genes are transcribed as single operons, except for *fox*GH and *fox*EF, which are bicistronic. Both *M. sedula* and *M. yellowstonii* have additional hypothetical proteins within the *fox*A-J gene cluster (*M. sedula* genes: msed0471, 0472, 0476, 0479, and 0482) not found in *S. metallicus* or *S. tokodaii* (Bathe and Norris, 2007). The ATPase-like sequence (msed0470) is fused to the homologue of msed0471 in *M. yellowstonii* and the *fox*GH and *fox*C/ msed 0479 genes are coded on opposite strands. In addition to a lack of synteny across the *fox* gene clusters in the two *Metallosphaera* organisms, the draft genome of *M. yellowstonii* contains a high frequency of transposable elements, similar to transposases from *Sulfolobus solfataricus* (She et al., 2001).

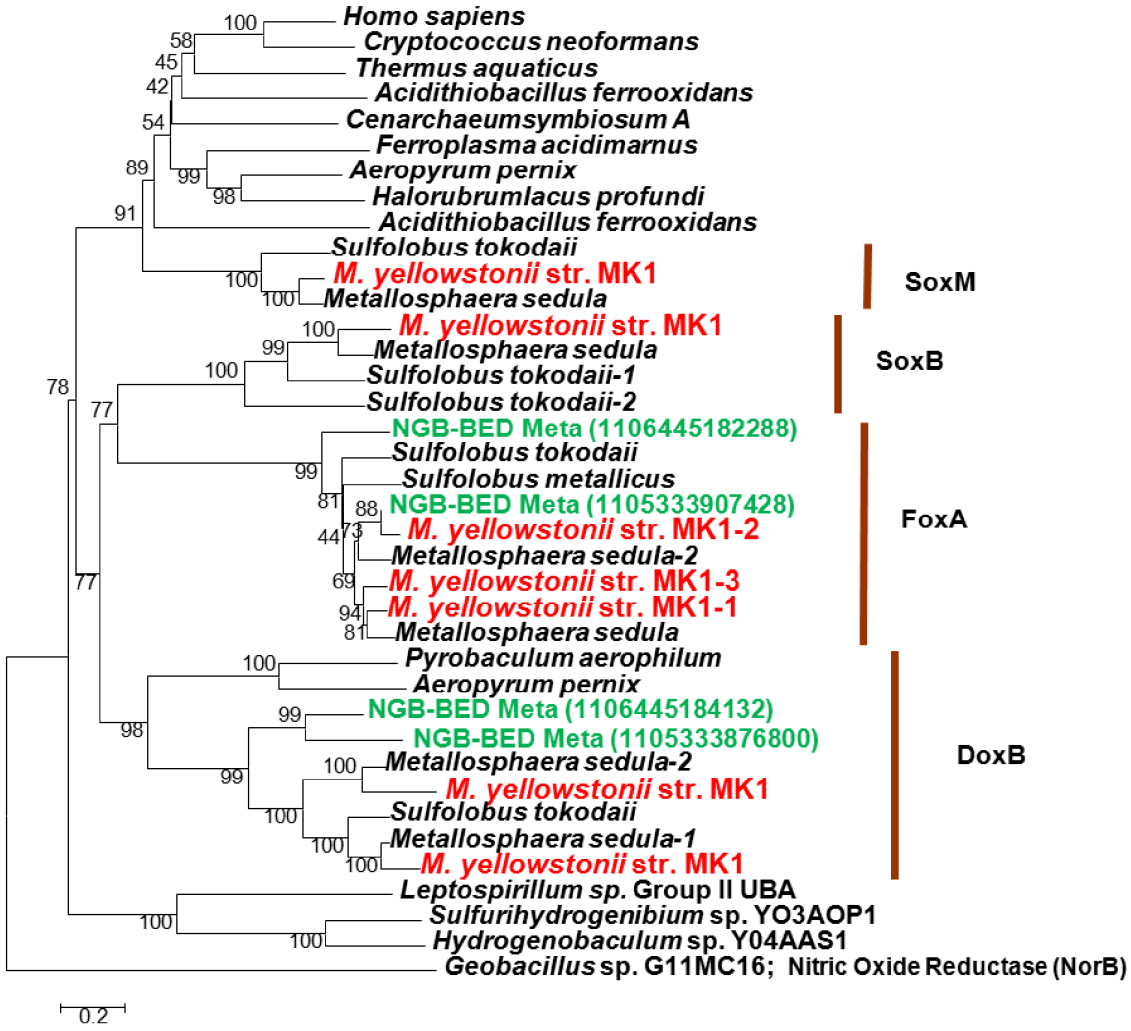

Figure 4.1 Protein tree of heme copper oxidases (subunit I) from all three domains of life. The extensive diversity of heme copper oxidases within the archaeal Order Sulfolobales and *Metallosphaera yellowstonii* strain MK1 includes DoxB, DoxB-2, FoxA, SoxB, SoxM). Entries from metagenome sequence collected at Beowulf Spring (NGB-BED) are labelled in green. [The Neighbour Joining tree was constructed with 1000 boot straps; nitric oxide reductase (NorB) from *Geobacillus* sp. G11MC16 was used as an outgroup]

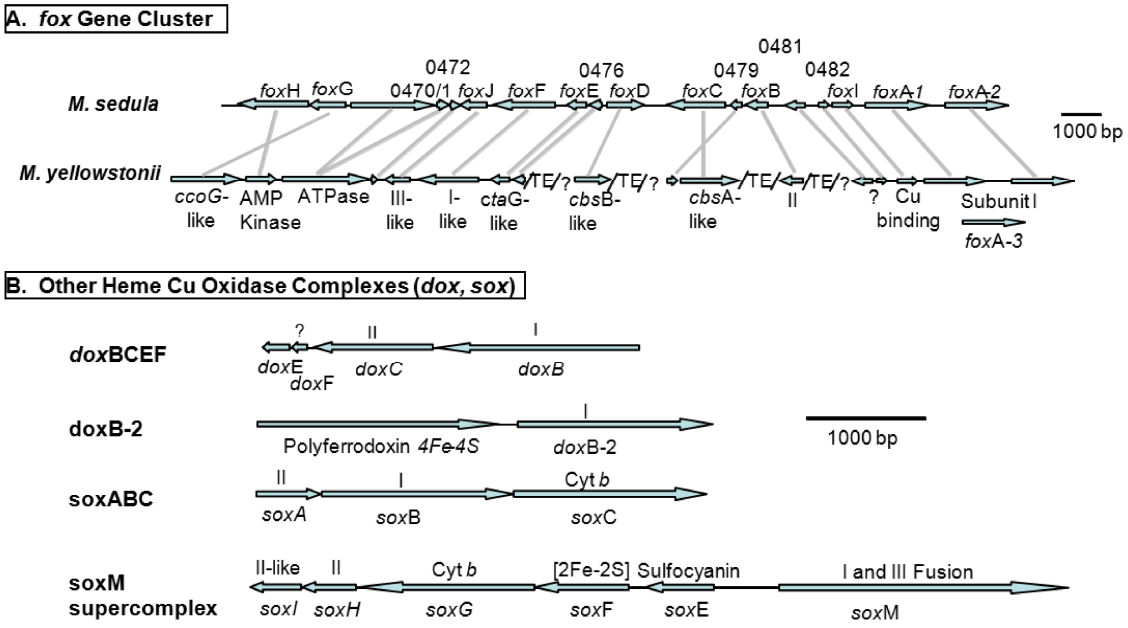

Figure 4.2. Gene arrangement of terminal oxidase (TO) complexes in *Metallosphaera yellowstonii* (strain MK1). (A) Comparison of the *fox* TO complex between *M. yellowstonii* and *M. sedula* showing annotation in *M. sedula* (top) and corresponding genes found in *M. yellowstonii* with additional description provided in Table 1 (*fox*C is the subject of further analysis and discussion). (B) Gene arrangement of additional TO complexes (*dox*BCEF, *dox*B-2, *sox*ABC, and *sox*M supercomplex) present in *M. yellowstonii* (Note: gene arrangements are identical to *M. sedula*). ? = putative protein function cannot be inferred.

Other genes with a potential role in the oxidation of Fe(II) were noted in recent gene expression studies in *S. metallicus* and *M. sedula* (Bathe and Norris, 2007; Auernik et al., 2008), and are also present in *M. yellowstonii*. These include genes that appear to encode a blue multi-copper protein (Mco), a Rieske-cytochrome *b* fusion protein (Rcbf), a cytochrome $b_{558/566}$ (CbsA) and two sulfocyanin subunits (SoxE-1 and SoxE-2). Putative sulfur-oxidizing genes are also present in *M. yellowstonii* strain MK1 and include sequences similar to a thiosulfate oxidase complex *tqo*AB (also referred to as

*dox*AD in *A. ambivalens*; Kletzin et al., 2005), and a sulfite-oxidase molybdopterin (*sox*) located directly upstream of *tqo*AB.

Table 4.1. Domain and structural predictions of putative proteins encoded by genes in the *fox* heme copper oxidase gene clusters. All modeling a structural predictions were done as a part of this study.

Gene	Modeled	Closest Protein Domain	Additional Comments
*fox*A	yes	Heme Cu oxidase, subunit I	Three copies in genome of *M. yellowstonii*
*fox*B	yes	Cytochrome oxidase, subunit II	Contains conserved Cu-binding ligands for Cu_A center similar to SoxH
*fox*C	yes (also see Results)	Cytochrome $b_{558/566}$, subunit A (pairs with FoxD)	Candidate for Fe(II) oxidation (also see Results)
*fox*D	no	Cytochrome $b_{558/566}$, subunit B, (pairs with FoxC)	10 transmembrane helices
*fox*E	no	Cytochrome c oxidase assembly factor (CtaG)	6 transmembrane helices
*fox*F	no	Faint structural similarity to a cbb_3-type cytochrome oxidase, subunit I (also similar to FoxA)	12 transmembrane helices
*fox*G	yes	Structurally similar to the ccoG protein required for biogenesis of cbb_3-type cytochrome c oxidase	9 transmembrane helices; NapH ferredoxin fold
*fox*H	partial	Two cystathionine-beta-synthase (CBS) domains: bind adenosyl group ligands (e.g. AMP, ATP S-AdoMet)	Senses changes in AMP/ATP ratios.
*fox*I	yes	Cu-resistance protein, CopC	binds Cu
*fox*J	no	Cytochrome oxidase subunit III	7 transmembrane helices

Metagenome Sequence

Four highly-related heme Cu oxidases (subunit I) were found in metagenome sequence obtained from an acidic Fe-oxide microbial mat in Norris Geyser Basin (YNP) where *M. yellowstonii*- like organisms are known to represent approximately 25-30% of the archaeal community (Figure 1; Kozubal et al., 2008; Inskeep et al., 2010). Two of the environmental sequences are closely related to the *fox*A from strain MK1, while the other two cluster with the *M. yellowstonii dox*B subunit I. These results have now been corroborated from metagenome sequence collected from two additional thermophilic and acidic Fe microbial mats in Norris Geyser Basin (data not shown). Both sites contain *M. yellowstonii*-like *foxA* gene sequences highly similar to those entries shown for *Beowulf Spring* (Figure 1), indicating that the metabolic potential for encoding Fox cluster proteins is common in these habitat types. Importantly, *fox* genes were not found in numerous other geothermal sites where *M. yellowstonii*-like populations are absent and where Fe-oxidation is not a dominant process (Inskeep et al., 2010).

Gene expression Studies in Pure Culture and Environmental Samples

Expression assays (mRNA) of all HCO (subunit I's) were obtained for *M. yellowstonii* cultures grown autotrophically on Fe(II)-ferrihydrite, pyrite, and elemental S, and heterotrophically on YE (Figure 4.3). All gene transcripts (mRNA) were confirmed by sequencing. Results indicated that *fox*A, *fox*B, *fox*D, *fox*EF, *fox*J and *mco* genes were all highly up-expressed in cultures grown on Fe(II)-ferrihydrite or pyrite (Figure 3). Conversely, *dox*B- and *dox*B2-like transcripts were the dominant mRNA products observed in cells grown on elemental S. The *dox*B and *dox*B-2 subunit I were

also present in treatments with pyrite (as expected in the presence of reduced S), but are clearly absent in cultures grown on Fe(II). Transcripts of the *cbs*A gene were detected in all treatments except cultures grown on YE, consequently, the activity of this gene was independent of whether Fe(II) or reduced S served as the electron donor. Cells grown on YE exhibited increased expression of *fox*HG, which was not observed in cultures grown on Fe(II) or elemental S. Cells grown on YE also showed expression of *dox*-B2 and weaker products of *fox*A, *fox*C, and *cbs*A.

Priority gene transcripts identified in expression assays (above) were then quantified in additional experiments using reverse transcriptase-quantitative PCR (RT-qPCR) including the heme Cu oxidases (subunit I) (e.g., *sox*A, *sox*M, *dox*B, *fox*A, *dox*B-2), a putative Fe(II)- oxidizing cytochrome $b_{558/566}$ (*fox*C), a multi copper oxidase (*mco*), and a thiosulfate oxidase (*tqo*B). Results from RT-qPCR were consistent with expression assays and showed that *M. yellowstonii* strain MK1 produces nearly an order of magnitude higher levels of *fox*A, *foxC* and *mco* gene transcripts when grown on Fe(II) or pyrite compared to cells grown on elemental S or YE. Conversely, *dox*B transcripts were only observed in cells grown on elemental S or pyrite, whereas *dox*-B2 was up-expressed in cells grown on elemental S, (or pyrite), or YE (Figure 4.4A). Cultures grown on YE also showed weak to modest up-expression of *fox*A, *fox*C and *sox*M subunit I. The putative thiosulfate oxidase (*tqo*B) was up-expressed in cultures grown on elemental S (or pyrite), but not on Fe(II).

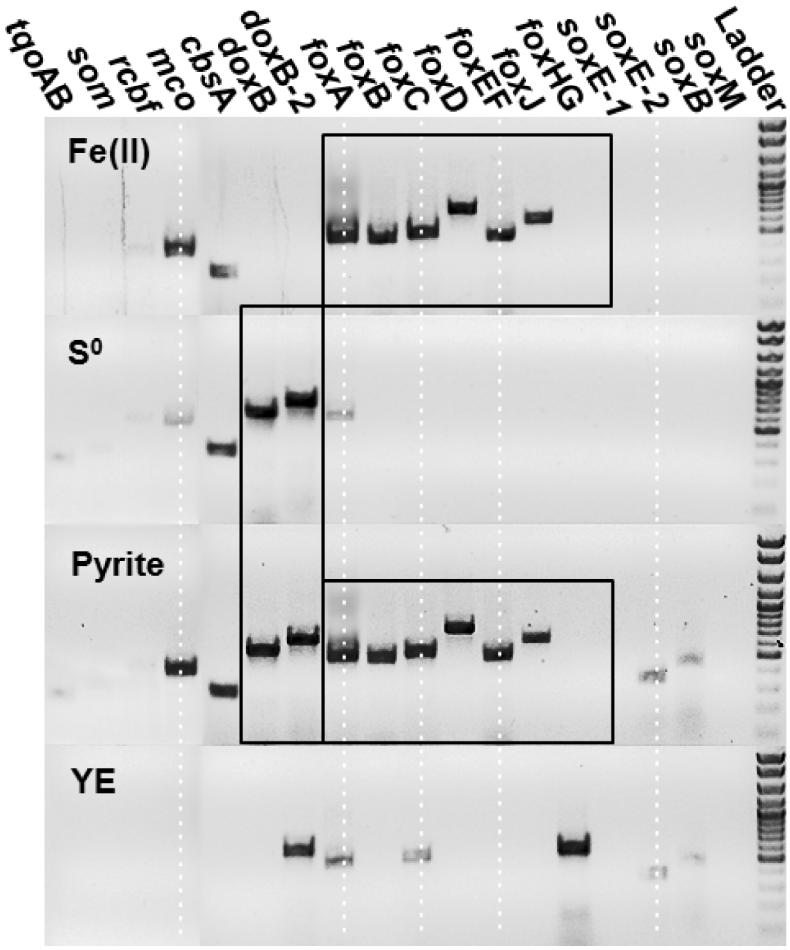

Figure 4.3. Agarose gels showing mRNA transcripts of target genes after cultivation of *Metallosphaera yellowstonii* on either Fe(II), pyrite, S^0, or YE, all at 70 ^oC and pH = 3.0.Gene expression assays of different heme Cu oxidases(subunit I), hypothetical fox genes, a multi copper oxidase (*mco*), thiosulfate oxidase (*tqo*), a rieske cytochrome b fusion protein (*rcbf*) and a sulfite oxidase molybterin (*som*).

Quantitative RT-PCR was also performed on samples from several acidic Fe-oxide mats in YNP, where organisms highly similar to *M. yellowstoni* strain MK1 (>98 % 16S rRNA gene nucleotide identity) are known to be important members of the microbial community (Kozubal et al., 2008; Inskeep et al., 2010). *fox*A was the only HCO (subunit I) expressed in four different Fe-oxide mat samples (Figure 4.4B), with the

exception of a considerably lower level of *sox*B in *Beowulf Spring* (BED). At this location, mRNA transcripts of *fox*A were found at concentrations nearly 10 times greater than *sox*B. mRNA transcripts of *fox*C were observed in all Fe mat samples (Figure 4.4B) at copy numbers roughly equivalent to *fox*A, which would be expected for a functional Fox complex. Moreover, with the exception of higher *fox*A levels in site BED, the other three sites yield similar ratios of *fox*A mRNA to *Metallosphaera yellowstonii*-like 16S rRNA.

Protein Sequence Analysis

Bioinformatic analysis was conducted on coding genes within the five HCO complexes to predict putative function using motif searches, structural analysis, and protein modeling. Of the genes in the *fox* gene cluster, *fox*C is an excellent candidate for protein sequence analysis (Table 4.1). This gene is highly up-expressed in all cultures and environmental samples where Fe(II)is used as an electron donor. The only close relatives (~ 25% amino acid identity) of this gene are cytochrome $b_{558/566}$ (*cbs*A) sequences found in several members of the Sulfolobales and *Caldivirga maquilingensis* (within the Thermoproteales). Three sequences related to *fox*C (>60% aa identity) were found in GenBank and belong to *M. sedula* (Msed_0478), *S. tokodaii* (ST2592/2593), and *S. metallicus* (accession ABG91824). The *fox*C in *S. tokodaii* is composed of two proteins (ST2592 and ST2593), which are fused in the other organisms. The *fox*C sequence from strain MK1 represents a fourth sequence and is related to Msed_0478 at 86% a.a. The *fox*C sequence present in strain MK1 has approximately 25% amino acid similarity to *cbs*A genes in the Sulfolobales.

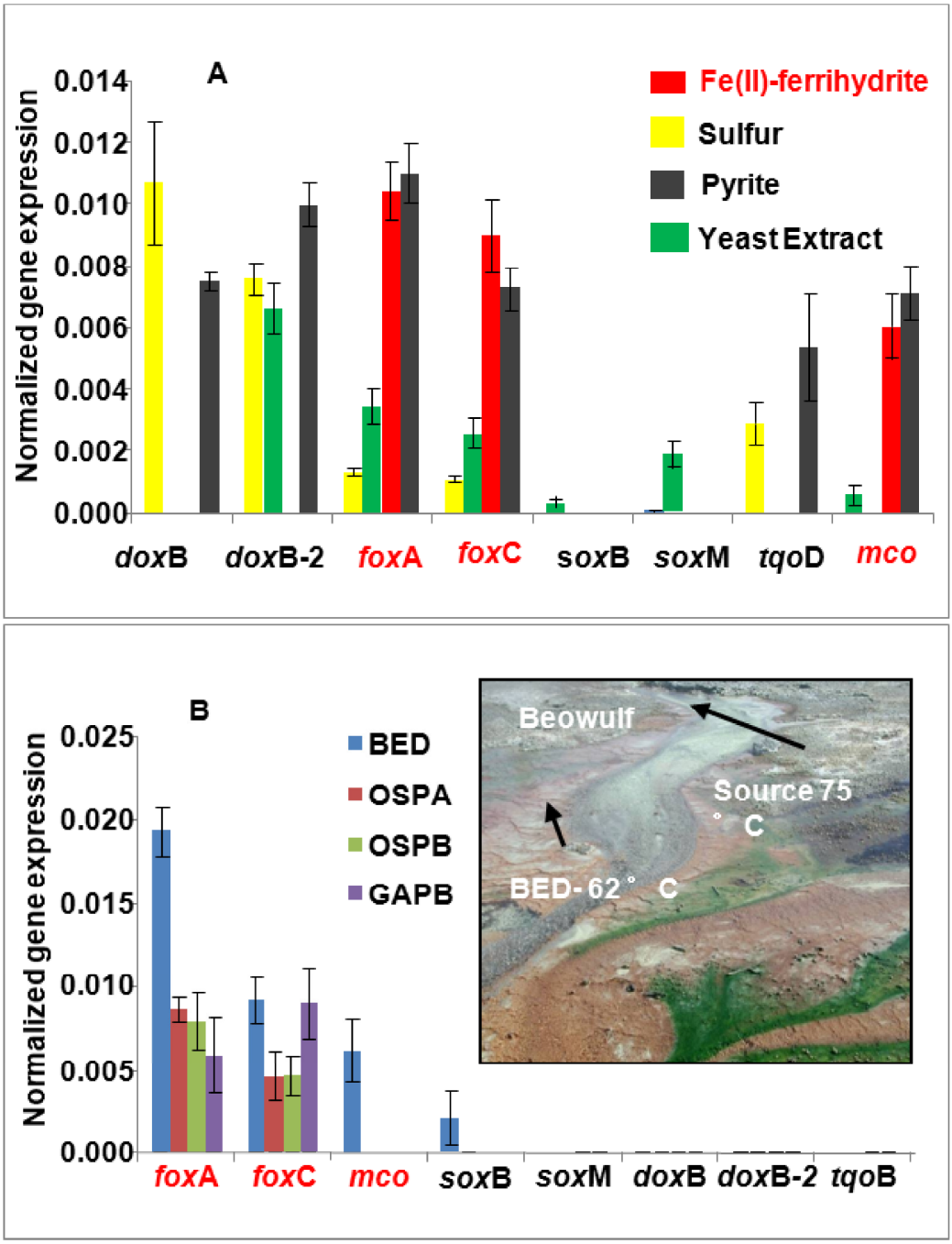

Figure 4.4. Normalized (relative to 16S rRNA) quantitative gene expression for heme copper oxidases (subunit I's include *dox*B, *dox*B-2, *fox*A, *sox*B, *sox*M,), *fox*C, *mco* and *tqo*B genes: A. *Metallosphaera yellowstonii* grown on Fe(II), pyrite, S^0, or YE, and B. Four high-temperature, acidic Fe(III) mats in Norris Geyser Basin (YNP). The inset shows a site photograph (*Beowulf Spring*) of one of three acidic geothermal systems sampled, indicating location of geothermal discharge and one of the sampling locations (BED) discussed herein.

Protein Modeling of FoxC

Sequence alignment of *fox*C and *cbs*A show highly conserved regions (Figure 4.5) at alignment positions 466-500 matching a heme *b* binding region of the gamma subunit of the ethylbenzene dehydrogenase (EBDH) crystal described in *Azoarcus* sp. EbN1 (Kniemeyer and Heider, 2001; Kloer et al., 2006). The EBDH heme *b* binding motif involves an unusual Lys-Met axial coordination. The conserved lysine in this coordination (K484 in our alignments) is shared in both *cbs*A and *fox*C (Figure 4.5). However, a conserved methionine is not found in either *fox*C or *cbs*A. Two candidate conserved amino acids for axial heme coordination with K484 are lysine and arginine (K103 or R289). Further evidence for this novel heme coordination was obtained by modeling the heme binding region with the EBDH crystal (Figure 4.6), which suggests the spatial location of heme *b* in relation to axial coordinating residues, arginines and phenylalanine. Conserved residues also include three tyrosines with possible roles in heme coordination.

Differences between *cbs*A and *fox*C are two conserved methionine residues 13 amino acids apart found in *cbs*A at alignment positions 293 and 307, which may be involved in coordination of an additional heme. The four *fox*C sequences contain multiple conserved residues in regards to amino acids necessary for heme, Fe or copper binding not found in *cbs*A. These include one cysteine at C132; four histidines at H96, H312, H360 and H465; and three methionines at M119, M312 and M313. All *cbs*A genes in the alignment contain a region high in threonine (T) at positions 507-535 indicating the possibility of a region of high glycosylation or a site for phosphorylation. This region is

not found in *fox*C. The threonine mol % composition is about 7% for *fox*C compared to about 11% for *cbs*A from strain MK1.

Sequence Analysis of Mco

The novel multi-blue Cu oxidase gene (*mco*) found in *M. yellowstonii* is also an excellent candidate for protein modeling. This gene was highly up-expressed (along with *fox*C and other *fox* cluster genes) under Fe(II)-oxidizing conditions. Bioinformatic analysis suggests that the hypothetical structure of Mco is related to eukaryal laccases and Fet3p proteins, which have been directly linked with the oxidation of Fe(II) (Quintanar et al., 2004; Stoj et al., 2006). The predicted protein (Mco) contains two active plastocyanin copper binding sites at sequence positions: His35, Cys93, His96, Met100 and His314, Cys373, His376, Met381 (Giri et al., 2004). However, the predicted Mco in *M. yellowstonii* strain MK1 does not have type II or III copper domains that are typical of eukaryal blue multi-copper proteins and are responsible for binding and reducing oxygen. The protein was modeled accurately around the plastocyanin domains, but a crystal structure is not yet available to allow accurate modeling of the remainder of the protein.

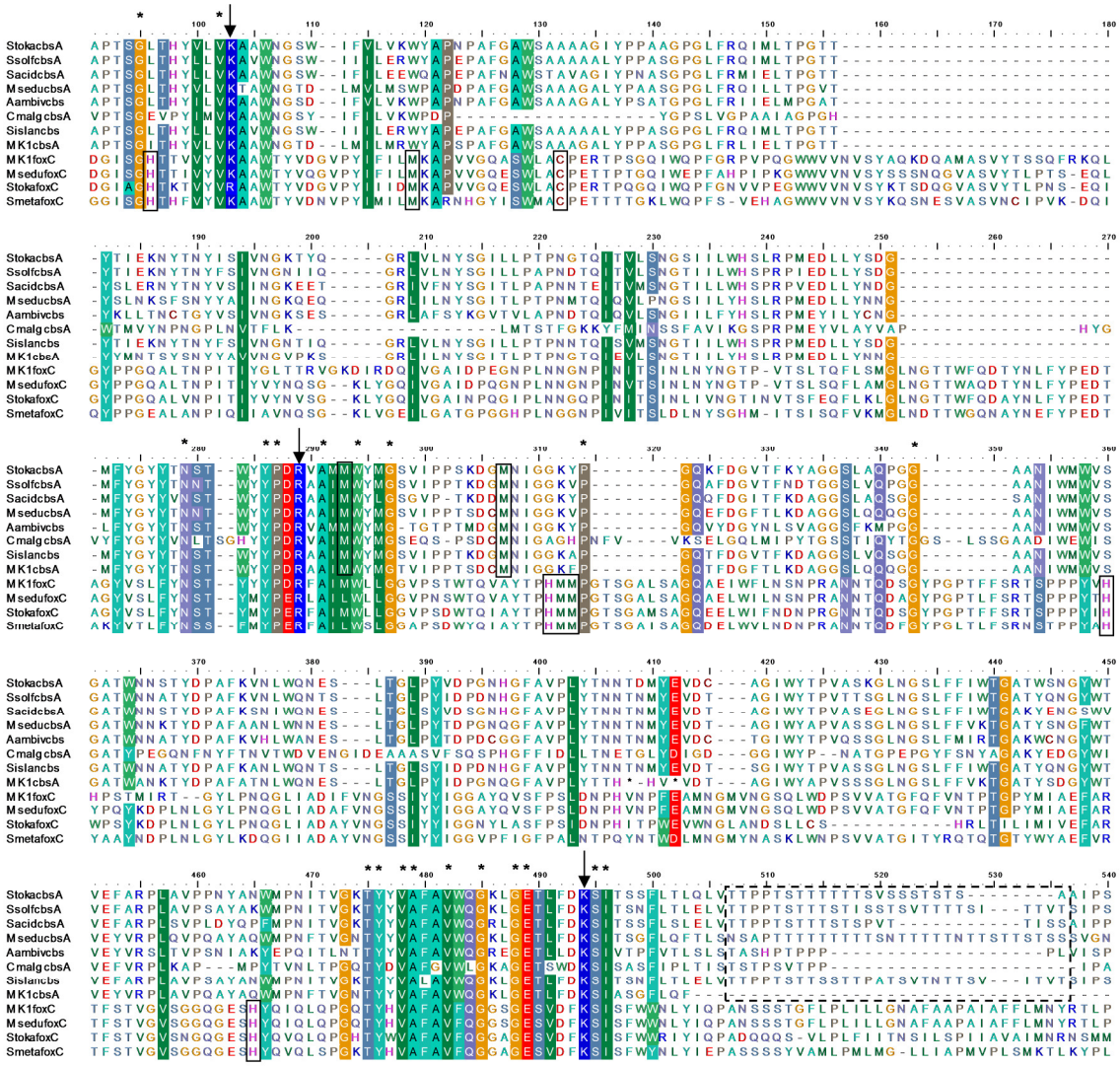

Figure 4.5. Protein alignment of FoxC and CbsA from Sulfolobales species and *Caldivirga maquilingensis* (CbsA only). Solid boxes indicate conserved histidine (H) and methionine (M) required for binding heme b and also illustrate a conserved cysteine (C) found only in the *fox*C sequences that may be used to bind Cu, Fe or heme b in a novel configuration. Conserved *fox*C sequences are at alignment positions C152, H97, M119, H311, H312, M313, H360 and H464. Arrows point to two conserved CbsA methionines that may be the heme b binding site. Dashed line is a region high in threonine (T), which is used in glycosylation and is not found in *fox*C.

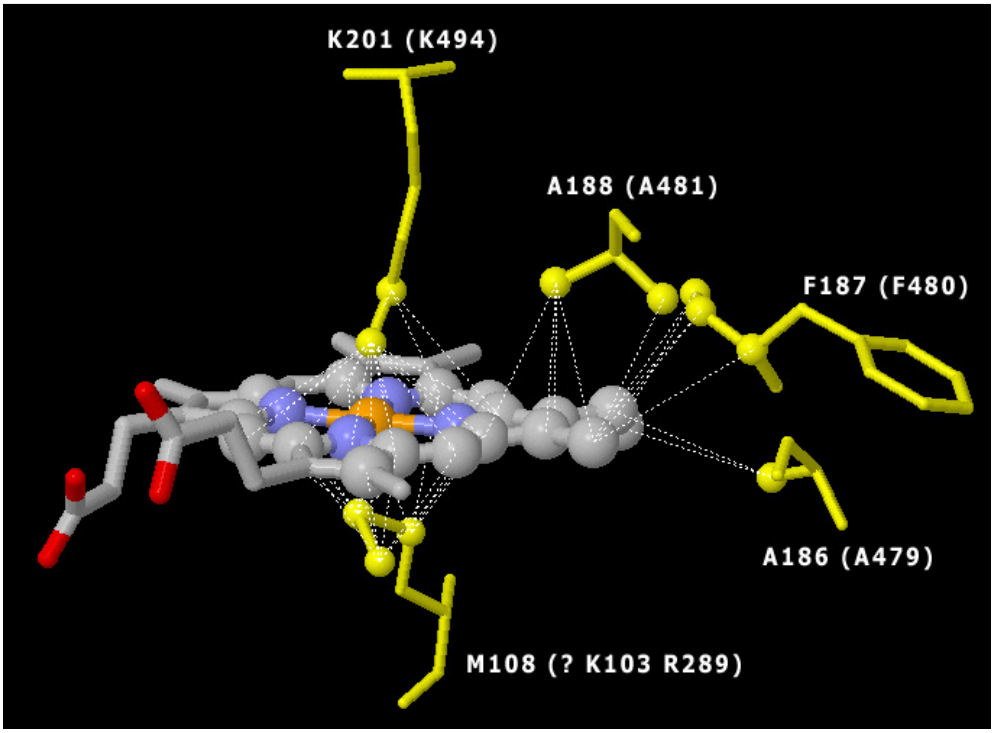

Figure 4.6. Model of FoxC putative heme *b* binding domain (orange = Fe, blue = N) indicating the spatial location of heme b relative to axial coordinating residues. The model shows lysine (K201) and methonine (M108) axial coordination for the EBDH crystal and corresponding lysine (K494) and arginine (R289) or lysine (K103) for the FoxC model. The model also shows conserved alanine (A188 and A186 for the EDBH crystal; A481 and A479 for FoxC) and phenylalanine (F187 for the EDBH crystal; F480 for FoxC).

Discussion

Metallosphaera yellowstonii strain MK1 contains up to 7 heme copper oxidase (subunit I) genes, which to our knowledge, is more than any other described microorganism. The putative FoxA (subunit I) appears to be involved in the final step in electron transfer from Fe(II) to O_2(aq). The fact that three copies of this gene are present in the draft genome sequence of strain MK1 further support its importance in the metabolism of this thermo-acidophile. The DoxBCEF complex was expressed only in treatments containing reduced S, and therefore appears to be important in sulfur

oxidation, as does the *doxB*-2/polyferredoxin bicistronic transcript, a novel putative terminal oxidase. This operon, known only in strain MK1 and *M. sedula,* does not contain a HCO subunit II, but rather a novel gene that encodes a putative polyferredoxin. Polyferredoxins have negative redox potentials ranging from -100 to -300 mV (Hedderich, 2004), which overlaps with values of half-reactions for the oxidation of reduced sulfur species. The potential utilization of a polyferrodoxin protein rather than a conventional heme copper cytochrome c or quinol oxidase subunit II (e.g., DoxC in the DoxBCEF complex) is a possibility, and this two protein complex would be one of the simplest electron transport systems in known aerobic organisms. *dox*B-2 is also expressed in cultures grown on YE and may, therefore, be involved in heterotrophic metabolism, along with the *sox*M supercomplex. The *fox*A, *dox*B, *dox*B-2 and *tqo*B are all expressed in pyrite grown cultures, consistent with the mechanism of pyrite dissolution by Fe(II)-oxidizing microorganisms involving the release of thiosulfate (Rohwerder et al., 2003).

Two *fox*A- and two *dox*B-like sequences were found in metagenome sequence obtained from *Beowulf Spring* (position BED), which corresponds to the location of original inoculum used to isolate strain MK1 (Kozubal et al., 2008; Inskeep et al., 2010). These sequences confirm that *M. yellowstonii* -like populations present *in situ* exhibit metabolic potential for the oxidation of both Fe(II) and elemental S. Although dominated by high-arsenic amorphous Fe-hydroxide (Inskeep et al., 2004), elemental S formed upstream in sulfidic zones can be transported into the Fe-mats and elemental S could be used as an electron donor in these environments (Inskeep et al., 2004; Macur et al., 2004; Inskeep et al., 2007). However, quantitative expression results show clearly that *fox* genes

(including *fox*A and *fox*C) are the dominant HCO genes expressed in allthe Fe(III)-microbial mats sampled. Although elemental S is abundant near the spring source (~ 70-75 ^{o}C in *Beowulf Spring*), *M. yellowstonii*-like organisms do not appear until theFe(III)-oxide depositional zone, which corresponds with oxygenation of the aqueous phase down gradient of discharge (Inskeep et al.. 2005).

The significant up-expression of *fox* cluster genes under Fe(II)-oxidizing conditions in the current, as well as previous studies (Kappler et al., 2005; Bathe and Norris, 2007; Auernik et al., 2008), suggests that the putative proteins encoded by these genes are excellent candidates for mediating electron transport from Fe(II) (Kappler et al., 2005). Prior work on the cytochrome spectra of thermo-acidophilic Sulfolobales cultivated on Fe(II) or pyrite had suggested that CbsA may be responsible for a unique absorption peak at 573 nm (Blake et al. 1993; Kappler et al., 2005). However, other findings on protein extracts indicate that this absorption peak is not due to CbsA (Hettman et al., 1998). Moreover, cbsA is found in species that are not capable of oxidizing Fe(II), and *cbs*A was equally expressed in the presence or absence of Fe(II) (Figure 4.3).

Instead, FoxC may be responsible for this unique spectral signature resulting from additional heme or metal binding site(s) not shared with CbsA (the predicted structure of FoxC contains four conserved histidines and a cysteine not found in CbsA).

Although His-His, His-Met or Met-Met axial coordination of heme *b* has been well-documented (Cowan 1993; Poulos 1996), Lys-Met coordination has been described for the EBDH gamma subunit, nitrate reductases, selenate reductase, chlorate reductases,

DMSO reductase heme b subunit from members of halophilic Euryarchaeota, and hypothetical cytochromes from *Sulfurihydrogenibium* spp. (Kniemeyer and Heider, 2001; Kloer et al., 2006). FoxC and CbsA align most closely to the EBDH gamma subunit (Figure 4.7 and 4.8), but alignment and protein modeling indicate a novel Lys-Lys or Lys-Arg coordination of heme *b* (Figure 4.6), which is a novel mechanism for axial coordination of heme with no obvious domain relatives found in Genbank. Lys-Met coordination imparts a more positive redox potential than other heme b proteins because lysine (and arginine) are less nucleophilic than methionine or histidine, which stabilizes the Fe(II) state. The Lys-Lys or Lys-Arg coordination proposed here would be expected to have an even higher Fe(II) stabilizing potential. In fact, previous studies have measured a very high redox potential for CbsA protein fractions at around +400 mV (Hettman et al., 1998). A higher redox potential would also be expected for FoxC to be effective in oxidizing Fe(II) at lower pH values (Amend and Shock, 2001). These properties appear to correspond quite well with the potentials necessary for an energetic electron transport from Fe(II) as an electron donor. Calculated redox potentials for the Fe(II)/Fe(III) half-reaction in these environments range between ~470 and 590 mV, depending on oxygen levels and pH (Inskeep et al., 2005).

CbsA has recently been implicated as the cytochrome b component of an archaeal bc_1 subunit III electron transport complex analogue (Bandeiras et al., 2009). Given the structural relatedness of components of FoxC and CbsA, it is expected that these proteins indeed play similar roles in electron transport. However, FoxC appears to be the heme b subunit of a larger protein complex with a function similar to the gamma subunit of the

EBDH heterodimer from *Azoarcus* sp. EbN1 (Kloer et al., 2006). The EBDH complex contains a molybpterin protein (alpha subunit) that contains a catalytic domain involved directly in the oxidation of ethylbenzene, and an Fe-S cluster (beta subunit) that is similar to ferredoxins. FoxG contains a ferredoxin fold (Table 4.1), and is therefore a candidate beta subunit for a hypothetical complex with FoxC. Finally, the predicted FoxH is similar to ATP/AMP sensor proteins and the putative FoxH may regulate expression of Fox components such as FoxC based on energy requirements.

The predicted blue multi-copper oxidase (Mco) of *M. yellowstonii* represents another novel protein and an interesting candidate for future study. Transcripts of *mco* were not observed in all HFO spring sites (only 1 of 4). Only two sequences similar to the *M. yellowstonii* strain MK1 *mco* were found in public databases including *M. sedula* and *Sulfolobus islandicus*. Interestingly, *mco*-like sequences were found in two of seven *Sulfolobus islandicus* strains, corresponding to those isolated from YNP (Reno et al., 2009). However, it is not known whether these *S. islandicus* strains are capable of oxidizing Fe(II). The translated 550 aa sequence contains two plastocyanin domains and models well with laccase proteins. Many type I domains in multi-copper oxidases are known to be non-specific in one electron transfers from a variety of chemical species including organic compounds (e.g. lignin phenolic groups), Fe(II) and Mn(II). However, a specific Fe(II) binding site has been found in Fet3P proteins, which show stronger ferrous iron oxidation activities than other blue multi-copper proteins (Quintanar et al., 2004; Stoj et al., 2006). Binding is believed to take place via a type I domain with two acidic residues (glutamic and aspartic acids). Whether Mco has a similar Fe(II) specific

binding region will require further protein analysis by either purification and specific activity assays or modeling with crystals not yet in the PDB dataset. The Mco in *M. yellowstonii* may represent an additional example of a fusion between two small blue copper proteins, believed to be an evolutionary step towards enzymes such as laccase in fungi and ceruloplasmin in higher mammals (Nakamura and Go, 2005). However, the putative Mco does not contain type II or III copper binding domains, which are typical of blue multi-copper proteins found in eukaryal species and are responsible for binding and reducing oxygen.

The predicted Mco may be involved in a variety of one electron transfers besides Fe(II) oxidation. Alternatively, Mco and or other blue copper proteins (SoxE-1 and SoxE-2) may function (like rusticyanin in *A. ferrooxidans*) as temporary storage for electrons (Rohwerder et al., 2003) or as an electron carrier between redox components of the Fox complex (i.e., FoxC, FoxA; Komorowski et al., 2001b). However, with the exception of the plastocyanin domains, Mco has little similarity to any known protein sequence and undoubtedly represents a novel family of multi-copper proteins that are quite different than small blue-copper proteins such as rusticyanin, which is only 187 aa in *A. ferrooxidans*.

The Sulfolobales do not have cytochromes *c*, which are important proteins for iron oxidation in *A. ferrooxidans* and *Leptospirillum* group II, and further supports the hypothesis that a different evolutionary path is responsible for iron oxidation in *M. yellowstonii*. Cytochromes *b* (i.e. FoxC and/or CbsA) and blue multi-copper (Mco) proteins likely have similar function to cytochrome *c* and rusticyanin for direct Fe(II)

oxidation and/or upstream/downstream electron transport. Expression and modeling results along with comparative genome analysis provides evidence to support a hypothetical model for iron oxidation in *M. yellowstonii* str. MK1 (Figure 5.4). This model assumes that FoxC is the direct oxidant of Fe(II) and that Mco acts much like a cytochrome *c* analog in transporting electrons either upstream for anabolic processes such as carbon fixation or downstream to the Fox HCO for energy gain and ATP synthesis.

The work presented in this study strongly suggests that the acidic Fe(II)-oxidizing niche realized by *M. yellowstonii*-like organisms in geothermal springs of YNP is linked directly with the metabolic capabilities imparted by putative proteins of the Fox complex, as well as possible roles for a unique multi-Cu oxidase containing two plastocyanin domains. These proteins are only observed (to date) in high-temperature Fe(II)-oxidizing habitats and are not present in other Sulfolobales habitats where S oxidation is the dominant electron donor (Inskeep et al., 2010). Consequently, these putative proteins are strong candidates for further study including verification of protein transcription in situ, as well as in vitro studies aimed at the isolation and characterization of these proteins.

Figure 4.7. Protein alignment of FoxC, CbsA and the cytochrome *b* subunit of the ethylbenzene dehrogenase from *Azoarcus* sp. EbN1. The conserved lysine (K484 from Figure 4.5 alignment) is indicated by an arrow. Stokoda- (*S. tokodaii*), Ssolf- (*S. solfataricus*), Sacido- (*S. acidocaldarius*), Msedul- (*M. sedula*), Silan- (*S. islandicus*), Apernnitra (*Aeropyrum pernix* nitrate reductase), MK1- (Strain MK1), EBDH (*Azoarcus* sp. EbN1 EBDH gamma subunit), Cmagu- (*C. maquilingensis*), Smetal- (*S. metallicus*).

Figure 4.8. Alignment of homologous sequences to the *Azoarcus* sp. EbN1 gamma EBDH Lys-Met axially coordinated heme *b* (alignment id: AzoarEBDH) which include: the EBDH from *Hydrogenivirga* sp. 128-5-R1-1 (HydroEBDH); nitrate reductases from *Aeropyrum pernix* (Apernnit) and *Pyrobaculum calidifontis* (Pcalnit); selenate reductase from *Thauera selenatis* (Selenate); DMSO reductase heme b subunit from *Halorubrum lacusprofundi* (HlacDMSOhem) and *Halorhabdus utahensis* (HutaDMSOhem); and hypothetical cytochromes from *Sulfurihydrogenibium yellowstonense* (Syellowst). The conserved methionine and lysine responsible for heme *b* coordination are indicated with arrows.

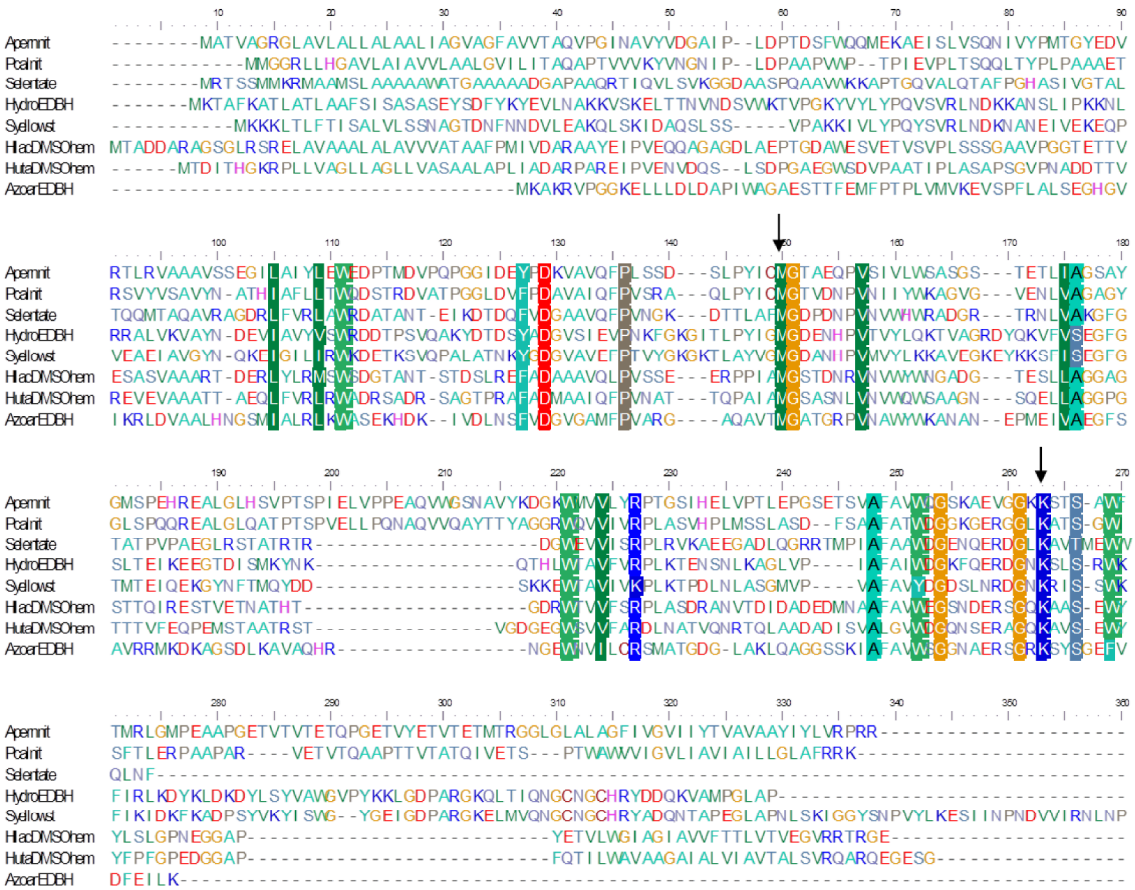

References

1. Amend, J.P., and E.L. Shock. 2001. Energetics of overall metabolic reactions of thermophilic and hyperthermophilic Archaea and Bacteria. FEMS Microbiology Reviews. 25: 175-243.

2. Appia-Ayme C, Guiliani N, Ratouchniak J, Bonnefoy V. 1999. Characterization of an operon encoding two c-type cytochromes, an aa3-type cytochrome oxidase, and rusticyanin in Thiobacillus ferrooxidans ATCC 33020. Appl Environ Microbiol. 65:4781–4787

3. Arnold K., Bordoli L., Kopp J., and Schwede T. 2006. The SWISS-MODEL Workspace: A web-based environment for protein structure homology modelling. Bioinformatics. 22:195-201.

4. Auernik K.S., Maezato Y., Blum P.H., and R. M. Kelly. 2008. The Genome Sequence of the Metal-Mobilizing, Extremely Thermoacidophilic Archaeon *Metallosphaera sedula* Provides Insights into Bioleaching-Associated Metabolism. Appl. Environ. Microbiol. 74: 682-692.

5. Auernik K.S., Kelly R.M. 2008. Identification of components of electron transport chains in the extremely thermoacidophilic crenarchaeon Metallosphaera sedula through iron and sulfur compound oxidation transcriptomes. Appl Environ Microbiol. 74:7723-32.

6. Baker, B.J. and J. F. Banfield. 2003. Microbial communities in acid mine drainage. FEMS Microbiology Ecology. 44: 139-152.

7. Bandeiras TM, Refojo PN, Todorovic S, Murgida DH, Hildebrandt P, Bauer C, Pereira MM, Kletzin A, Teixeira M. 2009. The cytochrome ba complex from the thermoacidophilic crenarchaeote Acidianus ambivalens is an analog of bc(1) complexes. Biochim Biophys Acta. 1787: 37-45.

8. Bathe, S. and P. R. Norris. 2007. Ferrous Iron- and Sulfur-Induced Genes in *Sulfolobus metallicus.* Appl. Environ. Microbiol. 73: 2491-2497.

9. Blake R.C, Shute EA, Waskovsky J, Harrison AP Jr. 1993. Respiratory components in acidophilic bacteria that respire on iron. Geomicrobiol J 10:173–192

10. Blake, R. and D.B Johnson. 2000. Phylogenetic and biochemical diversity among acidophilic bacteria that respire on iron. In: Environmental Microbe–Metal Interactions (Derek, L., Ed.). 53–78. ASM Press, Washington, DC.

11. Brierley, C. L., and J. A. Brierley. 1973. A chemoautotrophic and thermophilic microorganism isolated from an acid hot spring. Can. J. Microbiol. 19: 183–188.

12. Brock, T. D., K. M. Brock, R. T. Belly, and R. L. Weiss. 1972. Sulfolobus: a new genus of sulfur-oxidizing bacteria living at low pH and high temperature. Arch. Mikrobiol. 84: 54–68.

13. Cowan, J.A. 1993. Inorganic Biochemistry: An Introduction. VCH Publishers, New York.

14. Davis et al., A. Leaver-Fay, V. B. Chen, J. N. Block, G. J. Kapral, X. Wang, L. W. Murray, W. B. Arendal, Jack Snoeyink, J. S. Richardson and D. C. Richardson. 2007. MolProbity: all-atom contacts and structure validation for proteins and nucleic acids. Nucleic Acids Research 35:W375-W383.

15. Fuchs T., H. Huber, K. Teiner, S. Burggraf, and K.O Stetter. 1995. Metallosphaera prunae, sp. nov., a novel metal-mobilizing, thermoacidophilic Archaeum, isolated from a uranium mine in Germany. Syst. Appl. Microbiol. 18: 560-566.

16. García-Horsman J.A., Barquera B., Rumbley J., Ma J., and R.B. Gennis. 1994. The superfamily of heme-copper respiratory oxidases. J Bacteriol. 176: 5587-600.

17. Hallberg K.B, and D.B. Johnson. 2001. Biodiversity of acidophilic prokaryotes. Advances in Applied Microbiology. 49: 37-84.

18. Hallmann R, Friedrich A, Koops H-P, Pommerening-Röser A, Rohde K, Zenneck C, Sand W. 1993. Physiological characteristics of Thiobacillus ferrooxidans and Leptospirillum ferrooxidans and pyhsiochemical factors influence microbial metal leaching. Geomicrobiol J 10:193–206

19. Hedderich, R. 2004. Energy-Converting [NiFe] Hydrogenases From Archaea and Extremophiles: Ancestors of Complex I. Journal of Bioenergetics and Biomembranes. 36: 65-75

20. Hettmann T, Schmidt CL, Anemüller S, Zähringer U, Moll H, Petersen A, Schäfer G. 1998. Cytochrome b558/566 from the archaeon Sulfolobus acidocaldarius. A novel highly glycosylated, membrane-bound b-type hemoprotein. J Biol Chem. 273: 12032-40

21. Huber, G., C. Spinnler, A. Gambacorta, and K.O. Stetter. 1989. Metallosphaera sedula gen. nov. and sp. nov. represents a new genus of aerobic, metal-mobilizing, thermoacidophilic archaebacteria. Syst. Appl. Microbiol. 12: 38-47.

22. Huber G. and K.O. Stetter. 1991. Sulfolobus metallicus, sp. nov., a novel strictly chemolithoautotrophic thermophilic archaeal species of metal-mobilizers. Syst. Appl. Microbiol. 14: 372-378.

23. Inskeep W.P., R.E. Macur, G. Harrison, B.C. Bostick, S. Fendorf. 2004. Biomineralization of As(V)-hydrous ferric oxyhydroxide in microbial mats of an acid-sulfate-chloride geothermal spring, Yellowstone National Park. Geochimica et Cosmochimica Acta. 68: 3141–3155.

24. Inskeep W.P., G.G. Ackerman, W.P. Taylor, M. Kozubal, S. Korf, and R.E. Macur. 2005. On the energetics of chemolithotrophy in nonequilibrium systems: case studies of geothermal springs in Yellowstone National Park. Geobiology. 3: 297-320.

25. Johnson, D.B., and K.B. Hallberg. 2003. The microbiology of acidic mine waters. Research in Microbiology .154: 466-73.

26. Kappler, U., L.I. Sly, and A.G. McEwan. 2005. Respiratory gene clusters of *Metallosphaera sedula* – differential expression and transcriptional organization. Microbiology. 151: 35-43

27. Kletzin A., Urich T., Müller F., Bandeiras T.M., and C.M. Gomes. 2004. Dissimilatory Oxidation and Reduction of Elemental sulfur in thermophilic archaea. Journal of bioenergetics and biomembranes. 36: 77-91.

28. Kloer D.P., Hagel C., Heider J., and G.E. Schulz. 2006 Crystal Structure of Ethylbenzene Dehydrogenase from Aromatoleum aromaticum. Structure 14: 1377–1388.

29. Kniemeyer O and J. Heider. 2001. (S)-1-phenylethanol dehydrogenase of Azoarcus sp. strain EbN1, an enzyme of anaerobic ethylbenzene catabolism. Archives of microbiology. 176: 129-35.

30. Komorowski, L., Anemüller, S., and G. Schäfer. 2001a. First expression and characterization of a recombinant CuA-containing subunit II from an archaeal terminal oxidase complex. J Bioenerg Biomembr. 33: 27-34.

31. Komorowski, L. and G. Schäfer. 2001b. Sulfocyanin and subunit II, two copper proteins with novel features, provide new insight into the archaeal SoxM oxidase supercomplex. FEBS Letters. 487: 351-5.

32. Komorowski L., Verheyen W., and G. Schäfer. 2002. The archaeal respiratory supercomplex SoxM from S. acidocaldarius combines features of quinole and cytochrome c oxidases. Biol Chem. 383: 1791-9.

33. Kozubal M., Macur R.E., Korf S., Taylor W.P., Ackerman G.G., Nagy A., and W.P. Inskeep. 2008. Isolation and Distribution of a Novel Iron-Oxidizing Crenarchaeon from Acidic Geothermal Springs in Yellowstone National Park. Appl. Environ. Microbiol. 74: 942-949.

34. Kurosawa, N., Y.H. Itoh, and T. Itoh. 2003. Reclassification of *Sulfolobus hakonensis* Takayanagi et al. 1996 as *Metallosphaera hakonensis* comb. Nov. based on phylogenetic evidence and DNA G+C content. Int. J. Syst. Evol. Microbiol. 53: 1607–1608.

35. Li, X., Wei, Z., Zhang, M., Peng, X., Yu, G., Teng, M., and W. Gong. 2007. Crystal structures of E.coli laccase CueO at different copper concentrations. Biochem Biophys Res Commun. 354: 21-26

36. Lübben, M., Kolmerer, B. and M. Saraste. 1992. An archaebacterial terminal oxidase combines core structures of two mitochondrial respiratory complexes. EMBO J. 11: 805-812.

37. Lübben, M., Warne, S., Albracht, S. and M. Saraste. 1994a. The purified SoxABCD quinol oxidase complex of *Sulfolobus acidocaldarius*. Molecular Microbiology. 13: 327-35.

38. Lübben M., Arnaud S., Castresana J., Warne A., Albracht S.P., and M. Saraste. 1994b. A second terminal oxidase in Sulfolobus acidocaldarius. Eur J Biochem. 224: 151-9.

39. Lüthy R., Bowie JU, and D. Eisenberg. 1992. Assessment of protein models with three-dimensional profiles. Nature. 356: 83-5.

40. Macur, R.E., H.W. Langner, B.D. Kocar, and W.P. Inskeep. 2004. Linking geochemical processes with microbial community analysis: successional dynamics in an arsenic-rich, acid-sulfate-chloride geothermal spring. Geobiology. 2: 163-177.

41. Nakamura K, and N. GO. 2005 Function and molecular evolution of multicopper blue proteins. Cell Mol Life Sci. 62: 2050-66.

42. Pereira, M. M.,T. M. Bandeiras, A. S. Fernandes, R. S. Lemos, M. P. Melo, and M. Teixeira. 2004. Respiratory Chains From Aerobic Thermophilic Prokaryotes. Journal of Bioenergetics and Biomembranes. 36: 93-105

43. Poulos, T.L. 1996. The role of the proximal ligand in heme enzymes. J. Biol. Inorg. Chem. 1: 356-359.

44. Purschke, W.G., Schmidt, C.L., Petersen, A., and G Schäfer. 1997. The terminal quinol oxidase of the hyperthermophilic archaeon Acidianus ambivalens exhibits a novel subunit structure and gene organization. J Bacteriol. 179: 1344-53.

45. Quintanar L., Gebhard M., Wang T.P., Kosman and D.J. Solomon. 2004. Ferrous binding to the multicopper oxidases Saccharomyces cerevisiae Fet3p and human ceruloplasmin: contributions to ferroxidase activity. J Am Chem Soc. 126:6579-89.

46. Rawlings, D.E. 2002. Heavy metal mining using microbes. Annual Review of Microbiology. 56: 65-91.

47. Rawlings, D. E. 2005. Characteristics and adaptability of iron- and sulfur-oxidizing microorganisms used for the recovery of metals from minerals and their concentrates. Microbial Cell Factories. 4:13

48. Reno ML, Held NL, Fields CJ, Burke PV, Whitaker RJ. 2009. Biogeography of the Sulfolobus islandicus pan-genome. Proc Natl Acad Sci. 106:8605-10

49. Rohwerder, T., T. Gehrke, K. Kinzler, and W. Sand. 2003. Bioleaching review part A: progress in bioleaching: fundamentals and mechanisms of bacterial metal sulfide oxidation. Appl. Microbiol. Biotechnol. 63: 239-48.

50. Singer, S. W., C. S. Chan, A. Zemla, N. C. M. VerBerkmoes, M. Hwang, R. L. Hettich, J. F. Banfield, and M. P. Thelen. 2008. Characterization of cytochrome 579, an unusual cytochrome isolated from an iron-oxidizing microbial community. Appl Environ Microbiol. 74: 4454-62

51. Stoj C.S., Augustine A.J., Zeigler L., Solomon E.I., and D.J. Kosman. 2006. Structural basis of the ferrous iron specificity of the yeast ferroxidase, Fet3p. Biochemistry. 45:12741-9.

52. Suzuki, T., Iwasaki, T. Uzawa, T. Hara, K. Nemoto, N. Kon, T. Ueki, T. Yamagishi, A. and T. Oshima. 2002. *Sulfolobus tokodaii* sp. nov. (f. Sulfolobus sp. strain 7), a new member of the genus Sulfolobus isolated from Beppu Hot Springs, Japan. Extremophiles. 6: 39-44.

53. Takayanagi, S., H. Kawasaki, K. Sugimori, T. Yamada, A. Sugai, T. Ito, K. Yamasato, and M. Shioda. 1996. *Sulfolobus hakonensis* sp. nov., a novel species of acidothermophilic archaeon Int. J. Syst. Bacteroil. 46: 377–382

54. To, T.B., D.K. Nordstrom, K.M. Cunningham, J.W. Ball, R.B. McClesky. 1999. New method for the direct determination of dissolved Fe(III) concentration in acid mine waters. Environmental Science and Technology. 33: 807-813.

55. van der Oost J., de Boer A.P., de Gier J.W., Zumft W.G., Stouthamer A.H., and van Spanning R.J. 1994.The heme-copper oxidase family consists of three distinct types of terminal oxidases and is related to nitric oxide reductase. FEMS Microbiol Lett. 121:1–9

56. Wallner B., and A. Elofsson. 2003. Can correct protein models be identified? Protein Sci. 12(5):1073-1086

57. Wiederstein M., and M. J. Sippl. 2007. ProSA-web: interactive web service for the recognition of errors in three-dimensional structures of proteins.Nucleic Acids Research 35: W407-W410.

58. Yarzábal A, Brasseur G, Bonnefoy V. 2002a. Cytochromes c of Acidithiobacillus ferrooxidans. FEMS Microbiol Lett 209:189–195

59. Yarzábal A, Brasseur G, Ratouchniak J, Lund K, Lemesle-Meunier D, DeMoss JA, Bonnefoy V. 2002b. The high-molecular-weight cytochrome c Cyc2 of Acidithiobacillus ferrooxidans is an outer membrane protein. J Bacteriol 184:313–317

60. Zähringer U., Moll H., Hettmann T., Knirel Y. A., and G. Schäfer. 2000. Cytochrome b558/566 from the archaeon Sulfolobus acidocaldarius has a unique Asn-linked highly branched hexasaccharide chain containing 6-sulfoquinovose. European journal of biochemistry / FEBS. 267:4144-9.

CHAPTER 5

COMPARATIVE GENOME ANALYSIS OF *METALLOSPHAERA YELLOWSTONII* WITH ACIDOPHILIC IRON-OXIDIZING PROKARYOTES

Abstract

Given the importance of *M. yellowstonii* in geothermal habitats of YNP, one of the goals of this thesis was to obtain a genome sequence for comparison to other iron-oxidizing microorganisms. A draft genome has been assembled for *M. yellowstonii* MK1^T with adequate coverage (~6x) to compare putative genes involved in iron and sulfur oxidation, heavy metal resistance, carbon fixation, and oxygen reduction with a diverse group of iron-oxidizing acidophilic prokaryotes. The *M. yellowstonii* genome contains sequences similar to putative iron oxidizing orfs found in *M. sedula* and *S. tokodaii*, including a novel *fox* terminal oxidase gene cluster, a multicopper oxidase (*mco*), and the *cbs*AB-*sox*L2N operon. These genes differ considerably from the hypothesized cytochromes found in the genomes of *Acidithiobacillus ferrooxidans* and *Leptospirillum* group II. *M. yellowstonii* contains a conserved heterodisulfide (*hdr*) gene cluster believed to be involved in elemental sulfur oxidation and also contains sequences for sulfide (*sqr*), sulfite (*som*), and thiosulfate oxidation (*tqo*). Seven copies of the heme copper oxidase (HCO) subunit I were identified in the *M. yellowstonii* draft genome. *M. yellowstonii* also contains a *bd*-type terminal oxidase not found in other known members of the Sulfolobales. *M. yellowstonii* is similar to *M. sedula* regarding genes involved in CO_2 fixation (i.e., the 3-hydroxypropionate/ 4-hydroxybutyrate cycle) and heavy metal

resistance. Finally, *M. yellowstonii* is the only known Archaea to contain a methyl mercury lyase (*mer*B) gene. Analysis of gene sequence data suggest that, in addition to the diversity of HCOs, *M. yellowstonii* contains novel mechanisms of iron oxidation, sulfur metabolism, autotrophy, and heavy metal resistance consistent with the observed distribution of this organism in natural habitats.

Introduction

Chemolithoautotrophic growth on Fe(II) in acidic environments has gained significant attention because of potential commercial applications in bioleaching of mineral ores (Rawlings, 2002 and 2005; Olson et al., 2003), bioremediation of acid mine drainage (Johnson and Hallberg, 2005) and coal desulfurization (Clark et al., 1993). Diverse acidophilic organisms involved in Fe(II) oxidation include (i) the mesophilic *Acidithiobacillus ferrooxidans, Leptospirillum ferrooxidans, Leptospirillum ferriphilum,* and a dominant *Leptospirillum ferriphilum*-like population at Iron Mountain CA (*Leptospirillum* sp. group II; Konhauser, 1998; Blake and Johnson, 2000; Baker and Banfield, 2003; Johnson and Hallberg, 2003), (ii) moderately thermophilic *Sulfobacillus* spp., *Acidimicrobium ferrooxidans, Ferrimicrobium acidophilum,* and *Ferroplasma* spp. (Rawlings, 2002), and (iii) the thermophilic members of the crenarchaeal order Sulfolobales (i.e., *Metallosphaera sedula* (Huber et al., 1989), *Acidianus brierleyi* (Brierley and Brierley, 1973), *Sulfolobus metallicus* (Huber and Stetter, 1991), *Sulfolobus tokodaii* (Suzuki et al., 2002) and *Metallosphaera yellowstonii*).

The mechanism of iron oxidation has been studied extensively in *Acidithiobacillus ferrooxidans*, which is believed to utilize three cytochromes *c* (Cyc2,

Cyc1 and CycA1) and the blue-copper protein *rusticyanin* for Fe(II) oxidation. Cyc2 is believed to oxidize Fe(II) directly and reduce *rusticyanin*, which either passes electrons to CycA1 in a reverse electron flow mechanism for $NADP^+$ reduction or to Cyc1 (Quatrini et al., 2009). Cyc1 is thought to pass electrons directly to a aa_3 type heme copper oxidase complex for proton consumption and oxygen reduction. The resulting proton gradient is then utilized for ATP generation via an ATPase. A mechanism for Fe(II) oxidation has also been hypothesized in *Leptospirillum* group II and an outer membrane cytochrome cyt_{572} is believed to directly oxidize Fe(II), then transfer electrons to a periplasmic cytochrome cyt_{579}, which are ultimately passed to a terminal oxidase or used for reverse electron flow by an undefined mechanism (Jeans et al., 2008; Singer et al., 2008). In contrast, a small blue copper protein has been implicated in the direct oxidation of ferrous iron in *F. acidarmanus*, and the subsequent reduction of the subunit I of the HCO without intermediate electron carriers (Dopson et al., 2005). Knowledge of Fe(II) oxidation within the Sulfolobales is limited to a few gene expression studies (Bathe and Norris, 2007; Kappler et al., 2005; Auernik et al., 2008; Auernik and Kelly, 2008).

Metallosphaera yellowstonii MK-1^T (formerly referred to as *Metallosphaera* sp. strain MK1; T-designates type strain) was isolated from an acid sulfate chloride geothermal spring in Yellowstone National Park (YNP). The isolate is a chemolithotroph that is capable of autotrophic growth on Fe(II) sorbed to ferrihydrite, pyrite and elemental sulfur. A draft genome has been completed with sufficient coverage (~6x) for a comparative study with other chemolithoautotrophic iron-oxidizing acidophiles including *Metallosphaera sedula, Sulfolobus tokodaii, Ferroplasma acidarmanus, Acidithiobacillus*

ferrooxidans, and *Leptospirillum* sp. group II. Also, recent metagenome sequencing of ferric oxide mats of acidic geothermal springs in Yellowstone National Park (YNP) provide opportunities to compare gene sequences from acidophilic iron-oxidizing isolates to relatives found in natural environments (Inskeep et al., 2010).

The goals of the current study are to (1) describe metabolic attributes inferred from genes found in the draft *M. yellowstonii* genome with special focus on putative respiratory proteins and complexes, CO_2 fixation, oxygen reduction, and heavy metal resistance, (2) compare these putative genes to those found in *M. sedula*, *A. ferrooxidans*, *Leptospirillum* group II, *F. acidarmanus* , and *S. tokodaii,* and (3) compare HCO and *bd*-type terminal oxidase genes found in the genomes of iron-oxidizing acidophiles to gene sequences found in acidic ferric iron mats in YNP.

Materials and Methods

Genomic Sequences

M. yellowstonii gene sequences were obtained as described in Kozubal et al., (2008). All contigs were assembled in one file and both nucleotide and protein sequences were extracted. All sequences from other species were obtained at the NCBI GenBank website except *F. acidarmanus* which was acquired at the Oak Ridge National Laboratory website (http://genome.ornl.gov/microbial/faci/). All gene search sequences for blastp searches were obtained from NCBI GenBank. Blastp analysis was done with multiple search sequences from various bacterial and archaeal orders when available.

Most *M. yellowstonii* genes were found complete on single contigs and those found on multiple contigs were assembled and gaps were filled by primer walking when possible.

Metagenome Sequences

Yellowstone geothermal samples and sampling sites for metagenome sequence analysis are described by Inskeep et al., (2010). Of these samples, three hydrous-ferric-iron (HFO) mat samples from two geothermal springs were chosen for this study. The three mat samples from Norris Geyser Basin and their corresponding temperature are referred to as BED (62 °C) from *Beowulf* spring (site from which *M. yellowstonii* was isolated); OSP8 (75 °C) and OSP14 (81 °C) from OSP spring. Sequences for phylogenetic analysis were obtained by blastp through the Joint Genome institute IMG/ER database.

Bioinformatic Techniques

Gene sequences were translated with the EXPASY protein translation tool and annotated by homology comparisons with the *M. sedula* genome. Protein sequence alignments were performed using ClustalX (version 1.81) and unalignments/gaps were edited with Se-Al v2.0a11. Distance analysis was performed using the Jukes and Cantor correction, followed by phylogenetic tree construction using the maximum likelihood method of PAUP*4.0 software (Sinauer Associates, Sunderland, MA) after 1000 boot straps.

Several bioinformatic programs were used to determine putative functions of genes found in this study. Protein blast (blastp and PHI-BLAST) and conserved domain

searches were used initially to implicate the well conserved proteins with function based on homology in the NCBI databases. Multiple protein sequence analysis tools were used to determine structural relatives for sequences that could not be characterized with blastp and these include the Pfam database (a large collection of protein families, represented by multiple sequence alignments and hidden Markov models), SMART (Simple Modular Architecture Research Tool which analyses protein domain architectures and identifies and annotates genetically mobile domains), HHpred (Homology detection and structure prediction by HMM-HMM comparison), and the Bioinfobank Metaserver (protein structure and function prediction method assessed with a 3D-jury consensus). Structurally related sequences found with HHpred or the Bioinformatic Metaserver were aligned with ClustalX and the SwissView-Pdb viewer (V. 3.7) and models were created with the Swissmodel server (Arnold et al., 2006). The quality of the models were tested with ProQ (Wallner and Elofsson, 2003; Stockholm Bioinformatics Center), ProSa (Protein Structure Analysis; https://prosa.services.came.sbg.ac.at/prosa.php; Wiederstein and Sippl, 2007), MolProbity structural analysis tool (Davis et al., 2007) and the UCLA verify 3D-structure tool (Lüthy et al., 1992). The *Metallosphaera yellowstonii* draft genome contigs are available at the Joint Genome Institute IMG/ER website.

Results and Discussion

The diversity of known acidophilic iron oxidizing prokaryotes was compiled as a 16S rRNA phylogenetic tree (Figure 5.1) and includes representatives from the bacterial phylum Proteobacteria (*Acidithiobacillus ferrooxidans*), Nitrospirae (*Leptospirillum* group II), Firmicutes (*Sulfobacillus spp.* and *Alicyclobacillus* sp. Y0010), Actinobacteria

(*Ferromicrobium acidophilum*, *Acidimicrobium ferrooxidans*, *Rubrobacterales* sp. Pa33, and two un-named species Y005 and Y0010), as well as archaea within both the Euryarchaeota (*Ferroplasma acidarmanus)* and the Crenarchaeota (*Metallosphaera sedula*., *S. metallicus*, *S. tokodaii, S.* strain MK-3). The genomes completed to date cover the range of taxonomic groups of iron oxidizing acidophilic prokaryotes with the exception of members from the Actinobacteria and Firmicutes. This study describes putative genes involved in iron and sulfur oxidation, heavy metal tolerance, mercury and arsenic metabolism, CO_2 fixation, and oxygen reduction in the draft genome of *M. yellowstonii* as compared to other iron-oxidizing acidophilic bacteria and archaea.

General Features of the *M. yellowstonii* Genome

An analysis of select orfs from this study indicates significant synteny and gene similarity to *M. sedula*. *In-silico* hybridization indicates that 34% of the *M. yellowstonii* genome aligns with high similarity to *M. sedula* (see Appendix Chapter 2 for details). *M. yellowstonii* has a GC content = 48%, and has a high percentage of transposable elements (TEs). Initial estimates indicate approximately 10% of the genome is composed of TEs, similar to that observed in *S. solfataricus* (She et al., 2001).

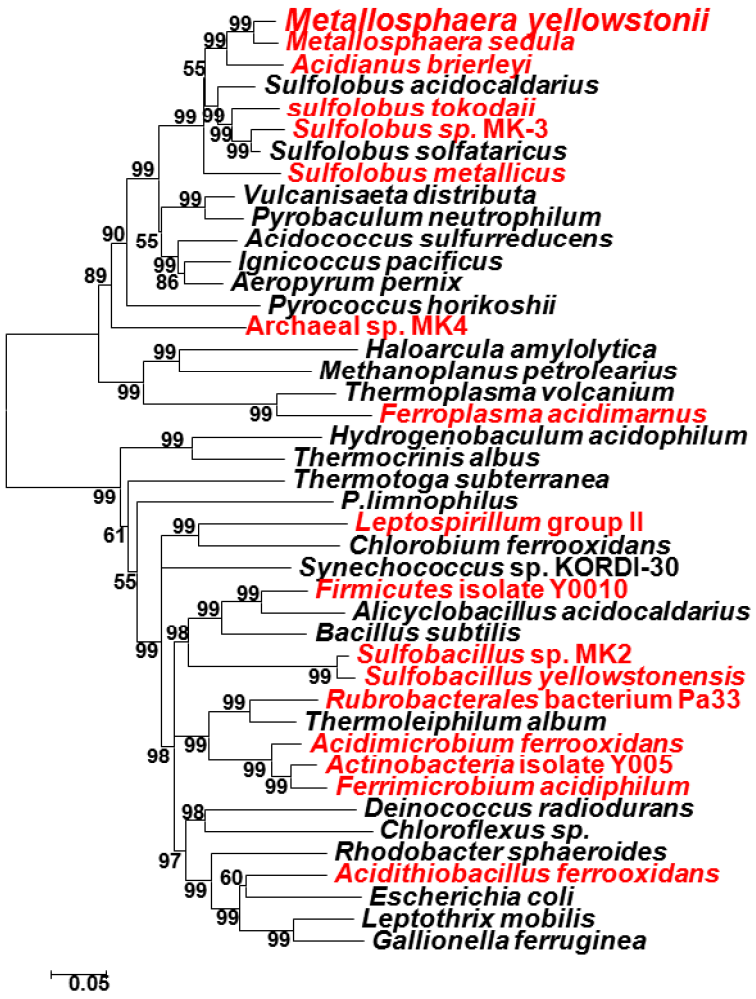

Figure 5.1. Phylogenetic tree (16S rRNA gene – approximately 1400 bp alignments) of all known acidophilic iron-oxidizing prokaryotes (indicated in red).

Oxygen Reduction

The acidophilic prokaryotes discussed in this study are all obligate aerobes that couple the oxidation of iron with oxygen reduction. All aerobic organisms reduce oxygen by a highly conserved subunit I of the heme copper oxidase (HCO) superfamily (García-Horsman et al., 1994). The wide variety of HCOs presumably allow organisms to use a myriad of electron donors (i.e. H_2, CH_4, Fe(II), H_2S, S^0, S_2O_3, tetrathionate, and As(III))

for energy conservation. Previous studies have linked gene expression of specific HCOs to oxidation of iron, sulfur or organic substrates (Purschke et al., 1997; Kappler et al., 2005; Bathe and Norris, 2007; see Chapter 4, this thesis). For example, expression of *fox*A-like sequences have been linked to iron oxidation, and are found only in iron-oxidizing Sulfolobales. Furthermore, specific HCOs may be necessary for growth under low O_2 concentrations (García-Horsman et al., 1994).

In addition to the HCO family, *bd*-type quinol oxidase complexes are found in several prokaryotes (Jünemann, 1997). The *bd*-type quinol oxidases are believed to have very high affinity for oxygen, and are likely important for aerobic growth under micro-aerophilic conditions (García-Horsman et al., 1994; Forte et al., 2007). Alternatively it has been suggested that *bd*-type quinol oxidases may protect cells from excessive nitric oxide (Mason et al., 2009).

HCO and *bd*-type terminal oxidase gene sequences from the acidophilic Fe(II) oxidizing species are shown with metagenome sequences from iron oxide mats (BED, OSP8 and OSP14) from Norris Geyser Basin (Figure 5.2 and 5.3). *M. yellowstonii* has seven subunit I HCO sequences (Figure 5.2), which include three *fox*A-like (Bathe and Norris, 2007), two *dox*B-like (Purschke et al., 1997), a *sox*M-like (Komorowski et al., 2002) and a *sox*B-like (Liibben et al., 1995) (discussed in detail in Chapter 4, this thesis). Unlike other known Sulfolobales, *M. yellowstonii* also has a *bd*-type terminal oxidase (Figure 5.3). The *M. yellowstonii bd*-type terminal oxidase sequence is flanked by insertion elements and is most closely related to the *bd*-type from *Thermoplasma acidophilum* possibly suggesting a horizontal gene transfer event. The presence of a *bd*-

type terminal oxidase may confer an additional advantage to *M. yellowstonii* for competition in micro-aerophilic zones. A significant number of HCO and *bd*-type terminal oxidase genes present in metagenome sequence correspond to the *fox* and *dox* HCOs found in *M. yellowstonii* (Figure 5.3), further supporting the importance of sulfur and ferrous iron as electron donors in these environments (see Chapter 4).

Iron Oxidation

The Fe(II)/Fe(III) redox pair has a Eh close to the O_2/H_2O couple under acidic conditions (Kappler and Straub, 2005) and therefore, the metabolic pathway involved in Fe(II) oxidation requires fewer electron transport steps than is required for more energy-rich substrates such as H_2 and glucose. The mechanism of Fe(II) oxidation in *M. yellowstonii* and the Sulfolobales is poorly understood and undoubtedly differs considerably from bacterial mechanisms. *M. yellowstonii* contains genes similar to those in *M. sedula* linked to iron oxidation (Auernik et al., 2008) including the *fox*A-J gene cluster (see Chapter 3, this thesis), the *cbs*AB-*sox*L2N operon, and a novel multi copper oxidase (*mco*). In addition, *M. yellowstonii* contains similar genes annotated as "major facilitator superfamily" orfs likely involved in $FeSO_4$ transport (related to Msed0467, -0907, -1001, -1095, -1181, and -1355). The best candidates for the direct oxidation of Fe(II) based on previous expression studies (Bathe and Norris, 2007; Auernik et al., 2008) and discussed in detail in Chapter 4 of this thesis are the blue multi copper oxidase (*mco*) and a novel cytochrome *b* located in the *fox* operon (FoxC).

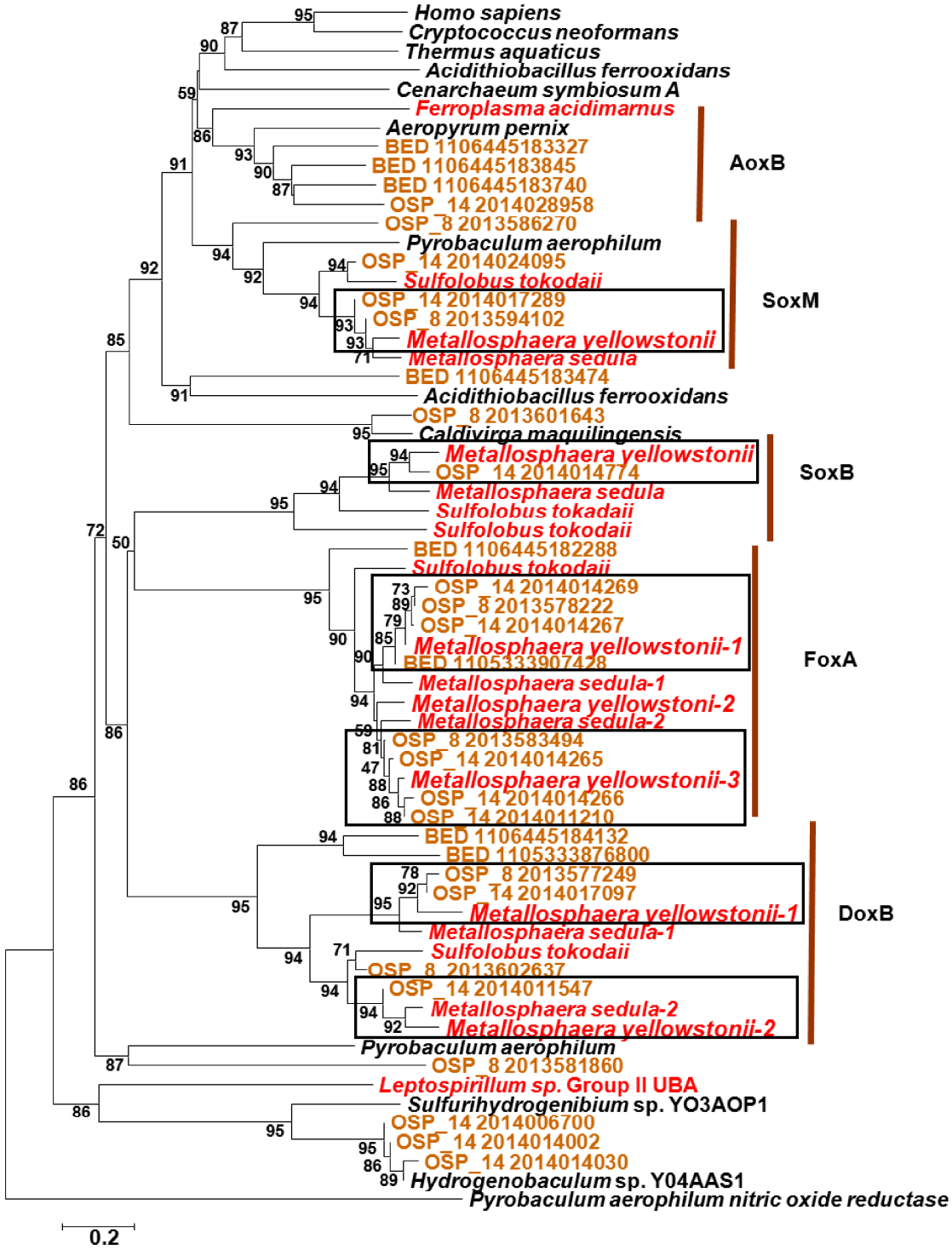

Figure 5.2. Phylogenetic tree of heme copper oxidase (HCO) subunit I showing acidophilic iron-oxidizing prokaryotes (red) and metagenome entries from acidic iron mats (orange). Numerous *M. yellowstonii*-like HCOs (boxed) were observed in

metagenome sequence (orange) obtained from three ferric iron mats (BED, OSP8, and OSP14; Norris Geyser Basin, YNP). Tree obtained from ~400 bp alignments.

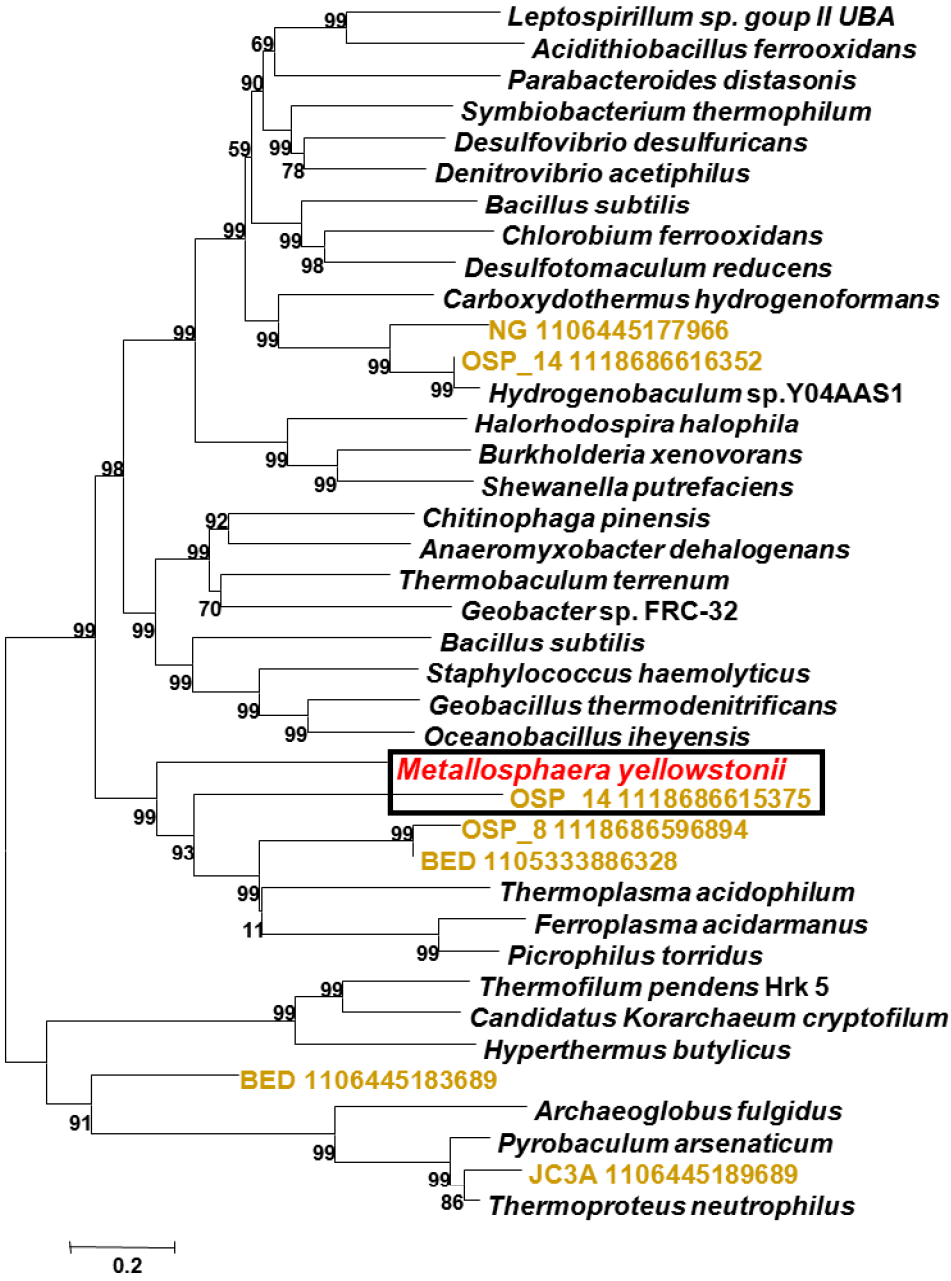

Figure 5.3. Phylogenetic tree of *bd*-type terminal oxidases showing acidophilic iron-oxidizing prokaryotes (red) and metagenome entries from acidic iron mats (orange) compared to *M. yellowstonii* sequences (bold). One *M. yellowstonii*-like *bd*-type terminal oxidase (boxed) was observed in metagenome sequence (orange) obtained from three ferric iron mats (BED, OSP8, and OSP14; Norris Geyser Basin, YNP).

The geochemical environment of each Fe(II) oxidizing species discussed in this study varies significantly and may explain convergent mechanisms of Fe(II) oxidation. *A. ferrooxidans* outcompetes other mesophilic iron oxidizing species (such as *Leptospirillum* sp. Group II) at lower redox potentials and is often the primary Fe(II) oxidizer in 'dump and heap' leaching environments (Rawlings, 2002). *A. Ferrooxidans* is generally favored within the temperature range 20–35 °C, between pH 2.0-2.5, and at high soluble Fe(II)/Fe(III) ratios. *Leptospirillum* sp. Group II thrives in stirred batch reactors and environments with high Fe(III)/Fe(II) ratios, pH values as low as 0.5, and high total iron concentrations inhibitory to other species (Richmond Mine in California; Bond et al., 2000). *A. ferrooxidans* is inhibited by iron concentrations over 3.1 mM compared to over 40 mM for *Leptospirillum* sp. Group II (Rohwerder et al., 2003).

The acidic geothermal iron mats of YNP, where *M. yellowstonii* predominates, have pH and temperature ranges of 2.6-3.3 and 58-75 °C, respectively (Macur et al., 2004; Inskeep et al., 2004; Inskeep et al., 2005; Kozubal et al., 2008), which are higher than habitats for *A. ferrooxidans* and *Leptospirillum* sp. Group II. Ratios of Fe(II)/Fe(III) range from 200 upon discharge to as low as ~0.5 in downstream locations. Measured redox potentials for the Fe(II)/Fe(III) couple range between approximately 0.47 and 0.59 V, which are lower than those discussed at the Richmond Mine or in environments where *A. ferrooxidans* predominates (Rohwerder et al., 2003; Inskeep et al., 2005). Among other factors, the differences in redox potential across natural environments, yields different mechanisms of iron oxidation across different phyla. The Sulfolobales do not have cytochromes *c*, which are important proteins for iron oxidation in *A. ferrooxidans*

and *Leptospirillum* group II, and further supports the hypothesis that a different evolutionary path is responsible for iron oxidation in *M. yellowstonii*. Cytochromes *b* (i.e. FoxC and/or CbsA) and blue multi-copper (Mco) proteins likely have similar function to cytochrome *c* and rusticyanin for direct Fe(II) oxidation and/or upstream/downstream electron transport. Expression and modeling results from Chapter 4 of this dissertation along with comparative genome analysis provides evidence to support a hypothetical model for iron oxidation in *M. yellowstonii* str. MK1 (Figure 5.4). This model assumes that FoxC is the direct oxidant of Fe(II) and that Mco acts much like a cytochrome *c* analog in transporting electrons either upstream for anabolic processes such as carbon fixation or downstream to the Fox HCO for energy gain and ATP synthesis.

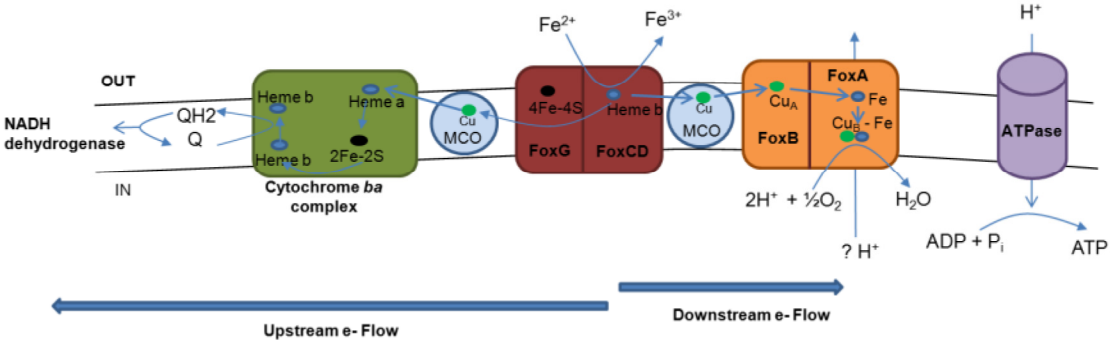

Figure 5.4. Hypothetical model of iron oxidation in *M. yellowstonii* str. MK1 based on annotation of draft genome sequence and functional modeling of putative proteins in the Fox 'supercomplex'. Blue arrows indicate path of electrons. Q – quinone; QH2 – hydroquinone.

Sulfur Oxidation

Reduced sulfur species that may serve as electron donors in natural environments include H_2S, S^0, $S_2O_3^{2-}$, and SO_3^{2-}. Sulfide (usually either H_2S or HS^- species) is oxidized

to elemental sulfur by either a sulfide quinine oxidoreductase (Sqr - via quinone) or a sulfide dehydrogenase (SudH - via cytochrome *c*). Both of these proteins belong to the superfamily of FAD dependent pyridine nucleotide-disulphide oxidoreductases. Other members of this protein family include MerA, heterodisulfide oxidoreductases, NADH dehydrogenase, thioredoxin reductases, and dihydrolipoamide dehydrogenase (Figure 5.6). There are currently four models for the oxidation of elemental sulfur in prokaryotes and include the (i) SOX system utilized in the *Alphaproteobacteria*, *Chromatiaceae* and *Chlorobi* (Friedrich et al., 2005), (ii) the dissimilatory sulfite reductase (DSR) system described in *A. vinosum* and green sulfur bacteria (Dahl et al., 2005; Sander et al., 2006) for the oxidation of sulfane sulfur species, (iii) the cytoplasmic sulfur oxidoreductase (SOR) model discussed in *A. ambivalens* (Kletzin et al., 2004), and (iv) a novel *hdr* gene cluster described in *A. ferrooxidans* and *M. sedula* (Auernik and Kelly, 2009; Quatrini et al., 2009), which contains a set of heterodisulfide reductase genes related to the *hdr* genes of *Methanothermobacter marburgensis* (Hedderich et al. 2005).

M. yellowstonii has one *sqr*- and two *sud*H-like sequences with similarity to sequences in *M. sedula* (Figure 5.6). The *hdr* gene cluster found in *A. ferrooxidans*, *M. sedula*, *M. yellowstonii* and *S. tokodaii* is highly conserved with respect to both protein similarity and synteny (Figure 5.5 and 5.6). *M. sedula*, *M. yellowstonii* and *S. tokodaii*, have a highly conserved gene cluster sequence (referred to in this study as the *trd* gene cluster) encoding a putative thioredoxin and a thioredoxin reductase directly upstream of the *hdr* operon, which has not been discussed prior to this study. The putative thioredoxin (Trd) may transfer reduced sulfur species to the Hdr cluster for further oxidation and

transfer of electrons to the quinone pool. However, the presence of a thioredoxin reductase (*trd*R) indicates $NADP^+$ or FAD are involved as oxidants. Perhaps, thioredoxin donates electrons obtained from reduced sulfur substrates to the thioredoxin reductase for production of NADPH for cell anabolic processes as an alternative to downhill electron transport to the terminal oxidase for ATP generation via a proton gradient. Microarray expression studies in *A. ferrooxidans* and *M. sedula* showed that genes in the *hdr* cluster were induced when cultures were grown on S^0 compared to Fe(II) (Auernik and Kelly, 2008), but the studies did not show induction of the *trd* gene cluster. However, the experiments were not performed using autotrophically grown cultures (0.1 % YE was added to the media), thus the cells did not need to shunt electrons for carbon fixation away from ATP synthesis.

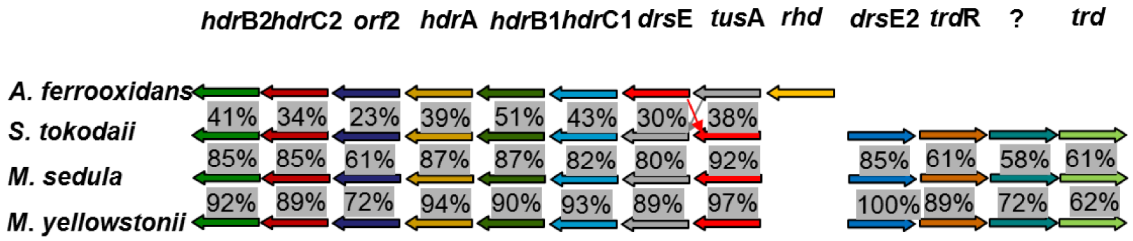

Figure 5.5. The *hdr* and *trd* gene clusters showing the gene arrangement synteny and a.a. similarity between species.

SO_3^{2-} (sulfite) is a common intermediate of both H_2S/S^0 oxidation and sulfate reduction. Two separate systems exist for sulfite oxidation and include the sulfite oxidase (SO) family of molybdopterin proteins and (APS) reductases (Kletzin et al., 2004). *M. yellowstonii* has two orfs coding for putative SO subunits (*M. yellowstonii* proteins are

related to *M. sedula* at ~66% each). *M. yellowstonii* and all known Sulfolobales also have a gene coding for a putative PAPS reductase, highly related to APS reductases. The PAPS reductase gene is encoded in a *cys* like operon, which is important for sulfate assimilation (Neumann et al., 2000) and is not likely involved in sulfur oxidation.

Thiosulfate ($S_2O_3^{2-}$) can form during the biological oxidation of sulfide minerals or from abiotic reactions involving S^0, tetrathionate and H_2S. Thiosulfate is unstable at pH levels below 5, and may disproportionate to form sulfite and elemental S (Wu et al., 1999). However, the rate of biotic oxidation has been found to compete with abiotic rates at the sulfide mineral interface at pH 5 or less (Nordstrom and Southam, 1997). Furthermore, thiosulfate may accumulate within the neutral cytoplasm as byproducts of S^0 and H_2S oxidation for further chemolithotrophic oxidation to sulfate or tetrathionate. Two protein systems exist for the oxidation of thiosulfate and include a thiosulfate oxidoreductase complex (TqoAB; Kletzin et al. 2005) and the bacterial specific molybdopterin SoxB protein of the SoxAXZYB complex (Friedrich et al., 2005). *M. yellowstonii* does not contain genes encoding for Sox proteins, but has a *tqo*AB orf found in all the Sulfolobales except *Sulfolobus acidicaldarius.* Interestingly, the *tqo*AB sequences of *M. yellowstonii* and *M. sedula* are directly upstream of a sulfite oxidase molybdopterin (*som*). One hypothesis that may explain the proximity of these genes is that oxidation of thiosulfate and sulfite is tightly coupled in *M. yellowstonii*. Tetrathionate may form as a product of TqoAB or may be introduced from abiotic reactions involving other S species. Genes similar to *tet*H are found in *M. yellowstonii*, *M. sedula*, *S. tokodaii* and *Leptospirillum* group II.

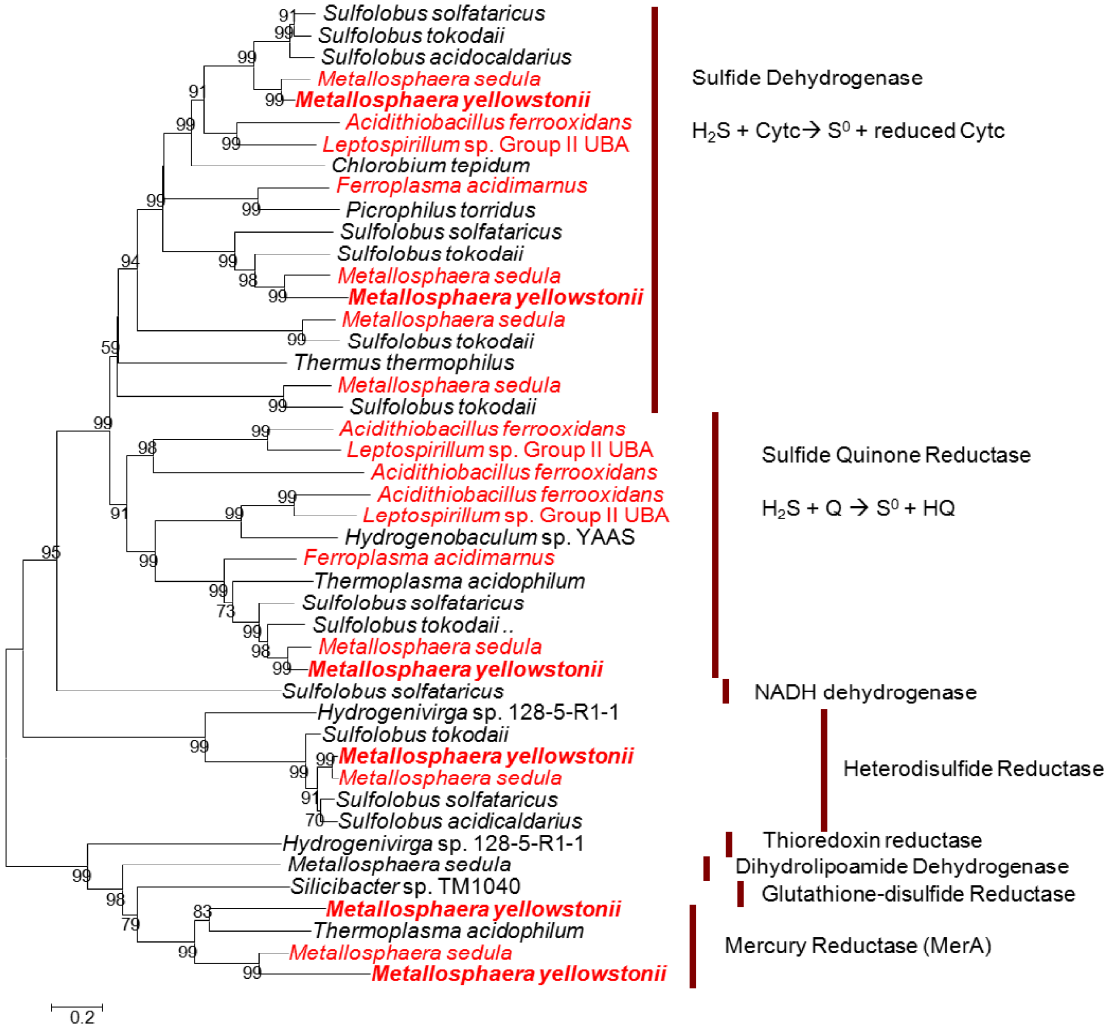

Figure 5.6. Phylogenetic tree of pyridine dinucleotide reductase sequences. Iron-oxidizing organisms discussed in the current study are emphasized (shown in red).

Carbon Fixation

There are six pathways for CO_2 fixation known across all three domains of life and include the Calvin cycle, reductive TCA cycle, reductive acetyl-CoA pathway, 3-hydroxypropionate pathway, the 3-hydroxypropionate/4-hydroxybutyrate cycle and the proposed dicarboxylate/4-hydroxybutyrate cycle (Berg et al., 2010). The 3-hydroxypropionate/4-hydroxybutyrate autotrophic pathway was recently characterized in

M. sedula (Berg et al., 2008) and similar sequences are found in all the Sulfolobales including the *M. yellowstonii* draft genome suggesting that *M. yellowstonii* fixes CO_2 using this mechanism. In fact, all key genes in the 3-hydroxypropionate/4-hydroxybutyrate pathway are found in the *M. yellowstonii* genome. Genes of the *nif* operon were not found in *M. yellowstonii*, consistent with the absence of this capability in any currently known thermophilic archaea. Although there may exist an undefined pathway for nitrogen fixation, it appears that thermophilic archaea evolved in environments with sufficient organic N and or other inorganic species of N. The concentrations NO_3^- (12-30 μM) and NH_4^+ (70-100 μM) in the native *M. yellowstonii* geothermal springs are sufficient for microbial growth, and calculations indicate that the total flux of N in these springs is not limiting biomass.

Trace Element Resistance and Metabolisms

Iron oxidizing chemolithotrophs live in environments such as acid mine drainage (AMD) and geothermal hot springs and are therefore exposed to high levels of trace elements such as Hg, Mn, Cu, As, Sb, Pb, Cd, and Cr (Johnson and Hallberg, 2005). Mechanisms must exist to allow these species to thrive in adverse conditions lethal to most organisms. Understanding mechanisms of trace element tolerance has implications for biotechnology such as the utilization of strains for bioleaching and bioremediation. Particularly adept metabolisms for trace element resistance may be targets for recombination into organisms for a myriad of industrial applications in contaminated conditions.

M. yellowstonii has two heavy metal efflux ATPases, one of which is most closely related to the *M. sedula* sequence (75% a.a. similarity), while a second is most related to a sequence from *S. solfataricus* (65% a.a. similarity). Similar genes to the *S. metallicus* polyphosphate mechanism (*pit*, *ppx*, *ppnk*; Cardona et al., 2002) are found in the genomes of all the Sulfolobales including *M. yellowstonii* with the exception of a *pit* homolog not found in *M. sedula*. This extrusion method appears to be specific to the Sulfolobales as a novel survival mechanism in sulfide mineral environments with high temperatures, low pH and extreme concentrations of heavy metals.

Sulfolobales spp. such as *M. yellowstonii* are found in geothermal springs with high concentrations of dissolved arsenic and HFO mats with over 20% sorbed arsenate (Inskeep et al., 2004). Sequences similar to *ars*A and *ars*C are not found in any of the genomes described in this study, but *ars*B is found in both mesophilic and thermophilic iron-oxidizers. Whether *ars*B alone is sufficient for arsenic resistance is unknown and RNA and protein expression work is crucial for determining additional mechanisms involved in arsenic resistance. An undefined metal efflux ATPase or the novel polyphosphate mechanism discussed above may play important roles in arsenic resistance along with components of the Ars protein complex in *M. yellowstonii*. Furthermore, *M. yellowstonii* is not capable of chemolithotrophic growth on arsenite and does not contain the *aro*AB genes necessary for this chemolithotrophic metabolism.

M. yellowstonii contains two copies of *mer*A; one related most closely to *M. sedula* at 61% (a.a relatedness) and one related most closely to *Thermoplasma acidophilum* at 41%. Directly upstream from the *T. acidiphilum*-like *mer*A is a novel

*mer*B sequence and is particularly interesting because *mer*B has not yet been described in the domain Archaea (Figure 5.7). The novel *M. yellowstonii mer*B sequence is most closely related to the sequence from *Arthrobacter chlorophenolicus* (at 24% a.a. similarity) suggesting a highly novel hypothetical methyl mercury lyase. The sequence alignment (Figure 5.8) highlights the active conserved region, which contains two cysteine residues at alignment position 107 and 174 required for activity (Di Lello et al., 2004; Pitts and Summers, 2002).

The *M. yellowstonii* deduced MerB sequence modeled well with the Protein Data Bank (PDB) 1S6LA MerB crystal (Lafrance-Vanasse et al., 2008), and the active site is shown in Figure 5.9. The conserved cysteine residues are shown with crystal model numbers. The proposed active site is quite similar to the 1S6LA crystal except *M. yellowstonii* has a proline in place of cys160 and the polar residues Phe103 and Try95 in place of tyrosines. Methyl mercury lyase activity has yet to be confirmed in *M. yellowstonii,* but the novel sequence likely codes for the highest temperature MerB observed to date.

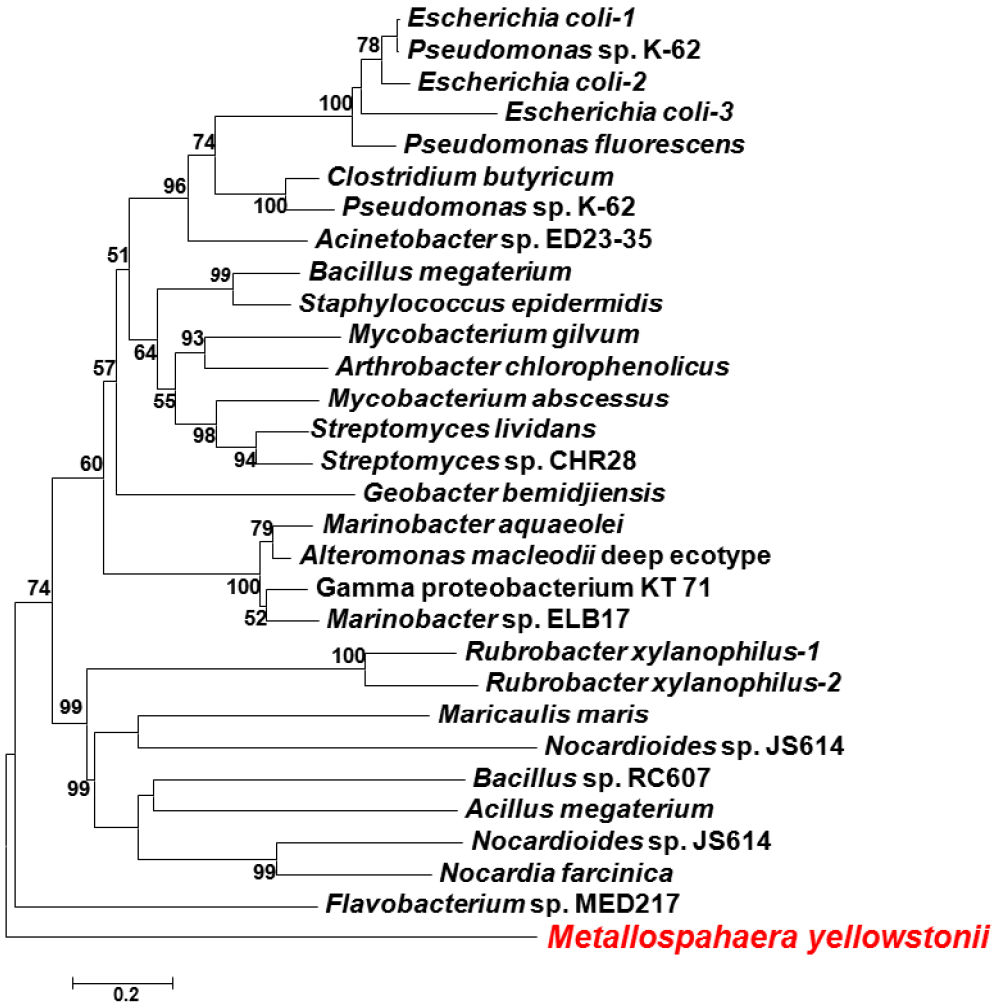

Figure 5.7. Phylogenetic tree of methyl mercury lyase (MerB) deduced protein sequences (sequence alignment of 240 a.a length). The deeply branching *M. yellowstonii* sequence is shown in bold and red and represents the only MerB sequence known in the archaeal domain.

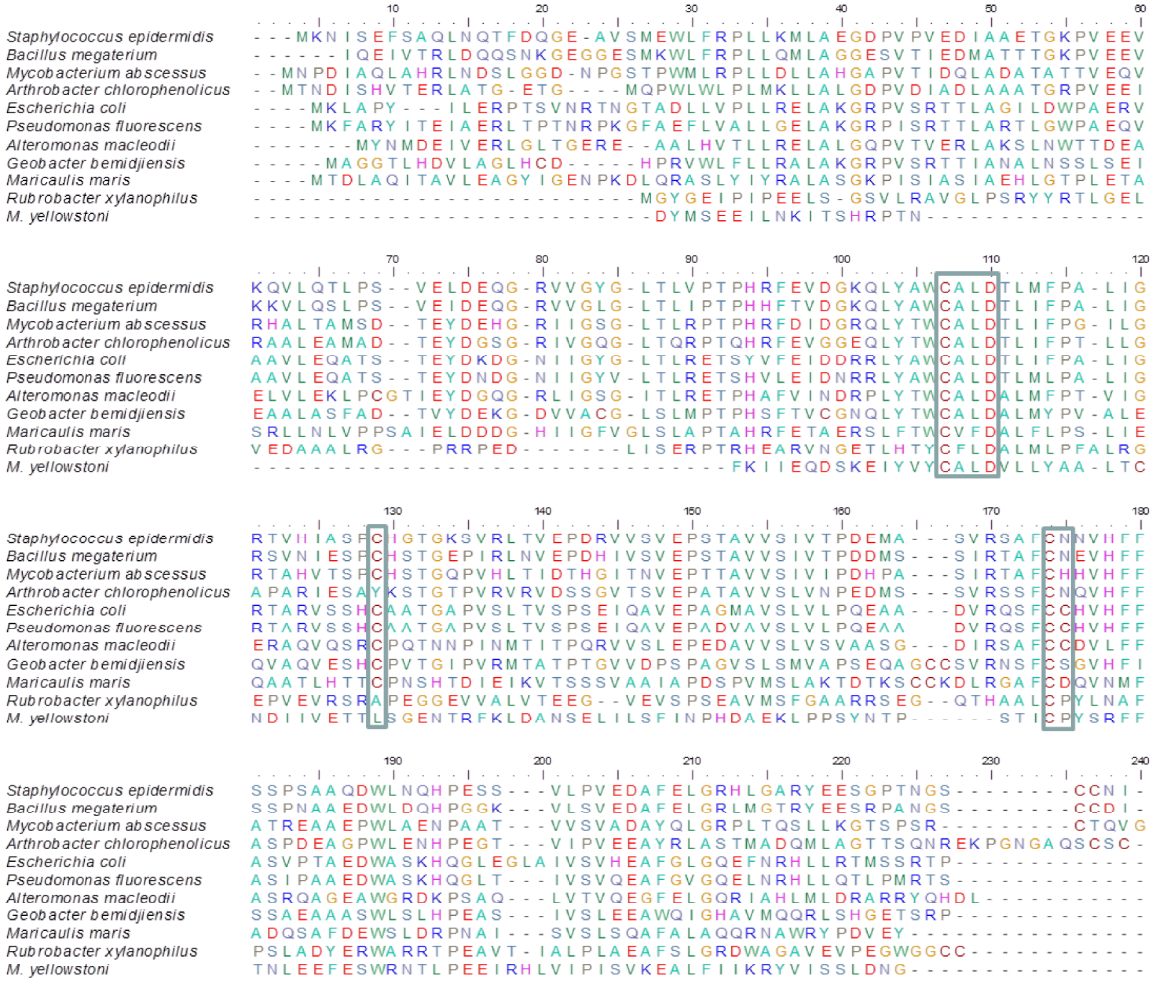

Figure 5.8. Alignment of mercuric lyase protein sequences including *M. yellowstonii*. Boxes indicate the active conserved regions, which include two cysteine residues at alignment position 107 and 174 required for activity.

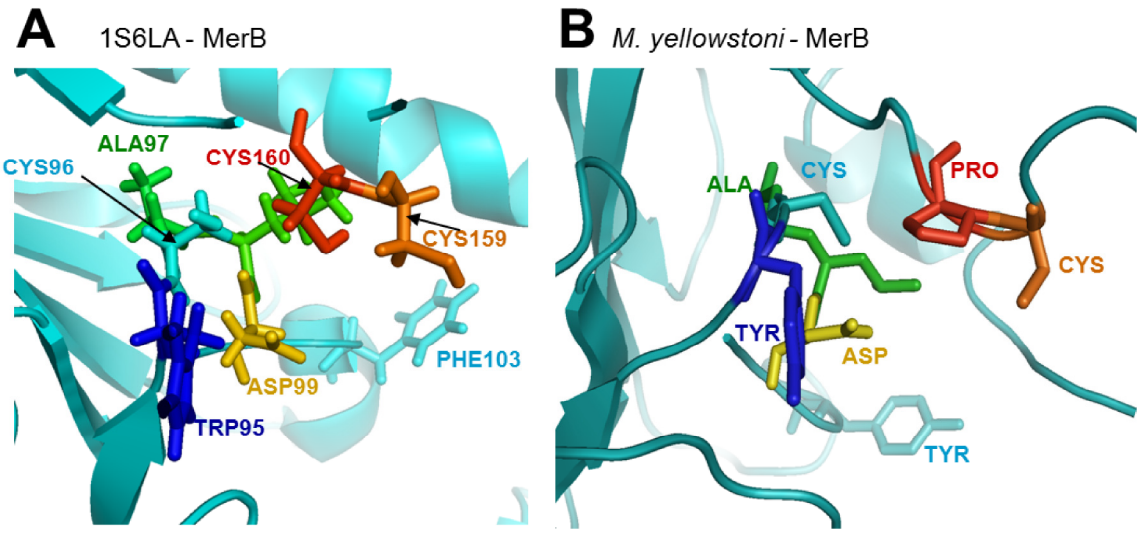

Figure 5.9 Active site of the crystal structure (A) of the methyl mercury lyase (MerB) determined in *E. coli* (PDB:1S6LA) and a structural model (B) of the *M. yellowstonii* MerB. The active residues responsible for methyl cleavage in the 1S6LA protein include Cys96 (cyan) and Cys159(orange). Corresponding Cys residues in cyan and orange are shown for the *M. yellowstonii* MerB model.

Summary

A summary of the different genes or metabolic pathways discussed in this study is shown in Table 5.1. Of particular interest is the diversity of terminal oxidases in iron-oxidizing species. A vast proportion of this known diversity belongs to the Crenarchaeota and especially the Sulfolobales, which has profound implications for origins of aerobic respiration in higher Eukaryotes. A high diversity of Sulfolobales HCOs may be linked to a myriad of electron donors and geochemical niches available to them. Furthermore, the Sulfolobales likely evolved over a long evolutionary period as compared to other prokaryotes and eukaryotes. The geological isolation of Sulfolobales acidic and thermophilic habitats may have allowed for high diversification of HCO sequences over

bilions of years especially given the varied oxygen levels, pH, temperature and electron donors available for chemolithotrophic growth in these environments. HCO sequences appear to have a high degree of horizontal gene transfer based on observations of phylogenetic trees and, therefore, Sulfolobales sequences may have transferred to mesophilic species and then evolved with higher eukaryotes.

Understanding the mechanisms of iron/sulfur oxidation, CO_2 fixation, and trace element resistance in acidophilic prokaryotes has implications in linking functional genes to environmental and geochemical niches. Additionally, enzymes that allow for a competitive advantage may be genetically engineered into desired microorganisms for bioremediation and biomining applications. Practical applications exist for utilizing thermophilic iron- and sulfur-oxidizing acidophiles in biomining of metal ores and bioremediation of heavy metal contaminated waste sites. The prospects of utilizing genetically engineered microorganisms in bioremediation and biomining are real possibilities once the metabolisms for sulfur and iron oxidation are determined.

Further studies utilizing genomic and proteomic techniques are necessary to fully understand these unique microorganisms and include but are not limited to, (1) differential protein and gene expression on entire genomes between sulfur/iron oxidation, heterotrophic vs. autotrophic growth, and heavy metal stress using microarray and 2-dimensional (or multidimensional) protein fractionation methods, (2) isolation of proteins differentially expressed between the aforementioned conditions in order to study their properties (specific activity, spectral properties, and redox potentials), (3) compare CO_2 fixation rates between species, (4) understand the fine structural details of heavy metal

ATPases by site directed mutagenesis, (5) characterize terminal oxidase complexes in regards to redox potentials and the geochemical and growth conditions required for their expression using site directed mutagenesis and knockout mutants, (6) study the evolution of heme copper oxidases, which has implications in understanding the origins of aerobic respiration .

Table 5.1. Putative genes involved in heavy metal resistance, mercury and arsenic metabolism, nitrogen fixation, oxygen reduction, carbon fixation, oxidation of sulfur chemical species, and oxidation of iron for Fe(II) oxidizing acidophiles with genomes available. nd = not detected.

	M. yellowstonii	***M. sedula***	***S. tokodaii***
Thiosulfate oxidation	*tqoAB* (msed0363/msed0364-like)	*tqoAB* (msed0363;msed0364)	*tqoAB* (ST1856;ST1855)
Sulfite oxidation	2 sulfite oxidase (*som*) molybdopterins (related 66% to msed0362;and 65% to msed1107)	2 sulfite oxidase (*som*) molybdopterin (msed0362;msed1107)	3 sulfite oxidase (*som*) molybdopterin (ST0819; ST1095; ST1010)
Sulfide oxidation	two sulfide dehydrogenases and one *sqr*	four sulfide dehydrogenases and one *sqr*	four sulfide dehydrogenases and one *sqr*
S^0 oxidation	*hdr* operon; novel *trd* gene cluster	*hdr* operon; novel *trd* gene cluster	*hdr* operon; novel *trd* gene cluster; *sor* (ST1127)
Fe(II) oxidation	*foxA-J* gene cluster; multi-blue copper protein (msed1206-like)	*foxA-J* gene cluster; multi-blue copper protein (msed1206)	*foxA-J* gene cluster (slow Fe(II) chemolithoautotrophic growth - no multi blue copper enzyme
CO_2 fixation	3-hydroxypropionate/4-hydroxybutyrate cycle	3-hydroxypropionate/4-hydroxybutyrate cycle	3-hydroxypropionate/4-hydroxybutyrate cycle
mercury Metabolism	*mer*AH related 61% to *M. sedula*; *mer*A related 41% to *T. acidophilum*; *mer*B	*merAH*	*mer*AHR
Arsenite Oxidase	nd	nd	*aro*AB (ST2391/ST2392)
Arsenic resistance	*ars*B/R; second *ars*B	*ars*B/R	*ars*B/R
Additional Heavy metal resistance	*znta* ATPase (msed0490-like); Phoshpate export system (*ppnk*: msed0740-like, *ppx*: msed0981-like; 2 *pits* ST0589-like)	*cop*D (msed_1208) without *cop*C; *znta* ATPase (msed0490); Phoshpate export system (*ppnk*: msed0740, *ppx*: msed0981; no *pit*)	*znta* ATPase (st1715); Phosphate export system (*ppnk*: ST2136, *ppx*: ST1544, *pit*: ST0589)
Terminal Oxidase Complexes	*sox*ABCD; *sox*M supercomplex; *dox*BCEF; *fox*A-J gene cluster with three *fox*A subunit I sequences; *dox*B-like (subunit I with polyferredoxin-like domain); a Thermoplasma volcanium-like (37%) *bd* type ubiquinol oxidase	*sox*ABCD; *sox*M supercomplex; *dox*BCE; *fox*A-J gene cluster with two *fox*A subunit I sequences; *dox*B-like (subunit I with polyferredoxin-like domain)	*sox*ABCD; *sox*BC with two sulfocyanins (*sox*E); *sox*M supercomplex; *dox*BCE; *fox*A-J gene cluster with one *fox*A subunit I sequences; *dox*B-like (subunit I with polyferredoxin-like domain)
Nitrogen Fixation	nd	nd	nd

Table 5.1 continued.

	F. acidarmanus	***A. ferroodoxins***	***Leptospirillum* group II**
Thiosulfate oxidation	nd	Thiosulfate oxidation operon (AFE_0041 to AFE_0048) includes *tqo*A (AFE_0044; AFE_0048),*tqo*B (AFE_0048) and a rhodanes-like sequence (AFE_0045)	nd
Sulfite oxidation	1 sulfite oxidase (*som*) molybdopterin (Faci_03001005); aps reductase	APS reductase sequence but no *som*	no *som* or APS reductase sequences
Sulfide oxidation	one sulfide dehydrogenases and one *sqr*	one sulfide dehydrogenases and three *sqr*	two sulfide dehydrogenases and two *sqr*
S^0 oxidation	*sor* (Faci_03001556)	*hdr* operon	none
Fe(II) oxidation	uncharacterized blue copper-haem protein and the a cbb3 terminal oxidase (subunit I - Faci_03001119)	*rus* operon -*coxABCD* (*aa3* type terimal oxidase) - *CysA1/Cys1/Cys2* (cytochromes c) - *rus* (rusticyanin); *cup*	*cyt*572 and *cyt*579 (Singer et al., 2008)
CO_2 fixation	Reductive acetyl-coA; possibly the 3-hydroxypropionate/4-hydroxybutyrate cycle (has 4-Hydroxybutyryl-CoA dehydratase but not the 4-Hydroxybutyryl-CoA synthetase)	Calvin Cycle	Calvin Cycle
mercury Metabolism	*mer*AH	*mer*RTCPADE; two copies of *mer*C	*mer*AH/TP but no *mer*C/F
Arsenite Oxidase	nd	nd	nd
Arsenic resistance	*ars*A/B	*ars*B/C/H, and a putative *arsR* gene	*ars*B (*ars*A in *L. ferrophilum*)
Additional Heavy metal resistance	Components of phosphate export system (*ppnk*: Faci_03001253; no *ppx*; *pit*: Faci_03000617)	*znta* ATPase; *Cop*C; Components of the phoshpate export system (has *ppk*-like sequence only)	*znta* ATPase; possible *copC;* Co/Zn/Cd efflux system components
Terminal Oxidase Complexes	*cbb3*-type terminal oxidase (subunit I - Faci_03001119); two *bd* type quinol oxidases (Faci_03001025; Faci_03000667)	two heme copper oxidases and one *bd*-type quinol oxidase	One heme copper oxidase and two bd ubiquinol oxidases
Nitrogen Fixation	nd	*nif*DK	nd

Acknowledgements

This work was supported by the National Science Foundation Microbial Observatory Program (MCB-0132022), the National Aeronautic and Space Administration (NASA) via funds provided to the Thermal Biology Institute at Montana State University (Project Numbers NAG5-8807, NNG04GR46G), and the Montana Agricultural Experiment Station (Project 911398). Special thanks to SymBio for sequencing efforts and DOE-JGI for annotation and orf calling. In addition, we would like to thank C. Hendrix and T. Olliff for permitting this work in Yellowstone National Park (Permit YELL-2007-SCI-1976).

References

1. Arnold K., Bordoli L., Kopp J., and Schwede T. (2006). The SWISS-MODEL Workspace: A web-based environment for protein structure homology modelling. Bioinformatics, 22,195-201.

2. Auernik K.S., Maezato Y., Blum P.H., and R. M. Kelly. 2008. The Genome Sequence of the Metal-Mobilizing, Extremely Thermoacidophilic Archaeon *Metallosphaera sedula* Provides Insights into Bioleaching-Associated Metabolism. Appl. Environ. Microbiol. 74: 682-692.

3. Auernik K.S., and RM Kelly. 2008. Identification of components of electron transport chains in the extremely thermoacidophilic crenarchaeon Metallosphaera sedula through iron and sulfur compound oxidation transcriptomes. Appl Environ Microbiol. 74: 7723-32.

4. Baker, B.J. and J. F. Banfield. 2003. Microbial communities in acid mine drainage. FEMS Microbiology Ecology. 44: 139-152.

5. Baker-Austin C, Dopson M, Wexler M, Sawers RG, Stemmler A, Rosen BP, Bond PL. 2007. Extreme arsenic resistance by the acidophilic archaeon 'Ferroplasma acidarmanus' Fer1. Extremophiles.11: 425-34.

6. Barkay T, Miller SM, and A.O. Summers.2003. Bacterial mercury resistance from atoms to ecosystems. FEMS Microbiol Rev. 27: 355-84.

7. Bathe, S. and P. R. Norris. 2007. Ferrous Iron- and Sulfur-Induced Genes in *Sulfolobus metallicus.* Appl. Environ. Microbiol. 73: 2491-2497.

8. Berg I.A., Kockelkorn D, Buckel W, Fuchs G. A. 2007. 3-hydroxypropionate/4-hydroxybutyrate autotrophic carbon dioxide assimilation pathway in Archaea. Science. 318: 1782-6.

9. Berg I.A., Ramos-Vera W.H., Petri A, Huber H, Fuchs G. 2010.Study of the distribution of autotrophic CO_2 fixation cycles in Crenarchaeota. Microbiology. 156: 256-69.

10. Blake, R. and D.B Johnson. 2000. Phylogenetic and biochemical diversity among acidophilic bacteria that respire on iron. In: Environmental Microbe–Metal Interactions (Derek, L., Ed.). 53–78. ASM Press, Washington, DC.

11. Bond PL, Druschel GK, Banfield JF. 2000. Comparison of acid mine drainage microbial communities in physically and geochemically distinct ecosystems. Appl Environ Microbiol. 66: 4962-71.

12. Branco R, Chung AP, Johnston T, Gurel V, Morais P, Zhitkovich A. 2008. The chromate-inducible chrBACF operon from the transposable element TnOtChr confers resistance to chromium(VI) and superoxide. J Bacteriol. 190: 6996-7003.

13. Brierley, C. L., and J. A. Brierley. 1973. A chemoautotrophic and thermophilic microorganism isolated from an acid hot spring. Can. J. Microbiol. 19: 183–188.

14. Brock, T. D., K. M. Brock, R. T. Belly, and R. L. Weiss. 1972. Sulfolobus: a new genus of sulfur-oxidizing bacteria living at low pH and high temperature. Arch. Mikrobiol. 84: 54–68.

15. Bryan C.G., and D.B. Johnson. 2008. Dissimilatory ferrous iron oxidation at a low pH: a novel trait identified in the bacterial subclass Rubrobacteridae. FEMS Microbiol Lett. 288: 149-55.

16. Cardona, S. T., F. P. Chavez, and C. A. Jerez. 2002. The exopolyphosphatase gene from Sulfolobus solfataricus: characterization of the first gene found to be involved in polyphosphate metabolism in archaea. Appl. Environ. Microbiol. 68: 4812–4819.

17. Castresana J., Lübben M., and M. Saraste. 1995. New archaebacterial genes coding for redox proteins: implications for the evolution of aerobic metabolism. J Mol Biol. 250: 202-10.

18. Clark, T. R., F. Baldi, and G. J. Olson. 1993. Coal depyritization by the thermophilic archaeon *Metallosphaera sedula*. *Appl Environ Microbiol* 59: 2375–2379.

19. Cox J.C., and D.H. Boxer. 1978. The purification and some properties of rusticyanin, a blue copper protein involved in iron(II) oxidation from Thiobacillus ferro-oxidans.Biochem J. 174: 497-502.

20. Dahl C, Engels S, Pott-Sperling AS, Schulte A, Sander J, Lübbe Y, Deuster O, Brune DC. 2005. Novel genes of the dsr gene cluster and evidence for close interaction of Dsr proteins during sulfur oxidation in the phototrophic sulfur bacterium Allochromatium vinosum. J Bacteriol. 187: 1392-404.

21. Davis I.W., Leaver-Fay A, Chen VB, Block JN, Kapral GJ, Wang X, Murray LW, Arendall WB 3rd, Snoeyink J, Richardson JS, Richardson DC. 2007. Nucleic

Acids Res. MolProbity: all-atom contacts and structure validation for proteins and nucleic acids. 35(Web Server issue):W375-83.

22. de la Torre, J.R., B.M. Goebel, E.I. Friedmann, and N.R. Pace. 2003. Microbial diversity of cryptoendolithic communities from the McMurdo Dry Valleys, Antarctica. Applied Environmental Microbiology. 69: 3858-3867.

23. Di Lello P., Benison G.C., Valafar H., Pitts K.E, Summers A.O., Legault P., and Omichinski J.G. 2004. NMR structural studies reveal a novel protein fold for MerB, the organomercurial lyase involved in the bacterial mercury resistance system. Biochemistry.43: 8322-32.

24. Forte E., Borisov VB, Konstantinov AA, Brunori M, Giuffrè A, Sarti P. 2007. Cytochrome bd, a key oxidase in bacterial survival and tolerance to nitrosative stress. Ital J Biochem. 56: 265-9.

25. Friedrich CG, Bardischewsky F, Rother D, Quentmeier A, Fischer. 2005. Prokaryotic sulfur oxidation. J. Curr Opin Microbiol. 8: 253-9.

26. Fuchs T., H. Huber, K. Teiner, S. Burggraf, and K.O Stetter. 1995. Metallosphaera prunae, sp. nov., a novel metal-mobilizing, thermoacidophilic Archaeum, isolated from a uranium mine in Germany. Syst. Appl. Microbiol. 18: 560-566.

27. García-Horsman J.A., Barquera B., Rumbley J., Ma J., and R.B. Gennis. (1994). The superfamily of heme-copper respiratory oxidases. *J Bacteriol* 176: 5587-600.

28. Hallberg K.B, D.B. Johnson. 2001. Biodiversity of acidophilic prokaryotes. Advances in Applied Microbiology. 49: 37-84.

29. Hedderich R, Hamann N, Bennati M. 2005. Heterodisulfide reductase from methanogenic archaea: a new catalytic role for an iron-sulfur cluster. Biol Chem. 386: 961-70.

30. Huber, G., C. Spinnler, A. Gambacorta, and K.O. Stetter. 1989. Metallosphaera sedula gen. nov. and sp. nov. represents a new genus of aerobic, metal-mobilizing, thermoacidophilic archaebacteria. Syst. Appl. Microbiol. 12: 38-47.

31. Huber G. and K.O. Stetter. 1991. Sulfolobus metallicus, sp. nov., a novel strictly chemolithoautotrophic thermophilic archaeal species of metal-mobilizers. Syst. Appl. Microbiol. 14: 372-378.

32. Hugenholtz P., C. Pitulle, K.L. Hershberger, and N.R. Pace. 1998. Novel division-level bacterial diversity in a Yellowstone hot spring. J Bacteriol. 180: 366-376.

33. Inskeep W.P., R.E. Macur, G. Harrison, B.C. Bostick, S. Fendorf. 2004. Biomineralization of As(V)-hydrous ferric oxyhydroxide in microbial mats of an acid-sulfate-chloride geothermal spring, Yellowstone National Park. Geochimica et Cosmochimica Acta. 68: 3141–3155.

34. Inskeep W.P., G.G. Ackerman, W.P. Taylor, M. Kozubal, S. Korf, and R.E. Macur. 2005. On the energetics of chemolithotrophy in nonequilibrium systems: case studies of geothermal springs in Yellowstone National Park. Geobiology. 3:297-320.

35. Inskeep, W.P., D. Rusch, Z. Jay, M.J. Herrgard, M.A. Kozubal, T.H. Richardson, R.E. Macur, N. Hamamura, B. Fouke, A-L. Reysenbach, F. Roberto, M. Young, R. Jennings, A. Schwartz, S. Korf, E. Boyd, J. Badger, M. Bateson, G. Geesey, E. Mathur and M. Frazier. 2009. Geochemistry underpins metagenome composition (phylogeny and function) in high temperature geothermal springs in Yellowstone National Park. *PLoS One*. 5: e9773.

36. Jackson, C. R., H. W. Langner, J. Donahoe-Christiansen, W.P. Inskeep, and T.R. McDermott. 2001. Molecular analysis of microbial community structure in an arsenite-oxidizing acidic thermal spring. Environmental Microbiology. 3: 532-542.

37. Jan, R.L., J. Wu, S.M. Chaw, C.W. Tsai, and S.D. Tsen. 1999. A novel species of thermoacidophilic archaeon, *Sulfolobus yangmingensis* sp. nov. Int. J. Syst. Bacteriol. 49: 1809-1816.

38. Jeans C., Singer SW, Chan CS, Verberkmoes NC, Shah M, Hettich RL, Banfield JF, Thelen MP. 2008. Cytochrome 572 is a conspicuous membrane protein with iron oxidation activity purified directly from a natural acidophilic microbial community. ISME J. 2: 542-50.

39. Johnson, D.B., and K.B. Hallberg. 2003. The microbiology of acidic mine waters. Research in Microbiology. 154: 466-73.

40. Johnson D.B., and Hallberg K.B. 2005. Acid mine drainage remediation options: a review. Sci Total Environ. 338: 3-14.

41. Jünemann S. 1997. Cytochrome bd terminal oxidase. Biochim Biophys Acta. 1321: 107-27.

42. Kanao T, Kamimura K, Sugio T. 2007. Identification of a gene encoding a tetrathionate hydrolase in Acidithiobacillus ferrooxidans. J Biotechnol. 132: 16-22.

43. Kappler, U., L.I. Sly, and A.G. McEwan. 2005. Respiratory gene clusters of *Metallosphaera sedula* – differential expression and transcriptional organization. Microbiology. 151: 35-43.

44. Kappler A. and K. L. Straub. 2005. Geomicrobiological Cycling of Iron. Reviews in Mineralogy and Geochemistry; 59: 85-108.

45. Kletzin A., Urich T., Müller F., Bandeiras T.M., and C.M. Gomes. 2004. Dissimilatory Oxidation and Reduction of Elemental sulfur in thermophilic archaea. Journal of bioenergetics and biomembranes. 36: 77-91.

46. Komorowski L., Verheyen W., and G. Schäfer. 2002. The archaeal respiratory supercomplex SoxM from S. acidocaldarius combines features of quinole and cytochrome c oxidases. Biol Chem. 383: 1791-9.

47. Konhauser, K. O. 1998. Diversity of bacterial iron mineralization. Earth-Science Reviews. 43: 91-121.

48. Kozubal M., Macur R.E., Korf S., Taylor W.P., Ackerman G.G., Nagy A., and W.P. Inskeep. 2008. Isolation and Distribution of a Novel Iron-Oxidizing Crenarchaeon from Acidic Geothermal Springs in Yellowstone National Park. Appl. Environ. Microbiol. 74: 942-949.

49. Lafrance-Vanasse J, Lefebvre M, Di Lello P, Sygusch J, Omichinski JG. 2008. Crystal structures of the organomercurial lyase MerB in its free and mercury-bound form: Insights into the mechanism of methylmercury degradation. J Biol Chem.

50. Lüthy R, Bowie JU, Eisenberg D. 1992. Assessment of protein models with three-dimensional profiles. Nature. 356: 83-5.

51. Liibben, M., Warne, S., Albracht, S. and M. Saraste. 1994. The purified SoxABCD quinol oxidase complex of *Sulfolobus acidocaldarius*. Molecular Microbiology. 13: 327-35.

52. Ma K., and M.W. Adams. 1994. Sulfide dehydrogenase from the hyperthermophilic archaeon Pyrococcus furiosus: a new multifunctional enzyme involved in the reduction of elemental sulfur. J Bacteriol.176: 6509-17.

53. Macur, R.E., H.W. Langner, B.D. Kocar, and W.P. Inskeep. 2004. Linking geochemical processes with microbial community analysis: successional dynamics in an arsenic-rich, acid-sulfate-chloride geothermal spring. Geobiology. 2: 163-177.

54. Mason MG, Shepherd M, Nicholls P, Dobbin PS, Dodsworth KS, Poole RK, Cooper CE. 2009. Cytochrome bd confers nitric oxide resistance to Escherichia coli. Nat Chem Biol. 5: 94-6.

55. Miroshnichenko, M.L. 2004 Thermophilic microbial communities of deep-sea hydrothermal vents. Microbiology. 73: 1–13.

56. Neumann S, Wynen A, Trüper HG, Dahl C. 2000. Characterization of the cys gene locus from Allochromatium vinosum indicates an unusual sulfate assimilation pathway. Mol Biol Rep. 27: 27-33.

57. Nordstrom, D.K. and G. Southam. 1997. Geomicrobiology of sulfide mineral oxidation. Reviews in Mineralogy. 35: 361-390.

58. Peeples, T.L. and R.M. Kelly. 1995. Bioenergetic response of the extreme thermoacidophile *Metallosphaera sedula* to thermal and nutritional stresses. Appl. Environ. Microbiol. 61: 2314-2321.

59. Pitts K.E, and A.O. Summers. 2002.The roles of thiols in the bacterial organomercurial lyase (MerB). Biochemistry. 41: 10287-96.

60. Prieur, D., M.A Voytek, C. Jeanthon and A.L. Reysenbach. 2001. Deep-Sea Thermophilic Prokaryotes. "Thermophiles: Biodiversity, Ecology and Evolution" pp 11-22. A-L. Reysenbach, M.A. Voytek and R. Mancinelli (eds.). Kluwer Academic/ Plenum Publishers. New York, NY.

61. Purschke, W.G., Schmidt, C.L., Petersen, A., and G Schäfer. 1997. The terminal quinol oxidase of the hyperthermophilic archaeon Acidianus ambivalens exhibits a novel subunit structure and gene organization. J Bacteriol. 179: 1344-53.

62. Quatrini R, Appia-Ayme C, Denis Y, Jedlicki E, Holmes DS, Bonnefoy V. 2009. Extending the models for iron and sulfur oxidation in the extreme acidophile Acidithiobacillus ferrooxidans. BMC Genomics.10: 394.

63. Rawlings, D.E. 2002. Heavy metal mining using microbes. Annual Review of Microbiology. 56: 65-91.

64. Rawlings, D. E. 2005. Characteristics and adaptability of iron- and sulfur-oxidizing microorganisms used for the recovery of metals from minerals and their concentrates. Microbial Cell Factories. 4:13.

65. Rohwerder, T., T. Gehrke, K. Kinzler, and W. Sand. 2003. Bioleaching review part A: progress in bioleaching: fundamentals and mechanisms of bacterial metal sulfide oxidation. Appl. Microbiol. Biotechnol. 63: 239-48.

66. Rosen BP. 2002. Biochemistry of arsenic detoxification. FEBS Lett. 529: 86-92.

67. Sander J, Engels-Schwarzlose S, Dahl C. 2006. Importance of the DsrMKJOP complex for sulfur oxidation in Allochromatium vinosum and phylogenetic analysis of related complexes in other prokaryotes. Arch Microbiol. 186: 357-66.

68. She, Q., R. K. Singh, F. Confalonieri, Y. Zivanovic, P. Gordon, G. Allard, M. J. Awayez, C.-Y. Chan-Weiher, I. G. Clausen, B. Curtis, A. De Moors, G. Erauso, C. Fletcher, P. M. K. Gordon, I. Heidekamp de Jong, A. Jeffries, C. J. Kozera, N. Medina, X. Peng, H. Phan Thi-Ngoc, P. Redder, M. E. Schenk, C. Theriault, N. Tolstrup, R. L. M. Charlebois, W. F. Doolittle, M. Duguet, T. Gaasterland, R. A. Garrett, M. Ragan, C. W. Sensen, and J. Van der Oost. 2001. The complete genome of the crenarchaeon *Sulfolobus solfataricus* P2. Proc. Natl. Acad. Sci. 98:7835-7840.

69. Silver S., and L. T. Phung. 2005. Genes and Enzymes Involved in Bacterial Oxidation and Reduction of Inorganic Arsenic. Appl Environ Microbiol. 71: 599–608.

70. Singer, S. W., C. S. Chan, A. Zemla, N. C. M. VerBerkmoes, M. Hwang, R. L. Hettich, J. F. Banfield, and M. P. Thelen. 2008. Characterization of cytochrome 579, an unusual cytochrome isolated from an iron-oxidizing microbial community. Appl Environ Microbiol. 74: 4454-6.

71. Stetter, K. O. 1999. Extremophiles and their adaptation to hot environments. FEBS Lett. 452: 22–25.

72. Suzuki, T., Iwasaki, T. Uzawa, T. Hara, K. Nemoto, N. Kon, T. Ueki, T. Yamagishi, A. and T. Oshima. 2002. *Sulfolobus tokodaii* sp. nov. (f. Sulfolobus sp. strain 7), a new member of the genus Sulfolobus isolated from Beppu Hot Springs, Japan. Extremophiles. 6: 39-44.

73. Tuffin IM, de Groot P, Deane SM, Rawlings DE. 2005. An unusual Tn21-like transposon containing an ars operon is present in highly arsenic-resistant strains of the biomining bacterium Acidithiobacillus caldus. Microbiology. 151: 3027-39.

74. Valdés J, Pedroso I, Quatrini R, Dodson RJ, Tettelin H, Blake R 2nd, Eisen JA, Holmes DS. 2008. Acidithiobacillus ferrooxidans metabolism: from genome sequence to industrial applications. BMC Genomics. 11: 9:597.

75. Wallner B., and A. Elofsson. 2003). Can correct protein models be identified? Protein Sci. 12: 1073-1086.

76. Wiederstein M.,and M.J. Sippl. 2007. ProSA-web: interactive web service for the recognition of errors in three-dimensional structures of proteins. Nucleic Acids Research. 35: W407-W410.

77. Yarzábal A, Brasseur G, Bonnefoy V. 2002a. Cytochromes c of Acidithiobacillus ferrooxidans. FEMS Microbiol Lett 209:189–195

78. Yarzábal A, Brasseur G, Ratouchniak J, Lund K, Lemesle-Meunier D, DeMoss JA, Bonnefoy V. 2002b. The high-molecular-weight cytochrome c Cyc2 of Acidithiobacillus ferrooxidans is an outer membrane protein. J Bacteriol 184:313–317

APPENDICES

APPENDIX A

MICROBIAL COMMUNITY STRUCTURE OF IRON OXIDE MATS FROM ACIDIC GEOTHERMAL SPRINGS IN YELLOWSTONE NATIONAL PARK: POPULATION DIVERSITY, ISOLATION OF NOVEL SPECIES AND IRON CYCLING

Abstract

Geochemical, molecular, and physiological analyses of microbial isolates were combined to study the geomicrobiology of acidic iron oxide mats in Yellowstone National Park (YNP). Eighteen sampling locations from ten geothermal springs were studied ranging in temperature from 53 to 84 °C and pH from 2.5 to 3.5. All iron-oxide mats exhibited high diversity of crenarchaeal sequences from the Sulfolobales, Thermoproteales, and Desulfurococcales. Sequences from the phyla Thaumarchaeota and Euryarchaeota are also found in numerous iron oxide mats. The predominant Sulfolobales sequences were highly similar to *Metallosphaera yellowstonii* str. MK1. Additional novel archaeal lineages were found to be consistently associated with different types of iron oxide mats. Bacterial sequences were dominated by close relatives of *Hydrogenobaculum* spp. above 65-70 °C, but diversity increased below 60 °C. Efforts to cultivate relevant microbial isolates from these systems were successful and six novel organisms (or co-cultures) were obtained including *M. yellowstonii* str. MK1, discussed previously (Chpater 3-4). The rates of iron oxidation measured in *M. yellowstonii* cultures were less than observed in geothermal springs, but still explain a significant contribution to the total Fe oxidation rate. . Analysis of ferric iron solid phasesfrom *M. yellowstonii* cultures revealed a mixture of hematite, jarosite, ferrihydrite and goethite, whileanalysis of ferric iron phases obtained from Crenarchaeaota sp. MK4 revealed jarosite and goethite. The combination of geochemical and molecular data as well as physiological observations of isolates obtained from these springs suggest that the community structure of acidic Fe

mats is linked with Fe cycling, although significant changes in specific populations were observed across temperatures ranging from 53 to 85 ^{o}C.

Introduction

Hydrous ferric oxide (HFO) and jarositic microbial mats are found in numerous environments and have been well studied in acid-mine-drainage systems such as Iron Mountain, CA (Edwards et al., 1999; Singer et al., 2008) where Fe(II) and H_2SO_4 are produced from the oxidation of sulfide minerals such as pyrite and chalcopyrite (Nordstrom and Southam, 1997; Rohwerder et al., 2003). Abiotic rates of Fe(II) oxidation are very slow at pH values less than 4.5 (1×10^{-7} mol Fe(II) min^{-1}; Singer and Stumm, 1970); therefore, acidophilic microbes have an advantage over neutrophiles by not having to compete for rapid disappearance of Fe(II). Biologically oxidized Fe(II) often accumulates as ferric oxide minerals, which range in thickness and hardness depending on the geochemistry, flow rate and microbial populations in the system (Konhauser 1998; Inskeep et al. 2004). A variety of geothermal ferric iron mats have been characterized in YNP, including 2-4 cm thick amorphous Fe-oxide mats in acid-sulfate-chloride (ASC) springs (pH ~3) at Norris Geyser Basin, and more crystalline ferric oxides (i.e., goethite, hematite) and jarosite in acid sulfate (AS) springs at Rainbow Springs and Joseph's Coat Hot Springs (Inskeep et al., 2005).

Numerous acidic geothermal springs in YNP provide an outstanding natural laboratory to study microorganisms that utilize ferrous iron as an energy source and fix CO_2 as their primary carbon source. Their ability to thrive in high-temperature

environments with minimal requirements other than CO_2 and inorganic constituents suggests that these organisms are important primary producers in acidic high-temperature environments. However, the limited energy available from the oxidation of Fe(II) results in the formation of copious amounts of iron oxides. It has been estimated that at pH 2, approximately 120 mols of Fe(II) must be oxidized for the formation of 1 mol of glucose. Thus, low cell numbers can result in the oxidation of large amounts of iron, which has implications in understanding the biomineralization of iron in many environments outside YNP, as well as throughout Earth's evolutionary history (e.g. banded iron formations; Konhauser 1998; Kappler and Straub, 2005).

Previous work has described the 16S rRNA gene sequence diversity in several iron-rich geothermal springs (Jackson et al., 2001; Inskeep et al., 2004; Macur et al., 2004; Kozubal et al., 2008). Gene (16S rRNA) sequences related to *Hydrogenobaculum*, *Metallosphaera*, *Sulfolobus*, *Acidimicrobium*, *Acidicaldus*, *Meiothermus* and *Sulfobacillus* spp., as well as several novel archaeal lineages have been described from these studies. The phylogenetic similarity of observed sequences to cultivated microorganisms (16S rRNA gene) is not sufficient to definitively link specific metabolisms to these novel microorganisms especially when several groups observed in the iron mats belong to novel clades with distant similarity to cultured organisms (e.g., < 90% 16S rRNA similarity). Therefore, cultivation of representatives from these groups is critical to implicate specific microorganisms and their corresponding metabolic pathways in biogeochemical processes.

The purpose of this study is to integrate past and current results on the geomicrobiology of ferric iron oxide mats in YNP. The specific objectives were to (i) describe the geochemistry of seven acid-sulfate-chloride (ASC) and three acid-sulfate (AS) springs in YNP over a temperature range of 53 to 85 °C and a pH range of 2.5 to 3.6, (ii) determine the community composition of ferric iron mats over a broad range of geothermal conditinos, and (iii) cultivate and study the physiology of novel bacteria and archaea identified using molecular surveys.

Material and Methods

Description of Sites

A total of ten geothermal springs in Yellowstone National Park were chosen for this study and include seven acid-sulfate-chloride springs (ASC) in Norris Geyser Basin, and three acid-sulfate springs (AS) springs from Joseph's Coat and Rainbow Springs. Each spring has one or more sampling points based on transects established witin the main flow channel as a function of distance (temperature) from the outflow source. The ASC springs sampled include *OSP Spring* (74 °C, NGB-OSP14, 62 °C NGB-OSP8), *Beowulf Spring* (62 °C, NGB-BE and 55 °C, NGB-BW), *Gap Spring* (84 °C, NGB-GAPA and 73 °C NGB-GAPB), *Echinus Geyser* (76 °C, NGB-EGA and 70 °C NGB-EGC), *Whirligig Geyser* (66 °C, NGB-WGA), and an unnamed spring in *Porcelain Basin* (referred to as *Big Red;* 85 °C, NGB-PBA). AS springs sampled include an unnamed spring at Joseph's Coat referred to as JC2 (75 °C JC2B, 65 °C JC2C, 56 °C JC2F); and

two unnamed springs at Rainbow Springs referred to as RS2 (73 °C RS2B,69 °C RS2C,53 °C RS2F) and RS3 (56 °C RS3A,53 °C RS3B).

DNA extraction and molecular cloning

The distribution and relative abundance of total archaeal and bacterial 16S rRNA gene sequences were examined for the geothermal springs described above. Microbial mat samples were obtained using sterile tools and collection tubes and were immediately placed on dry ice for transport to a –80°C freezer. Samples were taken at various times over a five year period from July 2003 to July 2008. Total DNA was extracted from the samples (or pure cultures) using a FastDNA SPIN kit for soil (Q-Biogene, Irvine, CA). The nearly full-length PCR primers targeting 16S rRNA genes were the *Bacteria*-specific primer Bac8f (5'-AGAGTTTGATCCTGGCTCAG-3') coupled with the universal primer Univ1392r (5'-ACGGGCGGTGTGTAC-3') and the *Archaea*-specific primer Arc2f (5'-TTCCGGTTGATCCYGCCGGA-3') also coupled with the universal primer Univ1392r. Briefly, each 50-µl PCR mixture contained 10 mM Tris-HCl (pH 8), 50 mM KCl, 0.1% Triton X-100, 4.0 mM $MgCl_2$, each deoxynucleoside triphosphate at a concentration of 800 µM, 0.5 µl of each primer, 1.25 U of *Taq* DNA polymerase (Promega, Madison, WI), and 1 to 5 µl of template DNA (2 to 20 ng). The thermal cycler protocol was 94°C for 6 min, 25 to 35 cycles of 94°C for 45 s, 54°C for 45 s, and 72°C for 110 s, and a final 7-min extension at 72°C. Negative control reactions (no template) were routinely performed to ensure purity. The purified PCR products were cloned using the pGEM-T vector system from Promega Corp. (Madison, WI), and the inserts were amplified and sequenced (TGEN, Phoenix, AZ, and the Ohio State Plant Genomics Facility, Columbus,

OH). In addition to the clone sequences obtained from the method described above, a total of 1348 sequences were obtained from the Joint Genome Institute (JGI) for OSP springs as part of a metagenomic study (Inskeep et al., 2009). The primers used by JGI are *Bacteria* specific 27F (5' -AGAGTTTGATCCTGGCTCAG-3') and 1391R (5'-GACGGGCRGTGWGTRCA-3'), and *Archaea* specific 4aF (5'-TCCGGTTGATCCTGCCRG - 3') and 1391R.

Cultivation and Isolation of Microorganisms

Approximately 2 g of an HFO microbial mat from NGB-BE, NGB-GAPA and NB-OSPB were placed into 60 ml serum bottles with synthetic growth medium as described by Kozubal et al., (2008) at various times between August 2003-August 2008. The cultivation and isolation of *Metallosphaera* sp. strain MK1 is described elsewhere (Kozubal et al., 2008). Isolation of *Sulfobacillus* sp. strain MK2 colonies was obtained by streaking approximately 0.5 ml of NGB-BE slurry on 1.5% agar plates in synthetic media with 0.5 % yeast extract and 10 mM $FeSO_4$. Plates were incubated at 58 °C for up to 12 days. Colonies were transferred to serum bottle cultures with 10 mM $FeSO_4$, 0.2% YE in synthetic media for further study. Pure cultures of Crenarchaeota sp. MK4 and *Acidicaldus* sp. MK6 were obtained by streaking approximately 0.5 ml of OSPB slurry on 1.2% Gelrite® plates in media described by Itoh et al., (2001) with 0.2 % yeast extract and 2 mM $FeSO_4$. Plates were incubated at 65 °C for up to 15 days. Pure colonies of *Acidicaldus* sp. MK6 were transferred to serum bottle cultures with synthetic media and 0.5% YE for further studies. Crenarchaeota sp. MK4 colonies were continuously streak transferred onto Gelrite® plates every 7 to 10 days and are capable of growth in liquid

culture with 0.2% YE, 10 mM glucose and synthetic media (Kozubal et al., 2008). Enrichment co-cultures of Sulfolobales sp. MK5 and *Acidicaldus* sp. MK6 were obtained on Gelrite plates as described above. Sulfolobales sp. MK5 was not viable after transfer to liquid media and co-culture colonies were kept viable by transferring to fresh Gelrite plates every 10-12 days. Sulfolobus sp. MK3 was obtained by dilution to extinction with 2% pyrite in synthetic media by the method described for *Metallosphaera* sp. strain MK1 except inoculum was obtained from GAPA and cultures were incubated at 75 °C. The progress of all cultures was monitored by extracting DNA from the serum bottles, followed by PCR amplification of 16S rRNA genes using universal bacterial and archaeal primers and separation and visualization of the PCR products using denaturing gradient gel electrophoresis (DGGE; Macur et al., 2004). The purity of cultures was also confirmed by cloning and sequencing of longer 16S rRNA gene fragments.

Growth Characteristics of the Isolates

pH and temperature optima was determined for all isolates in 20 mL serum bottles with 5-ml gas headspace composed of 25% O_2, 50% CO_2, and 25% air. Heterotrophic growth was determined with the addition of 0.5% Yeast Extract; autotrophic growth with either 2% pyrite, 2% S^0 or 5 mM Fe(II)SO_4 without added carbon; and mixotrophic growth with 5 mM Fe(II)SO_4 and 0.5% YE. Anaerobic growth was determined with Fe(III) a in 20 ml serum bottles with 15 ml of synthetic media, 0.5 grams of double autoclaved NGB-BE HFO mat (120 °C), 10 mM glucose, and 0.5% YE. Serum bottle cultures were sealed and purged with N_2 gas for 20 minutes to obtain anaerobic conditions.

Iron Oxidation and Reduction Rates

Iron oxidation rates were determined for *Metallosphaera* sp. MK1 in 120 ml serum bottles with 1 gram of crushed and triple autoclaved NGB-BE HFO mat and 60 ml of BED synthetic media with 10mM $FeSO_4$ without added carbon and a headspace composed of 50% O_2 and 50% CO_2. Fe(II) oxidation rates were determined with an initial cell culture of approximately 10^6 cells per ml added at exponential growth phase. Abiotic Fe(II) rates were determined with un-inoculated controls. 1 ml filtered (0.2 micron filters) samples were taken immediately after addition of 10 mM Fe(II) and every 10 minutes for four hours. Fe(II) was measured promptly by the ferrozine method (To et al., 1999).

Iron reduction rates were determined for *Acidicaldus* sp. MK6 in 120 ml serum bottles with 80 ml of synthetic medium, 10 mM glucose as the electron donor and 1-gram triple autoclaved HFO mat from NGB-BE which has been previously characterized (Inskeep et al., 2004). Serum bottles were purged with nitrogen gas for 20 minutes prior to inoculation. Samples were inoculated to an initial concentration of 10^5 cells/ml and 1 ml filtered samples were taken twice daily for 10 days and analyzed for Fe(II) as stated above. Cell concentrations were determined by SYBR gold staining and reduction rates were calculated as Fe(III) reduction per minute per 10^8 cells.

Solid Phase Chemical Analysis

Solid phase analysis was done on sample scrapings obtained from *Metallosphaera* sp. strain MK1 culture vessels after 11 days of incubation in spring water obtained from

Beowulf spring and 2% ground pyrite at 65 °C and pH 3.0. The culture vessel had two distinct phases of iron oxides including an approximately 0.5 cm dark red ring at the media/O_2 boundary beneath which was a yellow colored phase. Approximately 0.5-1 gram of each phase was scraped from the bottles and analyzed by X-ray diffraction (XRD) or X-ray absorption.

Synchatron Iron K-edge X-ray absorption spectroscopy was performed at SSRL on beamline 4–1 using an unfocused beam detuned approximately 50% to eliminate higher order harmonics. The transmitted energies were monitored using N_2-filled ionization chambers, the fluorescence yield was determined using a Stern-Heald type fluorescence detector equipped with 6 μM Mn filters. Spectra were obtained from about -200 to +1000 eV. To avoid self-absorption phenomena, the samples were dispersed and a thin film of solid phase was mounted on a polycarbonate membrane so that the change in optical density across the Fe K-edge was less than 0.1 U. Fluorescence spectra were then compared to transmission data to confirm that self-absorption dampening was eliminated. Iron X-ray absorption near edge structure (XANES) spectra of normalized spectra were compared to model compounds including (but not limited to) goethite, hematite, 6-line ferrihydrite, jarosite, lepidocrocite, magnetite, and vivianite. Linear combination fitting were obtained with the SixPack Version 0.62 software.

X-ray diffraction was obtained using a XRD on powderized fractions with grains in random orientations. Data reduction routines were utilized to determine peak position, relative intensities, and calculate intracrystalline d-spacing and compared to ASTM powder diffraction files for identification of crystalline minerals.

Microscopy

Optical images were obtained utilizing a Zeiss epifluorescence microscope (Zeiss Axioskop 2 plus; Zeiss, Oberkochen, Germany). Samples were stained with 10X SYBR-green for fluorescent images. Environmental samples for scanning electron microscopy (SEM) images were stored at 4 °C prior to analysis. Samples were analyzed with either a scanning electron microscope (SEM) equipped with an Energy-Dispersive X-ray Spectrometer (EDS) for elemental composition or a field emission scanning electron microscope (FE-SEM).

16S rRNA analyses

Consensus 16S sequences obtained by molecular cloning were obtained by assembling overlapped forward and reverse reads using Sequencher 4.8 (Ann Arbor, MI). 16S rRNA sequences were compared to deposited sequences in public databases using the blastn algorithm. 16S rRNA sequence alignments were performed using ClustalX (version 1.81) and gaps were edited with Se-Al v2.0a11. Distance analysis was performed using the Jukes and Cantor correction (1969), followed by phylogenetic tree construction using the maximum likelihood method of PAUP*4.0 software (Sinauer Associates, Sunderland, MA) after 1000 boot straps.

Results

Geochemistry of AS and AS springs

The major electron donors, pH, site temperature, oxygen concentration and solid phase geochemistry of three acid-sulfate (JC2, RS2, RS3) and seven acid-sulfate-chloride

geothermal springs (NGB-OSP, NGB-BE, NGB-BW, NGB-GAP, NGB-WG, NGB-EG, NGB-PB) are summarized across a total of 18 sampling positions (Table AA.1). Concentrations of ammonium (NH_4) are ~20-30 times higher in AS springs compared to ASC springs, however, in either spring type, NH_4 levels do not change as a function of distance from the spring source. Concentrations of arsenite (represented here as As(III)) are generally 10 to 100 times higher in ASC springs compared to AS springs, although one near-neutral AS geothermal pool at Joseph's Coat (referred to as JC3) contains up to 120 μM total soluble As (Taylor, 2007). Aqueous methane concentrations (CH_4(aq)) range from < 0.01 μM in NGB-GAP to 3.5 μM in RS3A and decrease as a function of distance from the source in RS2 and RS3. Aqueous hydrogen concentrations (H_2 (aq)) range from 11 nM in NGB-PB to 225 nM in NGB-GAP and concentrations generally decline downstream from spring discharge. Aqueous Fe(II) is available in all springs ranging from 25 μM in NGB-OSP to 236 μM in RS3. In the majority of systems studied here, aqueous Fe(II) concentrations do not decline significantly as a function of distance from discharge, although exceptions to this observation were noted in some sites (e.g., levels of Fe(II) decline from 81 to 34 μM in RS2).

Table AA.1. Geochemistry of acid-sulfate-chloride springs in Norris Geyser Basin (NGB) and acid-sulfate springs in Joseph's Coat (JC) and Rainbow Springs (RS) indicating concentrations of major electron donors, O_2 and solid phase analysis. nd = not determined; * = metagenome sample. See Table 3.1 for Lat-Long data.

Spring ID[2]	Position (m)	T (C°)	pH	NH_4 *µM*	As^{iii} *µM*	H_2S *µM*	H_2 *nM*	CH_4 *µM*	Fe^{II} *µM*	O_2 *µM*	Solid Phase Fe(III)
NGB-BE	***D (6)**	67	3.0	72	28	11.5	15	0.39	32	32	2-4 cm amorphous HFO
	E (7.5)	62	3.0	68	20.8	3.5	15.9	0.14	30	72	(~0.62 mol sorbed AsV)
NGB-BW	**D (8.4)**	55	3.0	68	21.5	2.4	10.8	0.3	30.5	87	~0.2 cm amorphous HFO (~0.62 mol sorbed AsV)
NGB-OSP	**A (0)**	74	3.4-3.6	nd	20.4	13.0	89	0.1	37.6	13	2-4 cm amorphous HFO
	***14/B(2)**	63-74	3.4-3.6	80	20.1	12.1	108	0.35	25.6	42	(~0.62 mol sorbed AsV)
	***8 (3)**	62	3.6	80	20.6	0.1	nd	nd	25.0	76	OSPB Grey streamers
NGB-GAP	**A (0)**	84	3.3	69	22.9	10.7	225	<0.01	76.9	28	2-4 cm amorphous HFO
	B (0.12)	73	3.2	71	20.2	1.9	20.9	<0.01	63.3	32	(~0.62 mol sorbed AsV)
NGB-WG	**A (0)**	66	3.4	74	nd	< 0.3	20	0.36	nd	nd	amorphous HFO w/ sorbed AsV
NGB-EG	**A (0)**	76	3.5	66	nd	3.5	111	0.37	nd	nd	goethite and hematite
	C (10)	70	3.4	69	nd	< 0.3	nd	nd	nd		
NGB-PB	**A (0)**	85	3.4	68	nd	1.3	11	<0.01	nd	nd	amorphous HFO
JC2	**B (2.7)**	75	2.5	2180	0.18	2	52.6	0.3	80.6	9	JC2B/C – Hematite
	C (7.1)	65	2.5	2420	0.08	3.8	65.7	0.3	68.5	43	JC2F – S^0
	F (22.0)	58	2.4	2350	0.25	20.2	27.0	2.6	78.9	47	
RS2	**B (2.2)**	73	2.5	1740	2.5	2.8	32	2.2	81.2	22	jarosite, goethite
	D (8.3)	69	2.6	1760	3.0	1.8	36.7	0.9	78.4	44	
	F (12.6)	53	2.5	1750	1.0	0.1	28.3	<0.01	33.8	102	
RS3	**A (0)**	54	3.3	1560	1.0	< 0.3	11	3.46	219	< 1	goethite, jarosite
	B (0.9)	54	3.3	1560	1.7	< 0.3	nd	nd	236	14	

Solid phase analysis has been completed for iron-oxide mat samples from all sites discussed in the current study (Inskeep et al., 2004; 2005). Springs in NGB containing high levels of arsenate (oxidized by *Hydrogenobaculum*-like organisms, Hammamura et al., 2009) tend to form amorphous hydrous ferric oxide (HFO) phases (As:Fe=0.6-0.7) with particle sizes near 1 nm (e.g., sites NGB-BE, -BW, -OSP, -GAP). Arsenate (As(V)) is sorbed to HFO edge sites via a bidentate, binuclear surface complex (Inskeep et al., 2004). Sites containing more crystalline phases such as hematite, goethite and jarosite ($KFe_3(OH)_6(SO_4)_2$) contain much lower levels of As, higher concentrations of Fe(II) and

or lower pH (Table AA.1; i.e., sites JC2, RS1 and RS2). The outflow channels of RS1, RS2 and JC2 contain higher concentrations of sulfate, potassium and Fe(III) than other sites, and jarosite is a predominant phase in these systems. It is important to note that jarosite contains Fe(III), and requires that Fe(II) be oxidized by some mechanism (Kappler and Straub, 2005). As stated previously, the abiotic rate of Fe oxidation is quite slow at low pH, so biological mechanisms are likely responsible for the majority of iron-oxides and jarosite deposited in these systems.

Both RS2 and JC2 show significant oxidation of Fe(II) as a function of distance from the spring source as evinced by corresponding increases in aqueous phase Fe(III). The oxidation of Fe(II) in JC2 at six sampling points (Figure AA.1) shows that approximately 45% is oxidized by sampling position JC2D. The residence time from JC2A to JC2D is 35 seconds! At sampling position JC2E, a second spring source emerges and Fe(II) is reset to near 100% of the total dissolved iron; approximately 43% is oxidized to Fe(III) by sampling point JC2F, a 32 second residence time. Measurements of channel velocities and estimates of total flow rate were used to approximate in situ iron oxidation rates throughout the JC2, RS1 and RS2 channels. The average rate of Fe(II) oxidation observed between sampling points A-D and E-F was ~1.3 ± 0.3 μmoles Fe(II) L^{-1} sec^{-1}.

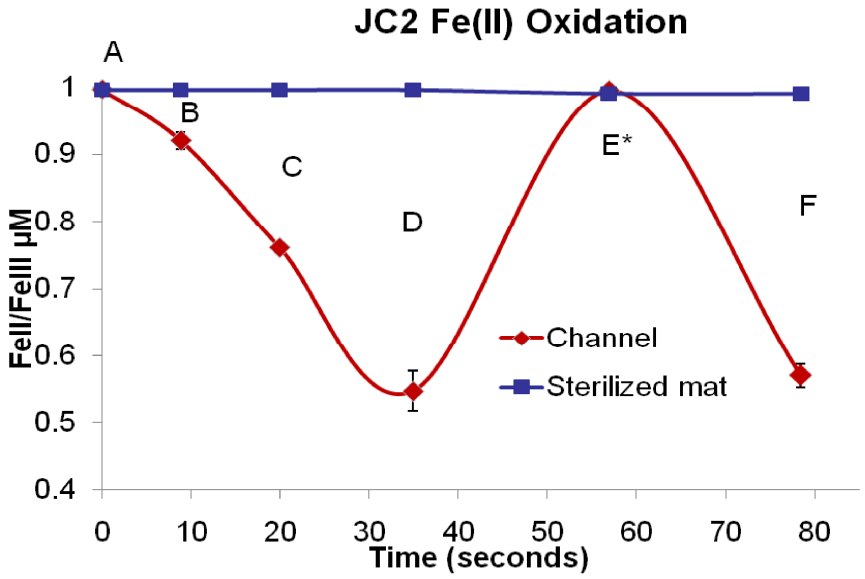

Figure AA.1. Iron oxidation (expressed as Fe(II)/Fe(III)) as a function of time in the outflow channel of an acidic geothermal spring at Joseph's Coat Springs (JC2). Total Fe at the source (JC2A) is 99.8 µM and is nearly 100% Fe(II). Approximately 45% of the total ferrous Fe is oxidized to form Fe(III) within 35 seconds corresponding to sampling position D. *Sampling position E is a second spring source that contains reduced iron.

Microbial diversity of ASC and AS springs

Sequences (16S rRNA) from all crenarchaeal orders (Sulfolobales, Desulfurococcales, and Thermoproteales) are found in ASC springs (Figure AA.2; colored green, AS springs are colored blue). In addition, these iron mats contain two deeply-rooted novel lineages (referred to as Crenarchaeota groups I and II), and a potential new genus within the order Sulfolobales. Sequences related to members of the candidate phylum Thaumarchaeota and Euryarchaeota were also observed in iron mats (Figure AA.3). The novel euryarchaeal sequences were observed in OSP and JC2 and are most closely related to *Thermoplasma volcanium*. In general, AS springs exhibit similar

microbial diversity compared to ASC springs, however, sequences from the Thermoproteales and Crenarchaeota group I are not represented.

Nearly 100% of bacterial 16S rRNA gene sequences were *Hydrogenobaculum*-like at sampling locations above 69 °C in both ASC and AS geothermal springs. Bacterial diversity tends to increase as temperature decreases especially below 55 °C (Figures AA.4 and AA.5). Below 55 °C, sequences related to *Acidimicrobium*, *Acidovorax*, *Acidicaldus*, *Methylacidiphilum*, *Meiothermus*, *Geothermobacterium* and *Sulfobacillus* spp. were observed. Many of these bacterial sequences are highly divergent from cultivated relatives (< 91% 16S rRNA similarity), and include a novel clade related to *Geobacter* spp. (represented by sequences RS2F-SK964 and RS2F–SK975; Figure AA.4). The *Geobacter*-like sequences are only approximately 83% (16S rRNA sequence similarity) related to the nearest cultivated delta proteobacteria *Geobacter uraniireducens*. Additionally, clone RS2F-SK971 is only related to *Acidimicrobium ferrooxidans* at 90%; RS2F-SK266 is related to *Sulfobacillus acidophilus* at just 89% and likely represents a new genus of *Sulfobacillus*-like organisms; finally, RS3B-SK292 is related to *Heliobacteriaceae* bacterium SLH at only 83%, representing a highly divergent sequence in the Firmicutes.

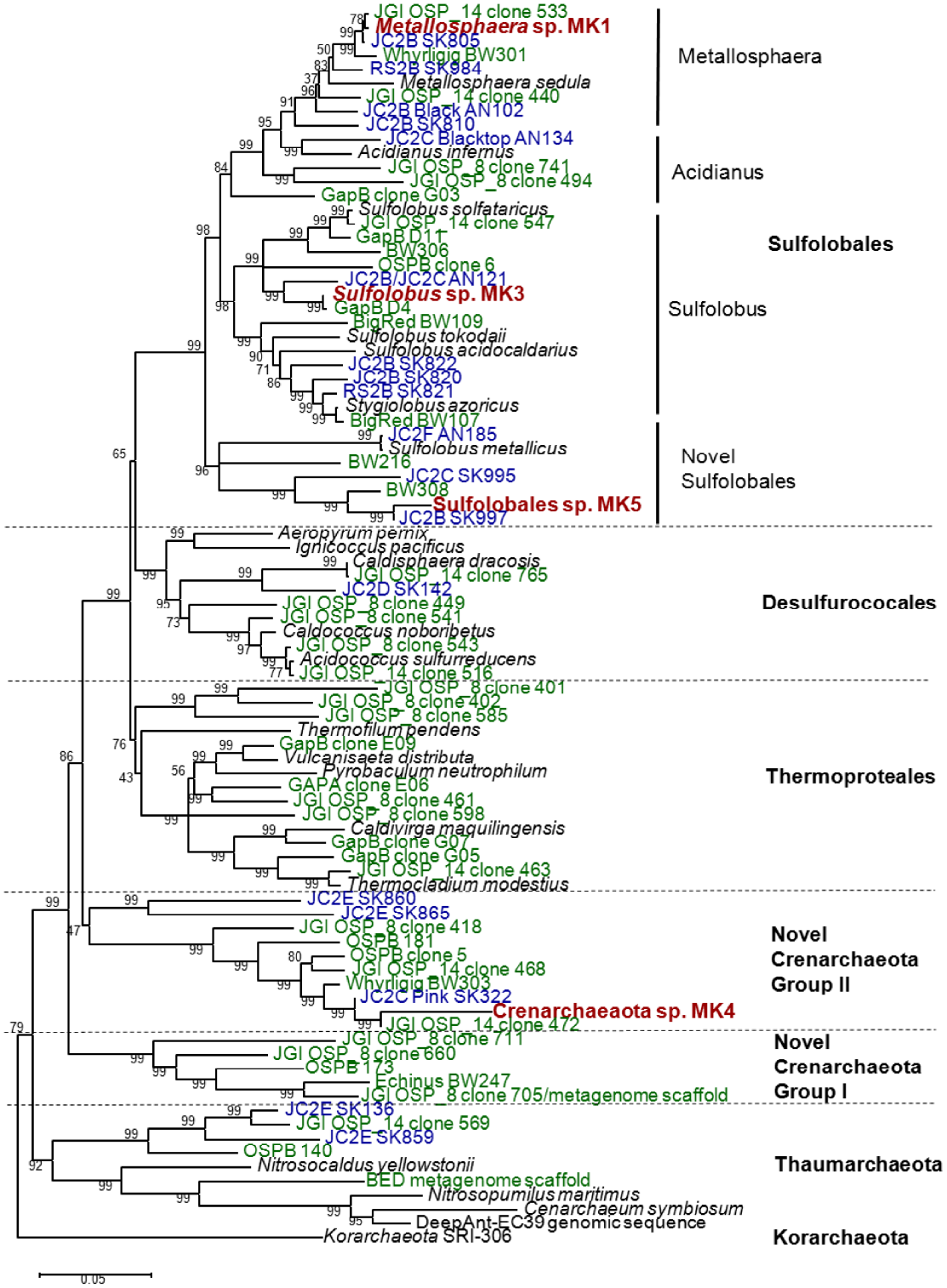

Figure AA.2. Phylogenetic tree of crenarchaeal and thaumarchael 16S rRNA sequences (sequence length ~1400 bp) observed across 18 different acidic iron mats in Yellowstone

National Park (ASC springs are shown in green, AS springs shown in blue, and isolates are highlighted in red).

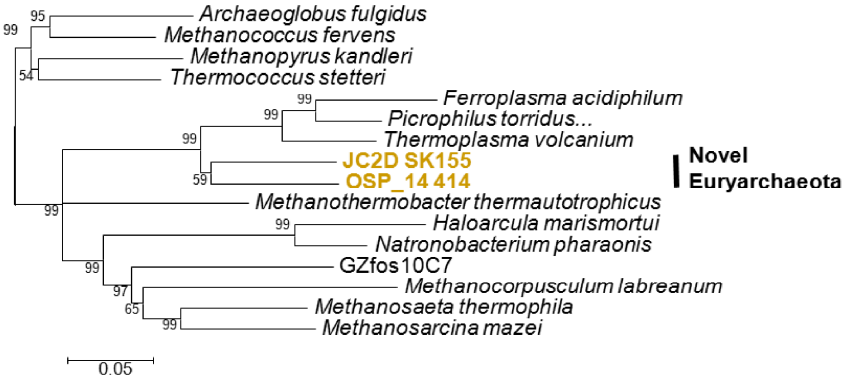

Figure AA.3. Phylogenetic tree of two predominant euryarchaeal 16S rRNA sequences (highlighted in yellow) from JC2 and OSP iron mats in Yellowstone National Park.

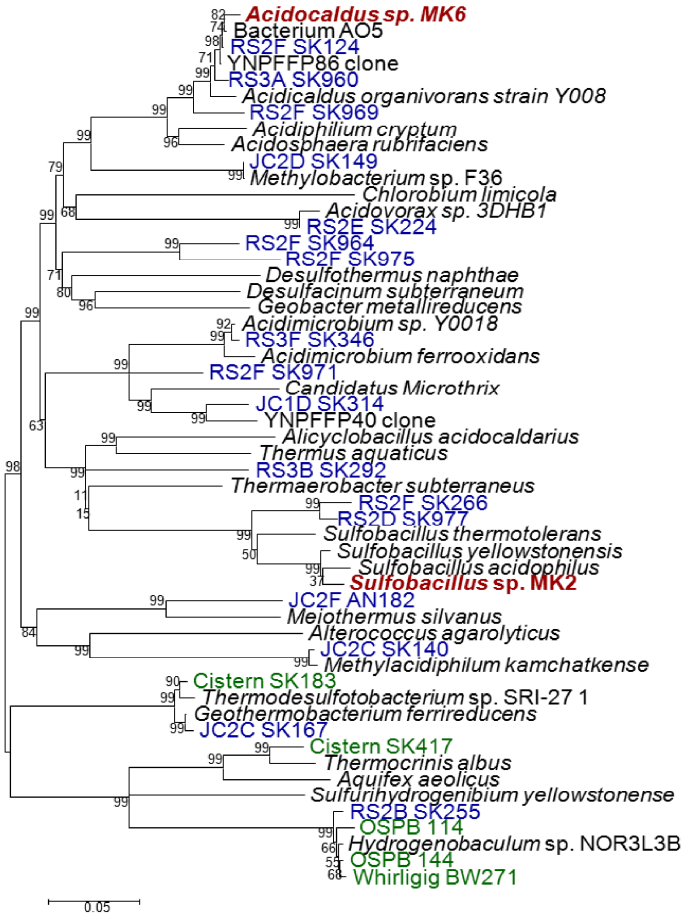

Figure AA.4. Phylogenetic tree of bacterial 16S rRNA sequences (~1400 bp) observed across 18 different acidic iron mats in Yellowstone National Park (ASC springs are shown in green, AS springs shown in blue, and isolates are highlighted in red).

Distribution of Microbial Sequences in Acid-Sulfate Springs

Metallosphaera yellowstonii str. MK1-like and *Hydrogenobaculum*-like 16S rRNA gene sequences represent the dominant archaeal and bacterial phyla detected in JC2 and RS2 above 65 °C. A small percent of sequences related to *Sulfolobus* sp. MK3 and *Stygiolobus* spp. are also found above 69 °C (Figure AA.5). Sequences related to Crenarchaeota Group II represent a high percentage of total archaeal sequences at temperatures below 69 °C, except in site RS3, which is less than 56 °C. Sequences clustering in a novel lineage of Sulfolobales were found at lower temperatures (i.e. RS2F and JC2F). Bacterial diversity increases below 65 °C (especially in RS2F) where *Hydrogenobaculum*-like populations are replaced by sequences related to multiple genera especially *Acidicaldus*, *Geobacter* and *Methylacidiphilum*. *Acidicaldus*-like sequences are especially important below 55 °C (e.g., 60-70% of bacterial clones observed at RS3A, RS3B and JC2C). Archaeal populations found in the lower temperature iron mats (RS3A and RS3B) are significantly different than those observed at higher temperatures (RS2 and JC2). For example, Thaumarchaeal- and *Thermocladium modestus*-like sequences are important in RS3 and were not found in RS2 or JC2.

Distribution of Microbial Sequences in Acid-Sulfate-Chloride Springs

Although similar archaeal populations were observed in acid-sulfate-chloride springs, there is considerably greater archaeal diversity in the amorphous iron oxide mats of Norris Geyser Basin (Figure AA.6). Sequences of particular interest belong to the novel Crenarchaeota Group II, Crenarchaeota Group I and Sulfolobales lineages along with sequences from the Thaumarchaeota (Candidate Phylum)and those related to *M.*

yellowstonii (Figure AA.2). Crenarchaeota Group II sequences are found in all spring locations below 85 °C and dominate in NG-EG, NG-BEE and NG-BWD. Crenarchaeota Group I sequences are particularly well represented in NG-EGA and NG-EGB, but are less important in other Fe mats (e.g. (e.g. NG-BWD, NG-BED and NG-WG). Interestingly, Crenarchaeota Group I sequences were not observed in AS spring locations.

Sequences related to the novel Sulfolobales clade are particularly well represented in NGB-WG, which also contains Crenarchaeota Group II and Crenarchaeota Group I sequences. *Metallosphaera yellowstonii*-like sequences were observedin all springs except the 88 °C NG-GAPA (note: distribution of *Metallosphaera* sequences is discussed in detail in Chapter 3 of this dissertation). The distribution of Thaumarchaeota-like sequences is interesting given that cultured members of this phylum are all mesophilic NH_4 oxidizers. Ammonia oxidation is not observed in AS or ASC springs and, therefore, Thaumarchaeota-like organisms from iron oxide mats represent an important thermophilic lineage with undefined metabolism. Clearly, cultivation of members from Crenarchaeota Group II, Crenarchaeota Group I, the novel Sulfolobales clade and the Thaumarchaeota would improve our understanding of the role of these organisms in microbial community function.

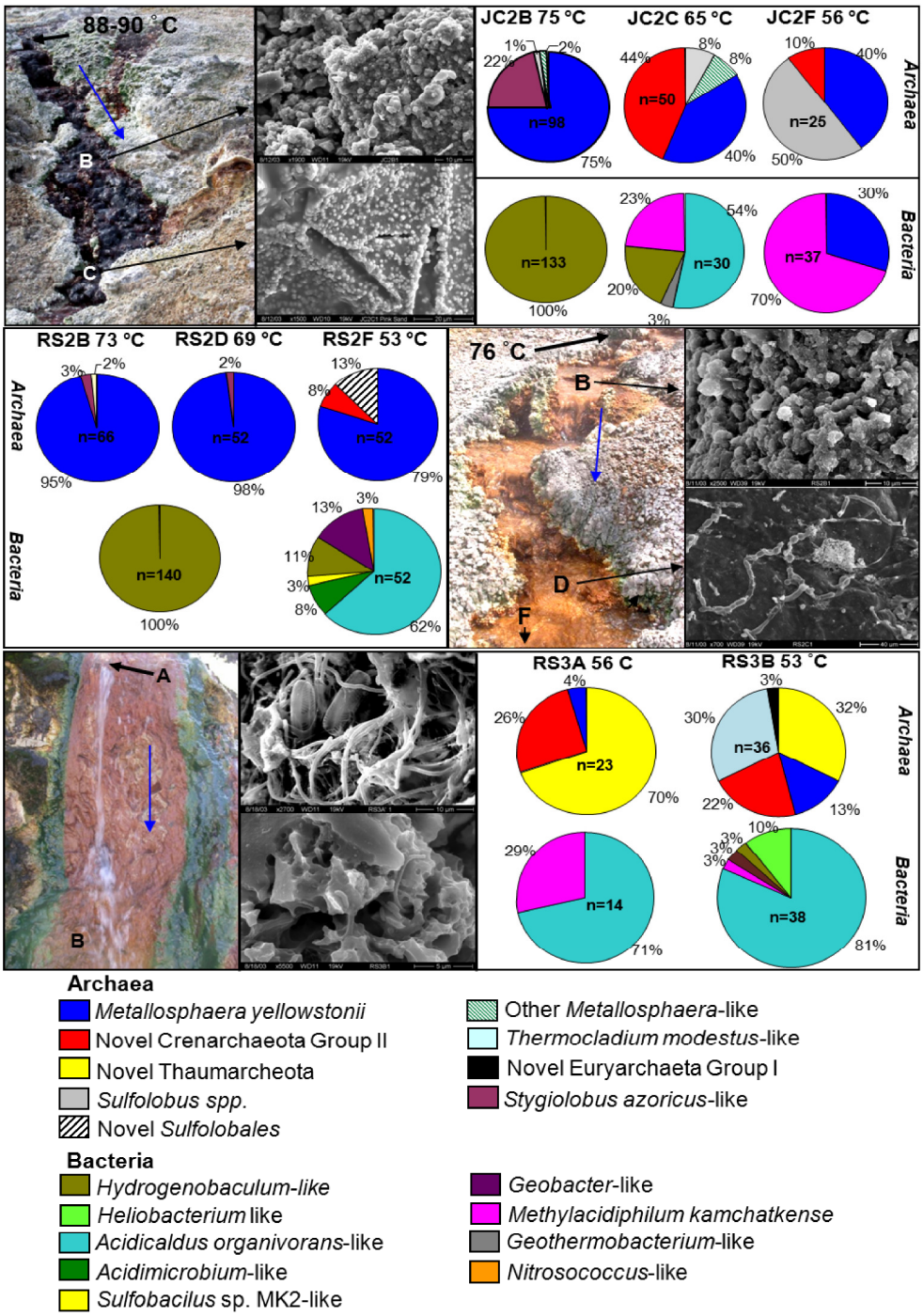

Figure AA.5**.** Images and distribution of 16S rRNA sequences in acid-sulfate (AS) springs. Left: images of springs with source locations and sampling positions labeled. Blue arrows indicate spring flow. Black arrows point to scanning electron micrograph images for various sampling points (Images used courtesy of R.E. Macur and W.P. Inskeep)

The predominant bacterial sequences observed in all ASC springs above 70 °C were closely related to *Hydrogenobaculum* spp. Bacterial clone libraries have yet to be completed on NG-BEE and NG-BWD, but cultivation from these sites indicates that *Sulfobacillus*- and *Acidicaldus*- like species are present. Additionally, previous DGGE analysis (Inskeep et al., 2004) found sequences related to *Meiothermus silvanus* (100% similarity to JC2F AN182; Figure AA.4), *Acidimicrobium ferrooxidans* (99% similarity to RS3F SK346), and *Acidosphaera* spp. (100% similarity to RS2F SK969).

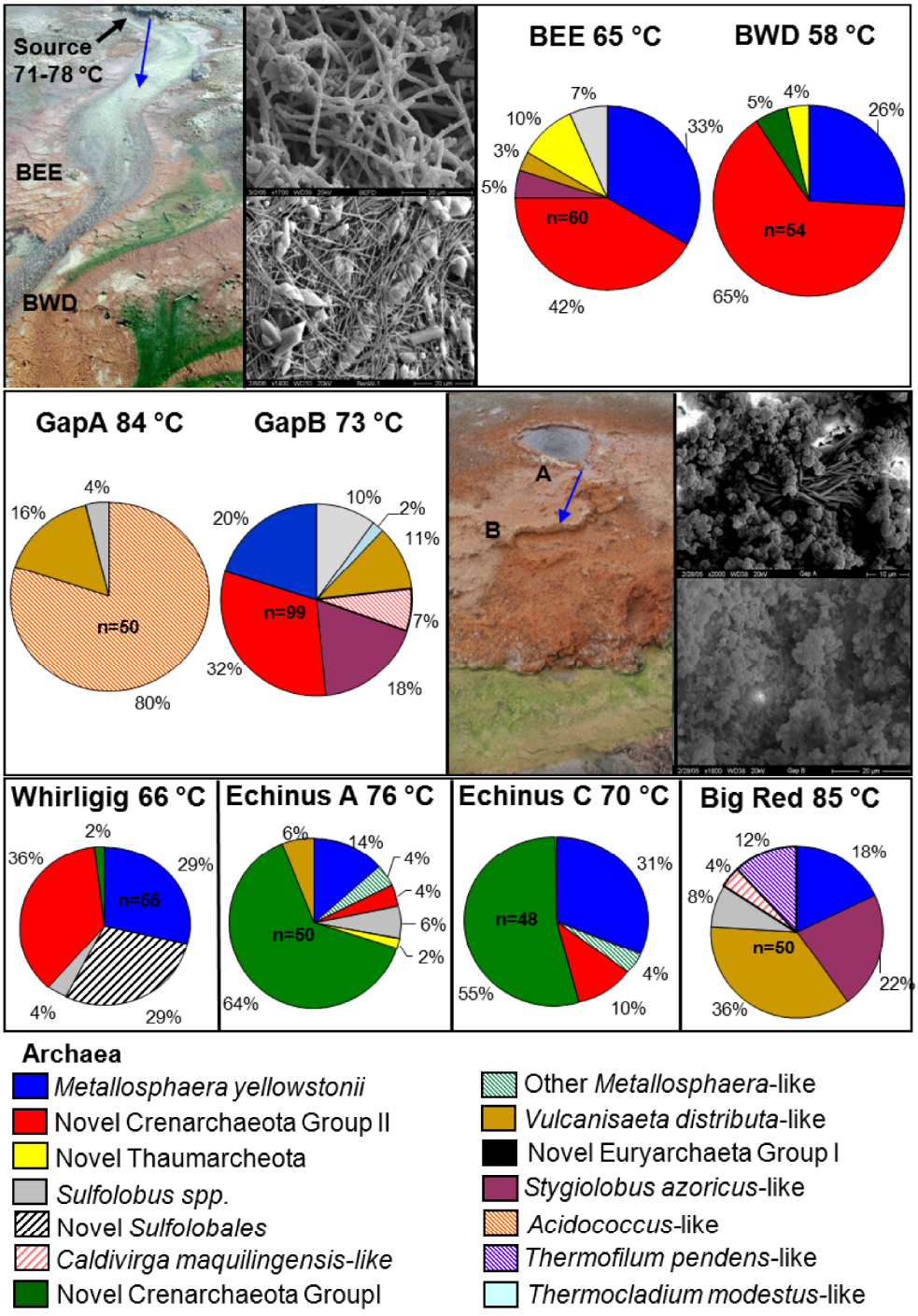

Figure AA.6. Images and distribution of 16S rRNA sequences in ASC springs. Left: images of springs with labeled source locations and sampling positions. Blue arrows indicate spring flow. Black arrows point to scanning electron micrograph images for various sampling points. Images not shown for WG, EG, and PB. (Images used courtesy of R.E. Macur and W.P. Inskeep)

Distribution of Microbial Sequences in the Acid-Sulfate-Chloride OSP Springs

A large clone library set was obtained from JGI for NG-OSP8 and NG-OSP14 (Figure AA.7 and AA.8; ~350 archaeal and bacterial clones generated per site) and representative sequences are shown in Figures AA.8 and AA.9 with percentages of clones belonging to each clade. NG-OSP8 contains sequences from all crenarchaeal orders with over 60% of clones related to Crenarchaeota Group I and approximately 13% related to *Metallosphaera yellowstonii*. NG-OSP14 also contains sequences from all orders in the crenarchaeota but 67% of sequences are related to *Metallosphaera* sp. MK1 and only about 2% are related to Crenarchaeota Group I. In addition, unlike NG-OSP8, NG-OSP14 has sequences related to the candidate Thaumarchaeota phylum and approximately 16% of total archaeal clones belong to a novel thermoplasma-like clade in the phylum Euryarchaeota.

A detailed phylogenetic analysis (Figure AA.10) of *Hydrogenobaculum*-like sequences in NG-OSP springs indicates different clades which can be divided between NG-OSP 8 and OSP14. 82% of NG-OSP14 sequences group with the cultivated *Hydrogenobaculum* spp. such as *H. acidophilum.* Conversely, NG-OSP8 sequences branch nearly exclusively with a clade with no cultured relatives.

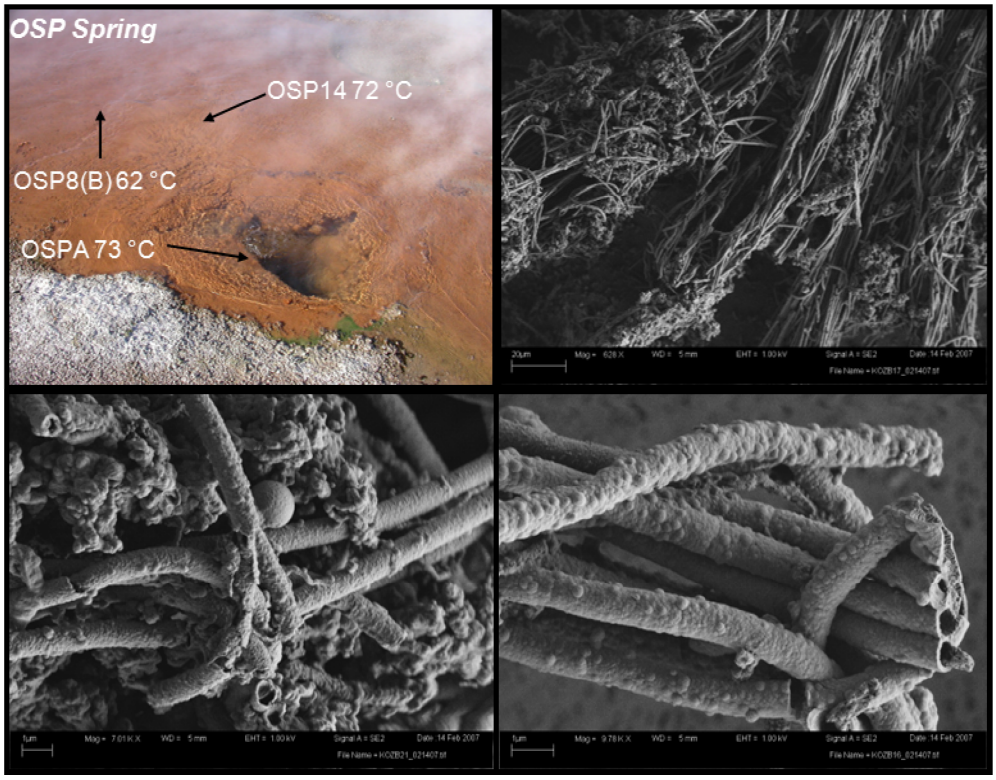

Figure AA.7. Image of the hydrous ferric oxide mat of NGB-OSP and spring source (top left) and electron micrograph images (F-SEM) showing ferric iron encrusted filamentous sheaths at the OSP14 sampling point. (Images used courtesy of R.E. Macur and W.P. Inskeep)

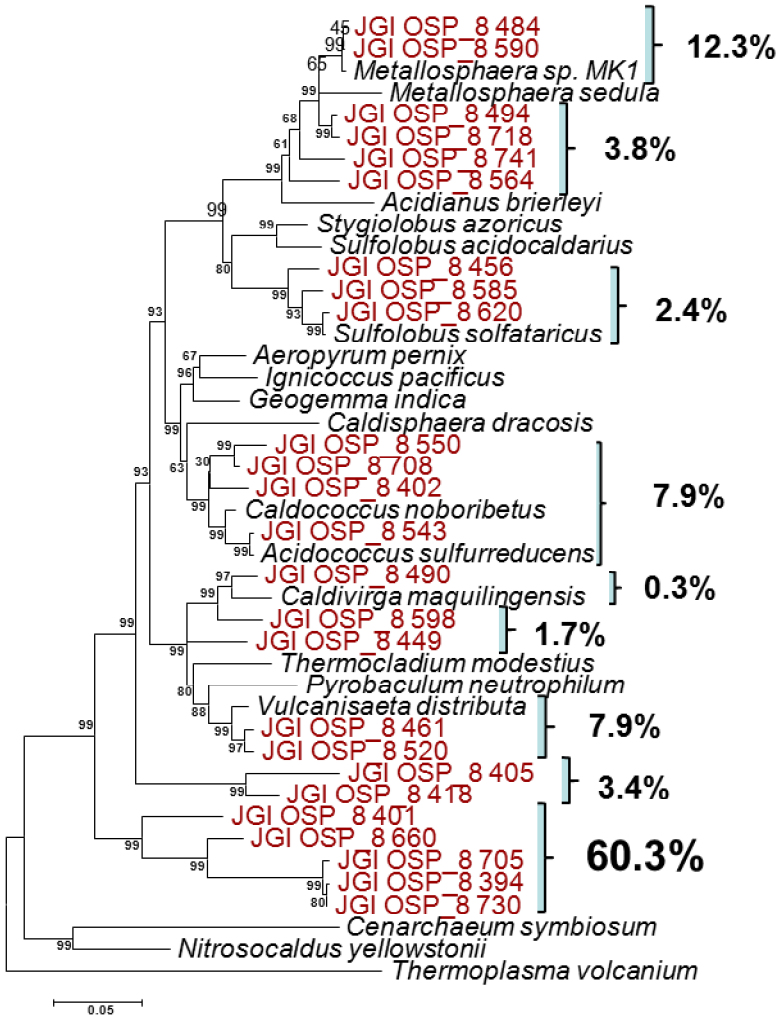

Figure AA.8. Phylogenetic tree of 16S rRNA sequences observed across the OSP_8 iron mat sampling site at Norris Geyser Basin, Yellowstone National Park. Clone sequences are highlighted in red and percentage of sequences belonging to sequence clades are indicated in brackets.

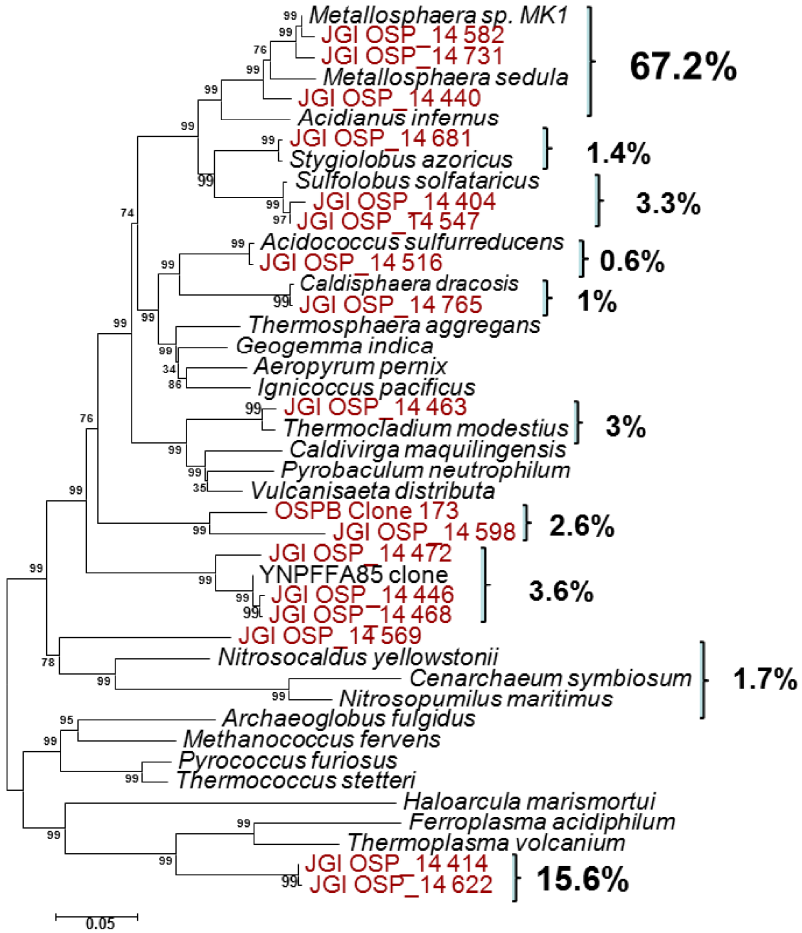

Figure AA.9. Phylogenetic tree of 16S rRNA sequences observed across the OSP_14 iron mat sampling site at Norris Geyser Basin, Yellowstone National Park. Clone sequences are highlighted in red and percentage of sequences belonging to sequence clades are indicated in brackets.

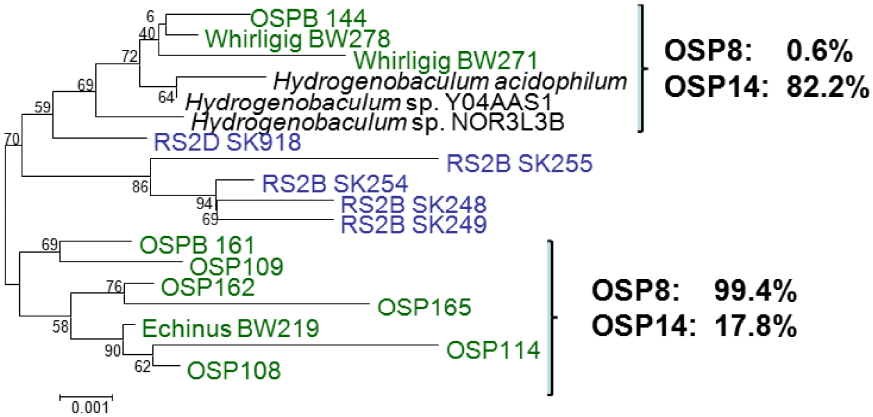

Figure AA.10. Phylogenetic tree of 16S rRNA *Hydrogenobaculum*-like sequences observed across the OSP and RS2 iron mats, Yellowstone National Park. Clone sequences in green are from the acid-sulfate-chloride OSP springs of Norris Geyser Basin and sequences in blue are from the acid-sulfate Rainbow Springs (RS2).

Description of novel isolates

Isolates were obtained from three ASC springs (Table AA.2; Figure AA.2, AA.3) and include *Metallosphaera* yellowstonii str. MK1 (see Chapter 3), *Sulfobacillus* sp. str. MK2, *Sulfolobus* sp. str. MK3, *Crenarchaeota* sp. str. MK4 and *Acidicaldus* sp. str. MK6. In addition, a co-culture of *Acidicaldus* str.MK6 and Sulfolobalesstr.MK5 was also obtained and is currently maintained on solid media Gelrite plates. Sulfolobales sp. MK5 could not be isolated on solid media and the co-culture would not grow in synthetic culture medium with YE, S^0, and pyrite as electron donors. The capabilities of the isolates to oxidize and/or reduce iron, and fix carbon were characterized (Table AA.2). All isolates were tested for growth using YE, Fe(II), S^0, pyrite, and solid media. *Metallosphaera* sp. MK1 and *Sulfolobus* sp. MK3 are capable of autotrophic growth and all isolates are capable of oxidizing iron except *Acidicaldus* sp. MK6. *Metallosphaera* sp. MK1 and *Sulfolobus* sp. MK3 are capable of pyrite oxidation. *Acidicaldus* sp. MK6 is capable of anaerobic growth with Fe(III) as an electron acceptor. The co-culture, *Crenarchaeota* sp. MK4, and *Acidicaldus* sp. MK6 are capable of growth on 1.2 % Gelrite® plates supplemented with synthetic growth media, 0.2% YE and 10 mM $FeSO_4$. *Acidicaldus* sp. MK6 colonies are fast growing white round colonies (colonies observed within 24 hours) while *Crenarchaeota* sp. MK4 colonies are slower growing, small and brownish in color, which become encrusted with ferric iron oxyhydroxides after 10 days incubation. *Sulfobacillus* str.MK2 grows on agar plates with 0.2% YE and 10 mM $FeSO_4$. Colonies were observed after 2-3 days and are round and brownish in color.

Metallospheara sp. MK1 and *Sulfolobus* sp. MK3 are not able to grow on Gelrite® or agar plate media supplemented with 10 mM $FeSO_4$ and 0.2% YE.

Isolate	Cell Morphology	pH_{optima}	T_{optima} (°C)	Fix CO_2	Plates	Fe^{2+}	S^0	Pyrite	Fe^{3+}
Metallosphaera sp. MK1	~1 µm lobed cocci	2.5-3.0	65-70	+	-	+	+	+	-
Sulfobacillus sp. MK2	1x3-5 µm rods	2.0-3.0	55-58	-	+	+	+	+	-
Sulfolobus sp. MK3	~ 1 µm cocci	2.0-2.5	75	+	-	+	+	+	-
Crenarchaeota sp. MK4	~1 µm cocci	nd	55-60	nd	+	+	-	-	-
Sulfolobales sp. MK5 co-culture with sp. MK6	~1 µm cocci	nd	nd	nd	+	+	nd	nd	nd
Acidicaldus sp. MK6	1x1.2-1.5 µm rods and 20-30 µm filaments	2.5-3.0	55-60	-	+	-	-	-	+

Table AA.2. Isolates and co-cultures obtained from acid-sulfate-chloride (ASC) springs and characterization of cell morphology, pH optima, temperature optima and growth on iron and sulfur substrates as electron donors or Fe(III)as an electron acceptor under anaerobic conditions. The ability to grow autotrophically on solid media is also indicated. nd = not determined.

Sulfolobus str. MK3 has the highest temperature optima at 75 °C. The bacterial isolates have the lowest temperature optima between 55-60 °C. All isolates grow optimally between pH 2.0 and 3.0 but *Sulfolobus* str. MK3 has a slightly lower pH optima ranging from 2.0 to 2.5. The cell morphologies of Sulfolobus sp. MK3 and *Crenarchaeota* sp. MK4 are ~1 µm cocci. *Sulfobacillus* sp. MK2 and *Acidicaldus* sp. MK6 are rod-shaped at ~1 x 5 and 1 x 3 µm, respectively (Figure AA.11).

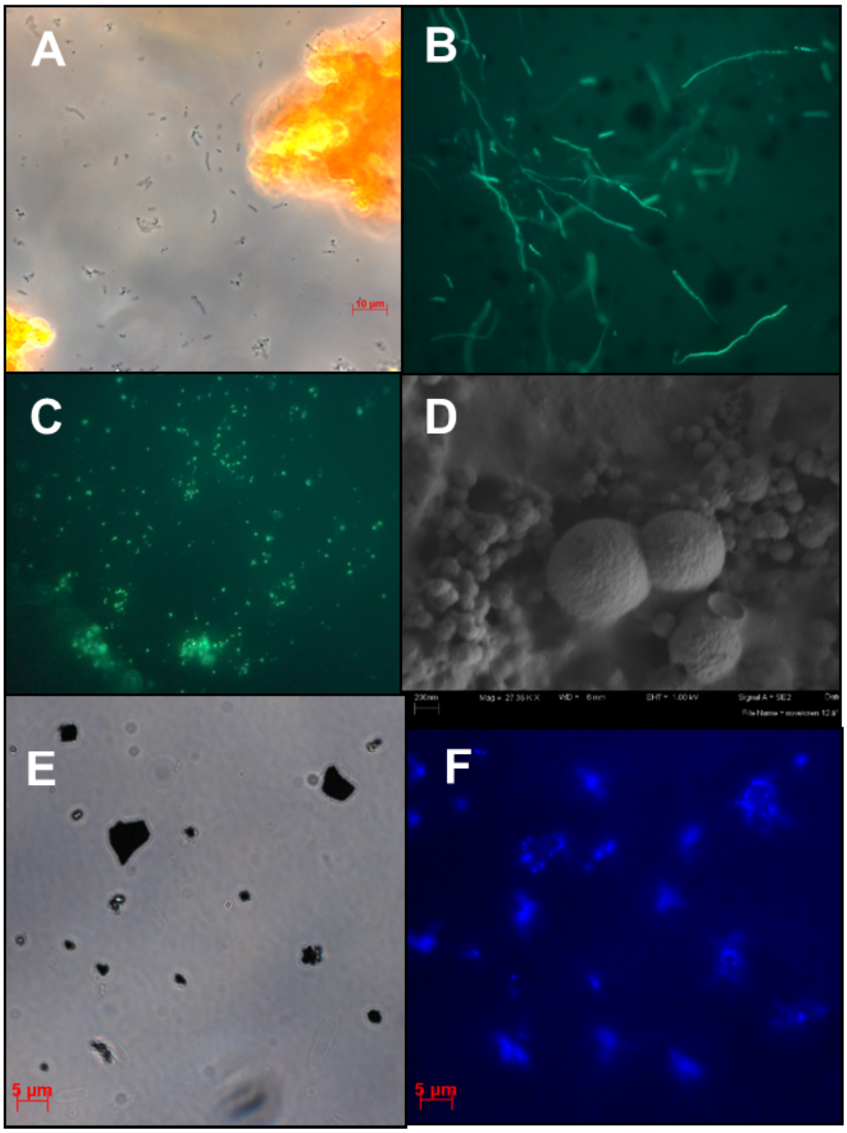

Figure AA.11. Microscopy images of isolates obtained from acid-sulfate-chloride springs in Yellowstone National Park. (A) Optical microscopy image of *Sulfobacillus* sp. MK2; (B) *Acidicaldus* sp. MK6 SYBR-green fluorescent image; (C) Crenarchaeota sp. MK4 SYBR-green fluorescent image; (D) FE-SEM micrograph image of Crenarchaeota sp. MK4; (E) *Sulfolobus* sp MK3 optical image with corresponding DAPI fluorescent image (F) showing cells bound to pyrite grains.

Iron oxidation and reduction rates

Iron oxidation rates were determined for *Metallosphaera yellowstonii* cultivated at 65 °C with 10 mM Fe(II) sorbed to iron oxide mat (obtained from NGB-BE). Iron

oxidation rates were 1.24 ± 0.31 and 0.74 ± 0.15 µmoles Fe(II) L^{-1} sec^{-1} at pH 2.5 and 3.2, respectively for exponential phase cultures with 10^8 cells mL^{-1}. Iron reduction rates were determined in *Acidicaldus* sp. MK6 cultures at pH 3.0 utilizing autoclaved HFO mat as the source of ferric iron (Figure AA.12) and 10 mM glucose as the electron donor. Rates of iron reduction were approximately 0.036 µmoles Fe(III) L^{-1} sec^{-1}.

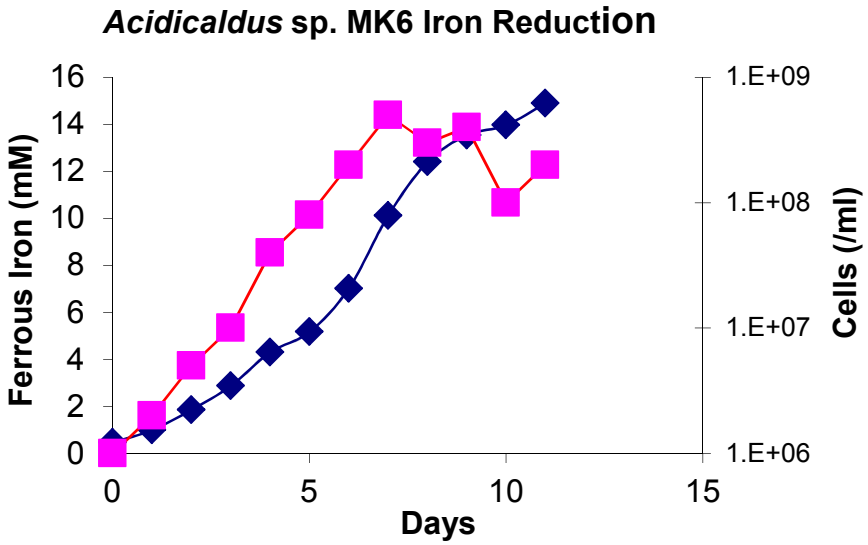

Figure AA.12**.** Ferrous iron accumulation (mM ferrous iron) and cell growth (cells/ml) as a function of time in anaerobic serum bottle cultures with *Acidicaldus* sp. MK6. Cultures were maintained at pH 3.0 with 10 mM glucose and 0.5 g of autoclaved HFO mat from NGB-BED. Squares = cells/mL; diamonds = Fe(II)(mM).

Analysis of Culture Fe Solid Phases

Ferric iron solid phases were formed on serum bottle surfaces after cultivation of *Metallosphaera yellowstonii* on pyrite or iron sorbed to ferrihydrite (Figure AA.13). Detailed geochemical analyses of these solid phases were performed using both x-ray diffraction (XRD) and extended-x-ray absorption fine-structure spectroscopy (EXAFS) (least-square fitting approach). After 11 days of incubation, XRD analysis indicates

hematite is the primary crystalline phase at the water-air interface, whereas jarosite is found below the water surface (Figure AA.13). EXAFS analysis of mixed solid phase from the vessel indicate ~ 41% ferrihydrite, 24% jarosite, 16% goethite and 12% hematite. XRD analysis of Crenarchaeota sp. MK4 revealed both goethite and jarosite as a slurry on the bottom of the serum bottle vessel (Figure AA.13).

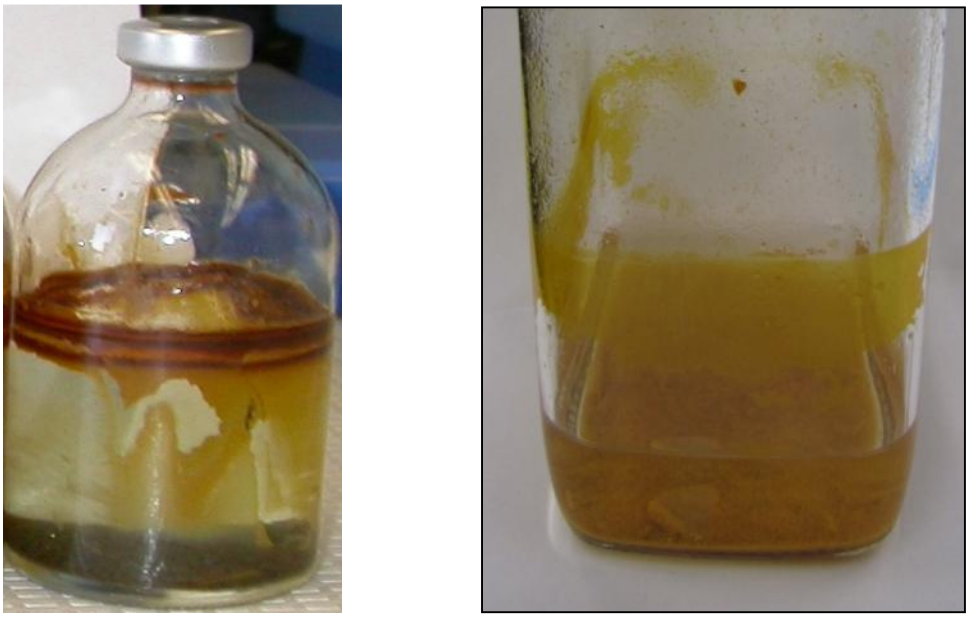

Figure AA.13. Left: Serum bottle culture of *Metallosphaera yellowstonii* str. MK1 after 11 days of incubation with pyrite as the electron donor. Red ring is primarily hematite and the lower yellow phase is principally jarosite. Right: Serum bottle culture of Crenarchaeota sp. MK4 after 8 days of incubation with 10 mM $FeSO_4$ as the electron donor.

Discussion

Ferric iron mats of ASC and AS springs in Yellowstone National Park exhibit considerable archaeal diversity, including representatives from the Crenarchaeota, Euryarchaeota and Candidate Phylum Thaumarchaeota, as well as new deeply-rooted

lineages (Figure AA.2). Members from all three orders of the Crenarchaeota are well represented. In addition, two new novel lineages were found from phylogenetic analysis of over 1500 16S rRNA gene sequences from the 18 sites included in this study. Highly divergent 16S rRNA bacterial sequences were also found in sites below 65-70 °C and especially at sites RS2F and RS3B (both 53 °C). Many of these sequences are less than 90% similar to cultivated relatives and represent three new taxonomic branches at the genera level or higher. Bacterial diversity is limited to *Hydrogenobaculum* spp. above 70 °C. Detailed 16S rRNA gene analysis of *Hydrogenobaculum*-like sequences in NG-OSP and RS2 springs reveals two distinct sub-clades. Sequences from NG-OSP14 cluster predominantly with the cultivated species *Hydrogenobaculum acidophilum*, *Hydrogenobaculum* sp. Y04AAS1, and *Hydrogenobaculum* sp. NOR3L3B while 99.4% of the NG-OSP8 sequences group with a clade that has no cultured relatives. Temperature may account for this divergence but H_2 and H_2S concentrations differ between these two spring locations: NG-OSP14 has 12.1 μM H_2S and 109 nm H_2 compared to 0.1 μM H_2S and 0.1 nm H_2 in NG-OSP8.

Microbial diversity in acidic iron mats is likely driven by the reduced inorganic electron donors available for growth and the increasing levels of oxygen down gradient from geothermal discharge. However, the most important parameter for overall diversity and distribution of microorganisms appears to be temperature. For instance, sequences related to *Acidococcus* spp., *Stygiolobus azoricus* and Thermoproteales spp. (i.e. *Vulcanisetta distributa*) dominate at higher temperatures, consistent with the range observed for cultivated relatives. *Metallosphaera* sp. MK1 is dominant especially in AS

springs between 60-75 °C (detailed diversity analysis of *Metallosphaera* sp. MK1 is the topic of chapter 3 of this dissertation). Sequences from Crenarchaeota Group II are found at temperatures up to 76 °C, but appear to be most dominant in the 58-65 °C range, which also corresponds to the optimal range of the novel Crenarchaeota sp. MK4 isolate.

Temperature does not explain all the diversity between the 18 spring sites discussed in this study. For instance, Crenarchaeota Group I- and Thaumarchaeota-like sequences are found at high percentages in Echinus Geyser (EG) and RS3, respectively, but do not appear in all spring locations with similar temperatures. Although a high number of total clones have been processed, a number of sites may not have a high enough sequencing depth to completely cover all 16S rRNA diversity due to the difficulty of DNA extraction from hard ferric iron phases and remote location of sites. Future work will require more detailed 16S rRNA analysis in combination with metagenome data.

Oxygen levels likely have an important effect on the distribution of microbial populations, expression of genes (i.e. heme copper terminal oxidases) and rates of geochemical processes such as Fe(II) oxidation. Abiotic Fe(II) oxidation rates are extremely slow at pH 2.6 and therefore, the observed Fe(II) oxidation in ASC and AS springs is driven by microbial metabolism. The slow rate of Fe(II) oxidation observed in filtered spring water confirms that microbial populations are responsible for the observed oxidation of aqueous iron (Figure AA.1). *Metallosphaera* str.MK1-like organisms contribute to the observed oxidation of iron based on the distribution of 16S rRNA

sequences in RS2 and JC2 above 65 °C; contributions to Fe(II) oxidation from the uncharacterized microorganisms present in these systems is also a strong possibility.

The average oxidation rate of Fe(II) in JC2 was approximately 0.270 ± 0.02g Fe L^{-1} h^{-1}, which is similar to the rates observed for *Metallosphaera* sp. MK1 in cultures (0.25±0.05 g Fe^{2+} L^{-1} h^{-1} at pH 2.5). These rates are also similar to those observed by other thermophilic bacterial species including *Sulfobacillus* spp. (0.5 g Fe^{2+} L^{-1} h^{-1}; Kinnunen et al., 2003) and higher than reported rates for any archaea (i.e. 0.1 g Fe^{2+} l^{-1} h^{-1} for *Acidianus brierleyi*; Nemati and Harrison, 1999). The oxidation rates reported for thermophilic microorganisms are lower than the mesophilic species such as *A. ferrooxidans* (26.4 g Fe^{2+} L^{-1} h^{-1}; Kauppi et al. 2001), although these rates were optimized in flow-through fluidized-bed reactors. Fe(II) oxidation rates in *A. brierleyi* increasing substantially as pH decreases (Nemati and Harrison, 1999). Similarly, *Metallosphaera yellowstonii* oxidizes Fe(II) at a higher rate at pH 2.5 than pH 3.2.

Cultivation efforts were successful in obtaining six novel microorganisms including one from Crenarchaeota Group II: Crenarchaeota sp. MK4 (Figure AA.2). This isolate will be a high priority for further study as it represents the only isolate from a deeply-rooted lineage. The phylogenetic data in this study indicate that in addition to the isolates obtained in this study, ferric iron mats in YNP contain numerous other uncultivated organisms. High priority targets include members from Crenarchaeota Group I, the Euryarchaeota (Thermoplasmatales-like) and bacteria distantly related to cultivated species in the Firmicutes and delta Proteobacteria.

Metallosphaera yellowstonii and *Sulfolobus* sp. MK3 were the only two species capable of autotrophic growth and may be a significant source of carbon for other microorganisms. Species such as *Acidicaldus* sp. MK6 may need this source of carbon for anaerobic growth on Fe(III). The diversity of uncharacterized archaeal and bacterial populations in ferric oxide mats may be linked to available electron donors besides Fe(II) (Table AA.1). For instance, *Methylacidiphilum*-like sequences are found in JC2F and RS3A at 70% and 29% of bacterial sequences, respectively, and may take advantage of the relatively high CH_4 concentrations (2.2 and 3.46 μM) compared to other spring locations.

Analysis of ferric solid phases on serum bottle cultures link observed biomineralized phases found in the springs to cultured organisms. Spring geochemistry (i.e. K^+ concentrations, pH, arsenic adsorption) plays an important role in the formation of mineral phases. However, ferric iron phases found in cultures of *Metallosphaera yellowstonii* and Crenarchaeota sp. MK4 differ in mineralogy and morphology. *Metallosphaera yellowstonii* forms hematite and jarosite on serum bottle surfaces and XRD analysis of Crenarchaeota sp. MK4 solid phases indicate jarosite and goethite as a slurry on the vessel bottom. Consequently, future efforts will continue to identify the individual contributions of different phyla to observed Fe(II) oxidation and the subsequent biomineralization of secondary phases.

Acknowledgements

This work was supported by the National Science Foundation Microbial Observatory Program (MCB-0132022), the National Aeronautic and Space Administration (NASA) via funds provided to the Thermal Biology Institute at Montana State University (Project Numbers NAG5-8807, NNG04GR46G), and the Montana Agricultural Experiment Station (Project 911398). The authors appreciate assistance from Bill Inskeep, Richard Macur, Sarah Korf, Peyton Taylor, Amanda Nagy and Galena Ackerman for field work regarding geochemical analyses, sample collection, and 16S rRNA sequence generation. The authors also appreciate C. Hendrix and T. Olliff for permitting this work in Yellowstone National Park (Permit YELL-2007-SCI-1976).

References

1. Amend, J.P., and E.L. Shock. 2001. Energetics of overall metabolic reactions of thermophilic and hyperthermophilic Archaea and Bacteria. FEMS Microbiology Reviews. 25: 175-243.

2. Amann, R.I., B. Zarda, D.A. Stahl, and K.H. Schleifer. 1992. Identification of individual prokaryotic cells by using enzyme-labeled, rRNA-targeted oligonucleotide probes. Appl. Environ. Microbiol. 58: 3007-3011.

3. Baker, B.J. and J. F. Banfield. 2003. Microbial communities in acid mine drainage. FEMS Microbiology Ecology. 44: 139-152.

4. Blake, R. and D.B Johnson. 2000. Phylogenetic and biochemical diversity among acidophilic bacteria that respire on iron. In: Environmental Microbe–Metal Interactions (Derek, L., Ed.). 53–78. ASM Press, Washington, DC.

5. Edwards K.J., Goebel B.M., Rodgers T.M., Schrenk M.O., Gihring T.M., Cardona M.M., Hu B., McGuire M.M., Hamers R.J., Pace N.R., and J.F. Banfield. 1999. Geomicrobiology of pyrite (FeS2) dissolution: case study at Iron Mountain, California. *Geomicrobiology Journal*. 16:155-179.

6. Hallberg K.B, D.B. Johnson. 2001. Biodiversity of acidophilic prokaryotes. Advances in Applied Microbiology. 49: 37-84.

7. Hugenholtz P., C. Pitulle, K.L. Hershberger, and N.R. Pace. 1998. Novel division-level bacterial diversity in a Yellowstone hot spring. J Bacteriol. 180: 366-376.

8. Inskeep W.P., R.E. Macur, G. Harrison, B.C. Bostick, S. Fendorf. 2004. Biomineralization of As(V)-hydrous ferric oxyhydroxide in microbial mats of an acid-sulfate-chloride geothermal spring, Yellowstone National Park. Geochimica et Cosmochimica Acta. 68: 3141–3155.

9. Inskeep W.P., G.G. Ackerman, W.P. Taylor, M. Kozubal, S. Korf, and R.E. Macur. 2005. On the energetics of chemolithotrophy in nonequilibrium systems: case studies of geothermal springs in Yellowstone National Park. Geobiology. 3:297-320.

10. Inskeep, W.P., D. Rusch, Z. Jay, M.J. Herrgard, M.A. Kozubal, T.H. Richardson, R.E. Macur, N. Hamamura, B. Fouke, A-L. Reysenbach, F. Roberto, M. Young, R. Jennings, A. Schwartz, S. Korf, E. Boyd, J. Badger, M. Bateson, G. Geesey, E. Mathur and M. Frazier. 2009. Geochemistry underpins metagenome composition

(phylogeny and function) in high temperature geothermal springs in Yellowstone National Park. *PLoS One*. In Review.

11. Itoh Y.H., Kurosawa N., Uda I., Sugai A., Tanoue S., Itoh T., Horiuchi T., and T. Itoh. 2001. Metallosphaera sedula TA-2, a calditoglycerocaldarchaeol deletion strain of a thermoacidophilic archaeon. Extremophiles. 5:241-5.

12. Jackson, C. R., H. W. Langner, J. Donahoe-Christiansen, W.P. Inskeep, and T.R. McDermott. 2001. Molecular analysis of microbial community structure in an arsenite-oxidizing acidic thermal spring. Environmental Microbiology. 3: 532-542.

13. Jennings, S. R. 1995. Geochemical characterization of sulfide mineral weathering for remediation of acid producing mine wastes. M.S. Thesis, Montana State University, Bozeman, MT. Publication No. 9502, 140 p.

14. Johnson, D.B., and K.B. Hallberg. 2003. The microbiology of acidic mine waters. Research in Microbiology .154: 466-73.

15. Kauppi P.H., Hautakangas H.J., Puhakka J.A. 2001. High rate iron oxidation in fluidized-bed bioreactors. Proc Int Biohydrometal Symp. 2001:385–392

16. Kinnunen P.H., Robertson W.J., Plumb J.J., Gibson J.A., Nichols P.D., Franzmann P.D., and J.A. Puhakka. 2003. The isolation and use of iron oxidizing moderately thermophilic acidophiles from the Collie coal mine for the generation of ferric iron leaching solution. Appl Microbiol Biotechnol 60: 748-753.

17. Konhauser, K. O. 1998. Diversity of bacterial iron mineralization. Earth-Science Reviews. 43: 91-121.

18. Langner, H.W., C.R. Jackson, T.R. McDermott, and W.P. Inskeep. 2001. Rapid oxidation of arsenite in a hot spring ecosystem, Yellowstone National Park. Environmental Science & Technology. 35: 3302-3309

19. Macur, R.E., H.W. Langner, B.D. Kocar, and W.P. Inskeep. 2004. Linking geochemical processes with microbial community analysis: successional dynamics in an arsenic-rich, acid-sulfate-chloride geothermal spring. Geobiology. 2: 163-177.

20. Miroshnichenko, M.L. 2004 Thermophilic microbial communities of deep-sea hydrothermal vents. Microbiology. 73: 1–13.

21. Nemati M., and S.T.L. Harrison. 2000. A Comparative Study on Thermophilic and Mesophilic Biooxidation of Ferrous Iron Minerals Engineering. 13:19-24.

22. Nordstrom, D.K. and G. Southam. 1997. Geomicrobiology of sulfide mineral oxidation. Reviews in Mineralogy. 35: 361-390.

23. Olson, G.J., J.A. Brierley, C.L. Brierley. 2003. Bioleaching review part B: Applied Microbiology and Biotechnology. 63: 249 – 257.

24. Rawlings, D.E. 2002. Heavy metal mining using microbes. Annual Review of Microbiology. 56: 65-91.

25. Rohwerder, T., T. Gehrke, K. Kinzler, and W. Sand. 2003. Bioleaching review part A: progress in bioleaching: fundamentals and mechanisms of bacterial metal sulfide oxidation. Appl. Microbiol. Biotechnol. 63: 239-48.

26. Schwertmann, U. and R.M. Cornell. 2000. Iron Oxides in the Laboratory. 2nd Ed., VCH, Weinheim, Germany. 105-107.

27. Singer, P.C., and M.W. Stumm. 1970. Acid mine drainage: The rate determining step. Science. 167: 1121–1123.

28. Singer, S. W., C. S. Chan, A. Zemla, N. C. M. VerBerkmoes, M. Hwang, R. L. Hettich, J. F. Banfield, and M. P. Thelen. 2008. Characterization of cytochrome 579, an unusual cytochrome isolated from an iron-oxidizing microbial community. Appl Environ Microbiol. 74: 4454-6.

29. Spurr A. R. 1969. A low-viscosity epoxy resin embedding medium for electron microscopy. J. Ultrastructure Res. 26: 31–43.

30. To, T.B., D.K. Nordstrom, K.M. Cunningham, J.W. Ball, R.B. McClesky. 1999. New method for the direct determination of dissolved Fe(III) concentration in acid mine waters. Environmental Science and Technology. 33: 807-813.

APPENDIX B

METALLOSPHAERA YELLOWSTONII SP. NOV., A NOVEL THERMOPHILIC, IRON OXIDIZING CHEMOLITHOAUTOTROPHIC ARCHAEON ISOLATED FROM AN ACIDIC FE^{III}-OXIDE MICROBIAL MAT IN YELLOWSTONE NATIONAL PARK

Abstract

A novel thermophilic, iron and sulfur oxidizing crenarcheaon, designated strain MK-1^T, was isolated from an acid-sulfate-chloride geothermal spring in Yellowstone National Park, USA. Strain MK-1^T is an obligate aerobe and is capable of autotrophic growth on reduced iron (ferrous iron sorbed to ferrihydrite), pyrite, elemental sulfur and hydrogen, and heterotrophic growth on yeast extract. Strain MK-1^T is morphologically similar to other members of the Sulfolobales (irregular shaped 0·8–1·0 µm diameter cocci). The isolate grows between temperatures of 45 and 85 °C (optimum 65-70 °C; 10-11 h doubling time), across a pH range of 1·0 to 5·0 (optimum pH 2·5-3·0), and between NaCl concentrations of 0.03 and 1.25 % (wt/vol). Phylogenetic analysis based on the 16S rRNA gene sequence and *in silico* DNA-DNA hybridization indicates that the isolate is a member of the genus *Metallosphaera*. The average G+C content obtained from a partial genomic sequence is 48 mol%. The widespread distribution of highly similar 16S rRNA gene sequences (> 99% nucleotide identity) in numerous acidic Fe-oxide mats throughout YNP suggests that strain MK-1^T occupies an Fe(II) oxidizing niche different from other Sulfolobales that prefer reduced forms of sulfur or H_2 as an electron donor. On the basis of the physiological and molecular characteristics of the new isolate, we propose the name *Metallosphaera yellowstonii* sp. nov. with MK-1^T.

Materials and Methods and Results

The Sulfolobales comprise one of three main orders within the domain *Archaea*, phylum Crenarchaeota. The first member of the Sulfolobales was isolated by Brierley *et*

al., (1966), and all subsequent organisms have been isolated primarily from solfatara fields, with a few species obtained from hot acidic soils, uranium mines and smoldering slag heaps (e.g., Brock *et al*., 1972; Golovacheva et al., 1987; Karavaiko et al., 1994; Fuchs *et al*., 1995; Huber *et al*., 1989; Huber *et al*., 1991; Jan *et al*., 1999; Kozubal *et al*., 2008; Segerer et al., 1986; Suzuki *et al*., 2002; Takayanagi *et al*., 1996; Zillig *et al*., 1980; Zillig *et al.,* 1986). Members of the Sulfolobales include six genera: *Metallosphaera, Sulfolobus, Acidianus, Sulfurisphaera, Sulfurococcus* and *Stygiolobus* spp.; all are thermophilic to hyperthermophilic, have a pH optima between 2-3, and exhibit regular or irregular cocci morphology with cell diameters between 1-5 μm (Huber & Prangishvili, 2007). Members of the Sulfolobales are known chemolithotrophs, capable of using reduced sulfur species ($S_2O_3^{2-}$, SO_3^{2-}, S_n^{x-}, H_2S, S^0), H_2, and Fe(II) as electron donors for growth (Huber & Prangishvili, 2007). However, many Sulfolobales are able to grow heterotrophically and or mixotrophically. *Sulfolobus* and *Metallosphaera* spp. are obligate aerobes, *Acidianus* and *Sulfurisphaera* spp. are facultative anaerobes, while *Stygiolobus azoricus* is an obligate anaerobe (Huber & Prangishvili, 2007). The reduction of elemental sulfur in the Sulfolobales is thought to occur via a sulfur reductase molybdopterin (Kappler et al., 2005).

The Sulfolobales contain the highest temperature Fe(II) and sulfur-oxidizing microorganisms cultured to date (Auernik et al., 2008; Bathe & Norris et al., 2007; Kappler et al., 2005; Kletzin et al., 2004; Peeples et al., 1995). Of the known Sulfolobales, only *Metallosphaera* spp., *Sulfolobus metallicus* strain DSM 6482^T and *Sulfolobus tokodaii* strain 7^T are capable of chemolithoautotrophic growth on both Fe(II)

and reduced sulfur (Bathe & Norris, 2007). The genome sequences are complete for a number of Sulfolobales including *Metallosphaera sedula* strain DSM 5348^T*, Sulfolobus solfataricus* strain P2^T*, S. acidocaldarius* strain DSM639^T, *S. tokodaii* strain 7^T (Auernik *et al*., 2008; She *et al.,* 2001), and *S. islandicus* (Reno *et al*., 2009). The goal of this study is to report additional growth characteristics and genomic data for a novel member of the Sulfolobales isolated from Yellowstone National Park (YNP), and provide evidence for placement of this organism within the genus *Metallosphaera* with the name *Metallosphaera yellowstonii* sp. nov., and MK-1^T as the type strain.

Microbial growth on reduced sulfur and Fe(II) minerals such as pyrite is of significant interest due to potential commercial applications in bioleaching of mineral ores (Olson *et al*., 2003; Rohwerder *et al*., 2003), bioremediation of acid mine drainage (Hallberg & Johnson, 2001; Johnson et al., 2003) and coal desulfurization (Clark *et al.,* 1993). Acidophilic bacteria involved in the oxidation of reduced sulfur and or Fe(II) in sulfidic ores include *Acidithiobacillus ferrooxidans, Acidithiobacillus thiooxidans, Leptospirillum ferrooxidans, Leptospirillum ferriphilum, Ferrimicrobium acidophilum,* and *Sulfobacillus* spp. (Blake & Johnson, 2000; Johnson *et al*., 2003). A model for electron transport from Fe(II) has been proposed for *A. ferrooxidans* (Quatrini *et al*., 2009) and more recently, a novel extracellular cytochrome (cyt_{579}) has been shown to be involved in Fe(II) oxidation in *Leptospirillum*, which is the dominant bacterial species from an acidic mine drainage at Iron Mountain, CA (Singer et al., 2008). The dominant archaeal member at the Iron Mountain site, (*Ferroplasma acidarmanus* strain Fer1^T) is also an iron-oxidizing organism, and a blue-copper protein is thought to be directly linked

to the oxidation of Fe(II) (Dopson et al, 2005). Conversely, the *fox* gene cluster represents a different putative Fe(II) oxidation pathway and has been described in *Metallosphaera sedula*, *Sulfolobus tokodaii* and *Sulfolobus metallicus* (Bathe & Norris, 2007; Auernik *et al*., 2008), and is found in the draft genome of strain MK-1^T (Kozubal et al., submitted) .

The isolation and growth of strain MK-1^T, and the distribution of MK-1^T-like 16S rRNA gene sequences was described previously (Kozubal *et al*., 2008). Briefly, inoculum was obtained from a 2 cm thick hydrous-ferric-oxide (HFO) mat (63 °C; pH 3.0) from Beowulf Spring in Norris Geyser Basin YNP (44°43'53.4"N, 110°42'40.9"W; YNP Thermal Inventory NHSP35). A pure culture of strain MK-1^T was obtained in sealed serum bottles under chemolithoautotrophic conditions (Kozubal *et al*., 2008) with pyrite as the electron donor, O_2 as the electron acceptor and CO_2 as the carbon source (serum bottle head-space: 25% O_2, 50% CO_2, and 25% air; total pressure = 1 atm). Growth of strain MK-1^T is easily verified by the formation of a continuous ring of amorphous Fe(III)-hydroxide solid phase at the air-water interface as well as subsequent formation of potassium jarosite ($KFe_3(SO_4)_2(OH)$), depending on levels of K^+ and SO_4^{2-} in the aqueous phase. Neither of these secondary solid phases are formed in un-inoculated controls. Autocatalytic oxidation of pyrite via Fe(III) (Nordstrom & Southam, 1997; Rawlings *et al.* 2003) is not kinetically favored at the optimum pH (2.5 - 3.0) and temperature (65-70 ºC) required for growth of strain MK-1^T. Growth curves were established using fluorescent optical microscopy (DAPI staining) and DNA analysis as a function of time. Growth was robust without the need for an added carbon source other

than CO_2. The purity of the isolate was verified repeatedly with standard protocols, including short-fragment and long-fragment 16S rRNA gene sequence analysis with universal bacterial and archaeal primers (Kozubal *et al*., 2008). The full-length 16S rRNA sequence for strain MK-1^T is 96.2% similar to *Metallosphaera hakonensis* strain HO1-1^T, 95.5% similar to *Metallosphaera sedula* strain DSM 5348T and 89.9% similar, to *Sulfolobus solfataricus* strain $P2^T$. Phylogenetic analysis based on the 16S rRNA gene places strain MK-1^T in the same genera as the five previously described *Metallosphaera* spp., although *M. yellowstonii* strain MK-1^T is the most deeply rooted organism within the genera (Figure AB.1).

Growth of strain MK-1^T was determined using both direct counting via DAPI stain and quantification of extracted DNA. Strain MK-1^T is an obligate aerobe that grows robustly on Fe(II) adsorbed to ferrihydrite, and iron sulfide minerals including pyrite, pyrrhotite, and chalcopyrite (Table AB.1); however, poor growth was observed on non-ferrous sulfide minerals (peak cell densities of 10^4 cells/mL on covellite and sphalerite). The isolate grows well on elemental sulfur (peak cell densities of 10^8 cells/mL; doubling time of 16 ± 2 hours), but no growth was observed in the presence of added dissolved sulfide, thiosulfate, or tetrathionate as electron donors with and without ferrihydrite-coated SiO_2 as an inert carrier material. Although strain MK-1^T grows well on Fe(II) adsorbed to ferrihydrite (peak cell density of 10^9 cells/mL; doubling time of 10.3 ± 0.5 hours), it grows poorly in the presence of aqueous $FeSO_4$ (peak cell density of 10^2 cells/mL), indicating the isolate likely needs solid phase substrates for optimal growth. Ferrous iron adsorbed to ferrihydrite has been shown to have a more negative redox

potential relative to aqueous Fe(II), which may allow the organism to gain more energy per mol of Fe(II) oxidized (Jeon *et al*. 2003).

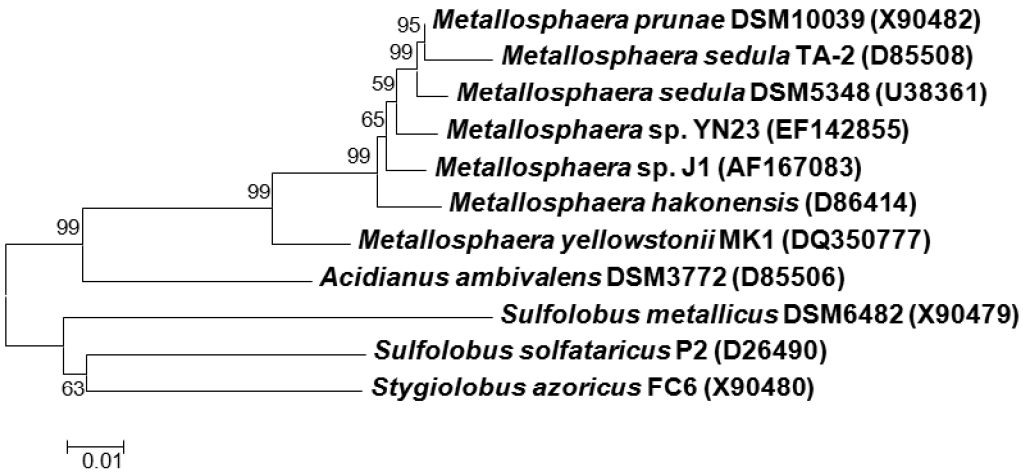

Figure AB.1. Phylogenetic (16S rRNA gene) tree showing the position of *Metallosphaera yellowstonii* (1332 bp fragment) relative to all *Metallosphaera* spp., and selected *Sulfolobus* and *Acidianus* spp.. Accession numbers of isolates are indicated in parentheses [The neighbor-joining tree was constructed using ClustalW and PAUP software (Swofford, 2003) and is consistent with results obtained using maximum parsimony methods. Bootstrap analysis of 1000 replicates was performed and values greater than 50 % are shown at nodes. Bar equals 0.01 substitutions per nucleotide position.]

Heterotrophic growth was determined in the presence of 0.2% YE and peak cell densities of 10^7 cells/mL were obtained after 9 days of growth (Table AB.1). Additions of YE and $Fe^{II}SO_4$ increased growth yields on elemental sulfur and pyrite. No growth was observed on starch, simple sugars, citric acid, succinic acid, or amino acids (Table AB.1), when added individually to serum bottles at final concentrations of 0.1% and 1% (wt/vol). All characterized *Metallosphaera* spp., and most of the *Sulfolobus* and *Acidianus* spp. are capable of growth using H_2 as the primary electron donor (Kletzin *et al*., 2004). To test for growth of strain $MK1^T$ on H_2, 50 mL of synthetic media was added

to 160 mL serum bottles with a headspace of equal parts O_2, CO_2 and H_2. Modest cell numbers were observed (10^6 cells mL^{-1}) after 14 d of growth. Previous work indicates that growth of *M. sedula* on H_2 is dependent on the ratio of H_2 to O_2 (Fuchs *et al*. 1995), and although *M. yellowstonii* strain MK-1^T is capable of growth on H_2 (Table 1), future work will be necessary to determine optimal growth yields on this particular electron donor.

Table AB.1. Peak cell densities[1] of *Metallosphaera yellowstonii* strain $MK1^T$ grown[2] in the presence of different inorganic and organic substrates (pH = 3, T = 65 °C).

[1] average of three triplicate cultures; "+++" = > 10^7 cells/mL; "++" = 10^5 – 10^7 cells/mL; "+" 10^2 – 10^5 cells/mL; "-" = < 10^2 cells/mL.

[2]All growth conditions included 20 mL of synthetic media (Kozubal et al., 2008) in 40 mL serum bottles. Aerobic cultures had a headspace consisting of 25% O_2, 50% CO_2, and 25% air (1 atm) except for cultures with H_2 as the electron donor. Anaerobic cultures were purged with N_2 gas and verified to be anoxic using resazurin. Cultures were inoculated with a total of 10^3 cells. Cell densities were checked daily over a 14 d incubation period.

[3] Sucrose, dextrose, D-fructose, D-lactose, D-xylose, D-galactose, D-ribose, L-arabinose, L-rhamnose

[4] L-aspartic acid, L-glutamic acid, L-tryptophane

Substrate	Growth1
Pyrite-enriched mine tailings (2% wt/vol)	+++
Fe(II) sorbed to ferrihydrite (2% wt/vol)	+++
Pyrite (FeS2; 2% wt/vol)+ (DSMZ 485 medium)	+++
Pyrrhotite (FeS; 2% wt/vol)	+++
Pyrite (FeS2; 2% wt/vol) + 20 mM Fe(II)	+++
Elemental sulfur (2% wt/vol)	+++
Elemental sulfur (2% wt/vol)+ 20 mM Fe(II)	++
Chalcopyrite (CuFeS2; 2% wt/vol)	++
Yeast extract (0.2%)	++
Covellite (CuS; 2% wt/vol)	+
Sphalerite (ZnS; 2% wt/vol)	+
H2 (33% H2, 33% O2 and 33% CO2 headspace)	+
Siderite (FeCO3; 2% wt/vol)	–
Magnetite (Fe3O4; 2% wt/vol)	–
FeSO4 (20 mM)	–
Tetrathionate (20 mM)	–
Na2S (5 mM)	–
Anaerobic (ferrihydrite/ sulfur; 2% wt/vol each)	–
Anaerobic (pyrite/10 mM NO3–;2% wt/vol)	–
Anaerobic [2% wt/vol Fe(II) ferrihydrite/10 mM NO3–)	–
Starch (2% wt/vol)	–
Casamino acids - 0.1% and 1% (wt/vol)	–
Citric acid - 0.1% and 1% (wt/vol)	–
Citric acid - 0.1% and 1% (wt/vol)	–
2Monosaccharides - 0.1% and 1% (wt/vol)	–
3Amino acids - 0.1% and 1% (wt/vol)	–

Growth on solid media was not achieved using plates with 1 to 1.5 % Gelrite® (Sigma, St. Louis, MO) media, pH 2.8 synthetic growth media and either 20 mM $FeSO_4$, 0.5g elemental sulfur, 0.5g pyrite (< 0.15-mm diameter), or 0.5g Fe(II) adsorbed to ferrihydrite (Kozubal *et al*., 2008). In addition, 5 mL of 0.4% Gelrite® was incubated at 65 ºC with 0.5 ml of *M. yellowstonii* pyrite slurry, then overlayed on solidified 0.8 % Gelrite® (Johnson, 1995). All plates were incubated at 65 ºC in sealed Ziploc® bags for ten days and no colonies were observed. Agar plates (1.5%) containing 20 mM $FeSO_4$ were incubated at 55 ºC (pH 3.0), and these attempts also did not produce colonies. Strain MK-1^T grows across a pH range of 1.0 to 5.0 (optimum = pH 2.5-3.0), a temperature range of 45 to 85 ºC (optimum = 65-70 ºC), and can tolerate up to 1.25 % NaCl (optimum = < 0.5 %). These attributes are similar to other members of the *Metallosphaera* genus (Fuchs *et al*., 1995; Huber *et al*., 1989; Takayanagi *et al*., 1996). Maximum growth rates at pH 3 and T = 65 ^oC were achieved using Fe(II) adsorbed to ferrihydrite ($2.1 \pm 0.5 \times 10^7$ cells ml^{-1} h^{-1}; doubling time = 10-11 hours) or pyrite. Under these growth conditions, a maximum cell density of 10^9 cells/mL was observed after 200 hours of incubation in closed serum bottles with 25% O_2, 50% CO_2, and 25% air headspace (Kozubal *et al.*, 2008). Cells observed (phase contrast and transmission electron microscopy) in late-exponential phase appear as immotile, irregular shaped cocci between 0.8 and 1.0 μm in diameter (Figure AB.2), and do not exhibit extracellular appendages (flagella were not observed in electron micrographs of negatively stained whole cells). Previous electron micrographs showed that strain MK1^T has a plasma

membrane and an S-layer cell wall typical of other members of the Sulfolobales (Kozubal *et al*., 2008; Huber & Prangishvili, 2007).

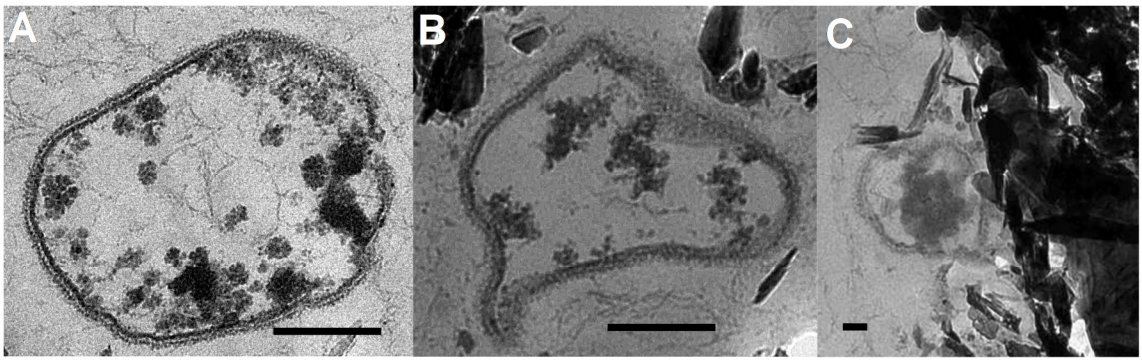

Figure AB.2. Transmission electron micrograph of *Metallosphaera yellowstonii* indicating irregular cocci morphology. Cells were prepared, stained and analyzed according to Kozubal *et al*. (2008). Scale bar = 200 nm.

The GC content of strain MK-1^T was determined to be 48 % from nearly 1.8Mb of assembled genome sequence that alsoaligned with the *M. sedula* genome. The draft genome sequence of strain MK-1^T is contained in 174 contigs larger than 5 kb (4.8x per contig) and is available from the DOE-Joint Genome Institute IMG/ER. The GC content of strain MK-1^T is consistent with values for *M. sedula* strain DSM 5348^T and *M. prunae* (GC contents of 45 and 46%, respectively), while other *Sulfolobus* spp. generally have GC contents ranging from 33-38 mol%. *In-silico* hybridization analysis against other members of the Sulfolobales (Table AB.2) was completed using the blastn discontiguous megablast algorithm with an E-value of one. The partial genome sequence of *M. yellowstonii* strain MK-1^T (draft consensus sequence = 2.3 Mb) was aligned with the genomes of *M. sedula* strain DSM 5348^T, *S. tokodaii* strain 7^T, *S. solfataricus* strain P2^T

and *S. acidicaldarius* strain DSM639^T, and values reported as percentage of MK-1^T sequence that is aligned between genome sequences (Table 2). Of the Sulfolobales genomes evaluated, strain MK-1^T is most similar to *M. sedula* strain DSM 5348^T, and using the above stated blastn criteria, 51% of the MK-1^T sequence aligns with *M. sedula*. When compared to the genomes of *S. acidicaldarius* strain DSM639^T, *S. tokodaii* strain 7^T, and *S. solfataricus* strain P2^T, alignment percentages were 23, 31 and 34 %, respectively. In addition, analysis of select genes indicates significant homology to *M. sedula* strain DSM 5348^T (unpublished data). However, strain MK-1^T appears to have a high percentage of transposable elements; initial estimates indicate that 10% of the genome may be composed of insertion elements, similar to *S. solfataricus* strain P2^T (She *et al*., 2001). Strain MK-1^T has unique genomic attributes compared to *M. sedula* strain DSM 5348^T as indicated by the divergence in nucleotide sequence relatedness, 16S rRNA gene sequence, and GC content. All these data indicate that strain MK-1^T is a new species in the genus *Metallosphaera*.

Description of *Metallosphaera yellowstonii* sp. nov.

Metallosphaera yellowstonii (yel.low.ston'i. N. L. gen n. yellowstonii,from Yellowstone National Park, the place of isolation). Cells are irregular cocci (0.8–1.0 μm in diameter). Growth occurs from 45 to 85 °C (optimum 65-70 °C), across a pH range of 1.0 to 5.0 (optimum 2.5-3.0) and up to 1.25 g/L NaCl. Electron donors include pyrite, Fe(II) adsorbed to ferrihydrite, elemental sulfur, 0.2% yeast extract, and ferrous sulfide minerals with molecular oxygen as an electron acceptor. The organism utilizes yeast extract as an organic carbon source or grows as an autotroph using CO_2. The G+C

content of genomic DNA is 48.0 mol% (based on partial genome sequence). The organism was isolated from Beowulf Spring in Norris Geyser Basin of Yellowstone National Park. The type strain is MK-1^{T}, which has been deposited in the American Type Culture Collection (ATCC) and the Japan Collection of Microorganisms (JCM).

Table AB.2. Characteristics of *Metallosphaera yellowstonii* strain MK-1^T relative to other isolates within the Crenarchaeal order.

Characteristic	***M. yellowstonii***	***M. sedula***	***M. hakonensis***	***M. prunae***
Temp range (°C)	45-85	50-80	50-80	55-80
Optimal temp (°C)	70	75	70	75
NaCl range (%,w/v)	0-1.25	ND	ND	ND
pH range	1-5	1-4.5	1-4	1-4.5
Optimal pH	2.5-3	2-3	3	2-3
Electron donors	Sulfide minerals; S^0; complex organics; Fe(II)	Sulfide minerals; S^0; complex organics; Fe(II)	Sulfide minerals; H_2; H_2S; $S_4O_6^{2-}$; S^0; organics	Sulfide minerals; H_2; S^0; organics; Fe(II)
Electron acceptors	O_2	O_2	O_2	O_2
G+C content (mol%)	48	45	46	46
Inoculum Source	Acidic iron mat, YNP, USA[1]	Thermal pond; Pisciarelli Solfatara, Italy[3]	Geothermal spring; Hakone NP, Japan[4]	Uranium mine Ronnenburg, Germany[5]
16S rRNA % similarity to *M. yellowstonii (%)*	100	95.5	96.1	96
Fraction of genome aligned to *M.yellowstonii**	100	51	no genome	no genome
Fraction of genome aligned to *S. solfataricus**	34	34	no genome	no genome

Characteristic	***A. ambivalens***	***S. solfataricus***	***S. tokodaii***	***S. metallicus***
Temp range (°C)	ND-87	50-87	70-85	50-75
Optimal temp (°C)	80	85	80	65
NaCl range (%,w/v)	ND	ND	ND	ND
pH range	1-3.5	2-5.5	2-5	1-4.5
Optimal pH	2.5	3-4.5	2.5-3	2-3
Electron donors	S^0; H_2 with S^0 as e^- acceptor	Complex organics; simple sugars; H_2	Organics; simple sugars; amino acids; S^0; Fe(II)	Sulfide minerals; S^0; Fe(II)
Electron acceptors	O_2; S^0	O_2	O_2	O_2
G+C content (mol%)	33	35	33	38
Inoculum Source	Geothermal Spring, Iceland[6]	Volcanic hot spring, Italy[7]	Geothermal spring, Kyushu Island, Japan[8]	Solfataric field, Iceland[9]
16S rRNA % similarity to *M. yellowstonii (%)*	91.4	88.4	90.6	89
Fraction of genome aligned to *M.yellowstonii**	no genome	34	31	no genome
Fraction of genome aligned to *S. solfataricus**	no genome	100	51	no genome

Table AB.2 continued

[1]Kozubal et al. 2008; [2]Simbahan et al. 2005; [3]Huber et al. 1989; [4]Takayanagi et al. 1996; [5]Fuchs et al. 1995; [6]Zillig et al. 1986; [7]Zillig et al. 1980; [8]Suzuki et al., 2002; [9]Huber and Stetter 1991; [10]Brock et al. 1972.

* Computed as the length of the aligned subsequence of the query (without gaps), divided by the total length of the query using blastn discontiguous megablast algorithm with an e-value of 1.

ND = Not Determined

Acknowledgements

This work was supported by the National Science Foundation Microbial Observatory Program (MCB-0132022), the National Aeronautic and Space Administration (NASA) via funds provided to the Thermal Biology Institute at Montana State University (Project Numbers NAG5-8807, NNG04GR46G), and the Montana Agricultural Experiment Station (Project 911398). The authors appreciate assistance from Y. Odake and S. Brumfield for transmission electron microscopy, and from C. Hendrix and T. Olliff for permitting this work in Yellowstone National Park (Permit YELL-2007-SCI-1976).

.

References

1. Amend, J.P., and E.L. Shock. (2001). Energetics of overall metabolic reactions of thermophilic and hyperthermophilic Archaea and Bacteria. *FEMS Microbiol. Rev*. 25: 175-243.

2. Auernik K.S., Maezato Y., Blum P.H., and R. M. Kelly. (2008). The Genome Sequence of the Metal-Mobilizing, Extremely Thermoacidophilic Archaeon *Metallosphaera sedula* Provides Insights into Bioleaching-Associated Metabolism. *Appl. Environ. Microbiol*. 74: 682-692.

3. Bathe, S. and P. R. Norris. (2007). Ferrous Iron- and Sulfur-Induced Genes in *Sulfolobus metallicus. Appl Environ Microbiol* 73: 2491-2497.

4. Blake, R. and D.B Johnson. (2000). Phylogenetic and biochemical diversity among acidophilic bacteria that respire on iron. In: Environmental Microbe–Metal Interactions (Derek, L., Ed.). 53–78. ASM Press, Washington, DC.

5. Brierley, C. L., and J. A. Brierley. (1973). A chemoautotrophic and thermophilic microorganism isolated from an acid hot spring. *Can J Microbiol* 19: 183–188.

6. Brock, T. D., K. M. Brock, R. T. Belly, and R. L. Weiss. (1972). Sulfolobus: a new genus of sulfur-oxidizing bacteria living at low pH and high temperature. *Arch Mikrobiol*84: 54–68.

7. Clark, T. R., F. Baldi, and G. J. Olson. (1993). Coal depyritization by the thermophilic archaeon *Metallosphaera sedula*. *Appl Environ Microbiol* 59: 2375–2379.

8. Dopson, M., C. Baker-Austin and P. L. Bond. (2005). Analysis of differential protein expression during growth states of *Ferroplasma* strains and insights into electron transport for iron oxidation. *Microbiol* 151: 4127–4137.

9. Fuchs T., H. Huber, K. Teiner, S. Burggraf, and K.O Stetter. (1995). *Metallosphaera prunae*, sp. nov., a novel metal-mobilizing, thermoacidophilic Archaeum, isolated from a uranium mine in Germany. *Syst Appl Microbiol* 18: 560-566.

10. García-Horsman J.A., Barquera B., Rumbley J., Ma J., and R.B. Gennis. (1994). The superfamily of heme-copper respiratory oxidases. *J Bacteriol* 176: 5587-600.

11. Hallberg K.B, D.B. Johnson. 2001. Biodiversity of acidophilic prokaryotes. Advances in Applied Microbiology. 49: 37-84.

12. Huber, G., C. Spinnler, A. Gambacorta, and K.O. Stetter. 1989. Metallosphaera sedula gen. nov. and sp. nov. represents a new genus of aerobic, metal-mobilizing, thermoacidophilic archaebacteria. Syst. Appl. Microbiol. 12: 38-47.

13. Huber G. and K.O. Stetter. 1991. Sulfolobus metallicus, sp. nov., a novel strictly chemolithoautotrophic thermophilic archaeal species of metal-mobilizers. Syst. Appl. Microbiol. 14: 372-378.

14. Huber H., and D. Prangishvili. 2007. Chapter 3, Sulfolobales. The Prokaryotes, 3rd ed., 2007, 7000 p.

15. Jan, R.L., J. Wu, S.M. Chaw, C.W. Tsai, and S.D. Tsen. 1999. A novel species of thermoacidophilic archaeon, *Sulfolobus yangmingensis* sp. nov. Int. J. Syst. Bacteriol. 49: 1809-1816.

16. Jeon, B., B.A. Dempsey, and W.D. Burgos. 2003. Kinetics and Mechanisms for Reactions of Fe(II) with Iron(III) Oxides. Environ. Sci. Technol. 37: 3309–3315.

17. Johnson, D.B. 1995. Selective solid media for isolating and enumerating acidophilic bacteria. Journal of Microbiological Methods. 23: 205-218.

18. Johnson, D.B., and K.B. Hallberg. 2003. The microbiology of acidic mine waters. Research in Microbiology.154: 466-73.

19. Johnson, D.B., N. Okibe and F.F. Roberto. 2003. Novel thermo-acidophilic bacteria isolated from geothermal sites in Yellowstone National Park: physiological and phylogenetic characteristics Archives of Microbiology. 180: 60-68.

20. Kappler, U., L.I. Sly, and A.G. McEwan. 2005. Respiratory gene clusters of *Metallosphaera sedula* – differential expression and transcriptional organization. Microbiology. 151: 35-43.

21. Kletzin A., Urich T., Müller F., Bandeiras T.M., and C.M. Gomes. 2004. Dissimilatory Oxidation and Reduction of Elemental sulfur in thermophilic archaea. Journal of bioenergetics and biomembranes. 36: 77-91.

22. Kozubal M., Macur R.E., Korf S., Taylor W.P., Ackerman G.G., Nagy A., and W.P. Inskeep. 2008. Isolation and Distribution of a Novel Iron-Oxidizing Crenarchaeon from Acidic Geothermal Springs in Yellowstone National Park. Appl. Environ. Microbiol. 74: 942-949.

23. Kurosawa, N., Y.H. Itoh, and T. Itoh. 2003. Reclassification of *Sulfolobus hakonensis* Takayanagi et al. 1996 as *Metallosphaera hakonensis* comb. Nov. based on

phylogenetic evidence and DNA G+C content. Int. J. Syst. Evol. Microbiol. 53: 1607–1608.

24. Macur, R.E., H.W. Langner, B.D. Kocar, and W.P. Inskeep. 2004. Linking geochemical processes with microbial community analysis: successional dynamics in an arsenic-rich, acid-sulfate-chloride geothermal spring. Geobiology. 2: 163-177.

25. Nordstrom, D.K. and G. Southam. 1997. Geomicrobiology of sulfide mineral oxidation. Reviews in Mineralogy. 35: 361-390.

26. Olson, G.J., J.A. Brierley, C.L. Brierley. 2003. Bioleaching review part B: Applied Microbiology and Biotechnology. 63: 249 – 257.

27. Peeples, T.L. and R.M. Kelly. 1995. Bioenergetic response of the extreme thermoacidophile *Metallosphaera sedula* to thermal and nutritional stresses. Appl. Environ. Microbiol. 61: 2314-2321.

28. Rawlings D. E. 2005. Characteristics and adaptability of iron- and sulfur-oxidizing microorganisms used for the recovery of metals from minerals and their concentrates. Microbial Cell Factories. 4: 13.

29. Rohwerder, T., T. Gehrke, K. Kinzler, and W. Sand. 2003. Bioleaching review part A: progress in bioleaching: fundamentals and mechanisms of bacterial metal sulfide oxidation. Appl. Microbiol. Biotechnol. 63: 239-48.

30. Segerer, A., A.M. Neuner, J.K. Kristjansson, and K.O. Stetter KO. 1986. *Acidianus infernus* gen. nov., sp. nov., and *Acidianus brierleyi* comb. nov.: facultatively aerobic, extremely acidophilic thermophilic sulfur-metabolizing archaebacteria. Int. J. Syst. Bacteriol. 36: 559–564.

31. She, Q., R. K. Singh, F. Confalonieri, Y. Zivanovic, P. Gordon, G. Allard, M. J. Awayez, C.-Y. Chan-Weiher, I. G. Clausen, B. Curtis, A. De Moors, G. Erauso, C. Fletcher, P. M. K. Gordon, I. Heidekamp de Jong, A. Jeffries, C. J. Kozera, N. Medina, X. Peng, H. Phan Thi-Ngoc, P. Redder, M. E. Schenk, C. Theriault, N. Tolstrup, R. L. M. Charlebois, W. F. Doolittle, M. Duguet, T. Gaasterland, R. A. Garrett, M. Ragan, C. W. Sensen, and J. Van der Oost. 2001. The complete genome of the crenarchaeon *Sulfolobus solfataricus* P2. Proc. Natl. Acad. Sci. 98:7835-7840.

32. Singer, S. W., C. S. Chan, A. Zemla, N. C. VerBerkmoes, M. Hwang, R. L. Hettich, J. F. Banfield, and M. P. Thelen. 2008. Characterization of cytochrome 579, an unusual cytochrome isolated from an iron-oxidizing microbial community. Appl. Environ. Microbiol. 74:4454-4462.
33. Suzuki, T., Iwasaki, T. Uzawa, T. Hara, K. Nemoto, N. Kon, T. Ueki, T. Yamagishi, A. and T. Oshima. 2002. *Sulfolobus tokodaii* sp. nov. (f. Sulfolobus sp. strain 7), a

new member of the genus Sulfolobus isolated from Beppu Hot Springs, Japan. Extremophiles. 6: 39-44.

34. Swofford, D. L. 2003. PAUP*: Phylogenetic analysis using parsimony (*and other methods), version 4. Sunderland, MA: Sinauer Associates.

35. Takayanagi, S., H. Kawasaki, K. Sugimori, T. Yamada, A. Sugai, T. Ito, K. Yamasato, and M. Shioda. 1996. *Sulfolobus hakonensis* sp. nov., a novel species of acidothermophilic archaeon Int. J. Syst. Bacteroil. 46: 377–382

36. Zillig, W., K. O. Stetter, S. Wunderl, W. Schulz, H. Priess, and I. Scholz. 1980. The Sulfolobus-‘‘Caldariella’’ group: taxonomy on the basis of the structure of DNA-dependent RNA polymerases. Arch. Microbiol. 125:259–269

37. Zillig, W, S. Yeats, L. Holz, A. Bock, M. Rettenberger, F. Gropp and G. Simon. 1986. *Desulfurolobus ambivalens*, gen. nov., sp. nov., an autotrophic archaebacterium facultatively oxidizing or reducing sulfur. Syst. Appl. Microbiol. 8: 197-203.

APPENDIX C

SUPPLEMENTAL TABLES AND FIGURES

APPENDIX TABLE AC.1

Accession numbers, spring locations and number of clones associated with each accession number. 86 accessions numbers associated with 383 clones were deposited in GenBank. All entries belong to *Metallosphaera*-like Group 1 clones identified in Fig. 3.1 of manuscript except where noted.

Spring and Location Identification	Accession #	# of clones
JC1B	AY882666	4
JC2C	AY882685	2
JC2C, NGB-GAPB	AY882686	2
JC2C	AY882687	1
NGB-PB, NGB-OSPA (Clone Group 2)	AY882688	2
JC2C	AY882689	1
RS1B	AY882788	1
RS1B	AY882789	2
RS1B	AY882790	2
RS1B	AY882791	6
RS2A, NGB-GAPB, NGB-WG, NGB-BEE	AY882800	14
RS2B	AY882806	4
RS2B	AY882807	1
RS2D	AY882814	2
RS3A, RS3B, NGB-BWD, NGB-BEE	AY882821	7
RS1B	AY882822	3
RS1B	AY882823	1
RS1B, RS2B, RS2D, RS2F	AY882824	13
NGB-PB, NGB-EG, RS3B, NGB-WG, NGB-GAPB, NGB-DWC, NGB-BEE, NGB-BWD, NGB-OSPA, NGB-OSPB	AY882836	35
RS3B	AY882852	1
RS2A, NGB-GAPB, NGB-BWD, NGB-BEE, NGB-OSPA, NGB-OSPB	DQ179029	27
RS2B	DQ179030	8
RS2B	DQ179031	1
NGB-PB, NGB-EG, NGB-WG, NGB-OSPB, NGB-GAPB, NGB-	DQ350777	49

BEE, NGB-DWC, NGB-BWD		
JC2B	DQ834052	2
JC2B	DQ834053	1
JC2B	DQ834054	1
JC2B	DQ834055	1
JC2B	DQ834056	1
JC2B	DQ834057	17
JC2B	DQ834058	1
JC2B	DQ834059	1
JC2B	DQ834060	10
RS2B	DQ834060	1
JC2B	DQ834061	1
JC2B	DQ834062	1
RS2B	DQ834141	1
RS2B, RS2D	DQ834142	15
RS2B, RS2D, RS2F	DQ834143	13
RS2B, RS2D	DQ834144	5
RS2B, RS2D	DQ834145	9
RS2B	DQ834146	1
RS2B	DQ834147	2
RS2B	DQ834148	2
RS2B, RS2F	DQ834149	6
RS2B	DQ834150	1
RS2B	DQ834151	1
RS2B	DQ834152	1
RS2B, RS2D	DQ834153	21
RS2B	DQ834154	1
RS2B	DQ834155	1
RS2D	DQ834191	2
RS2D	DQ834192	1
RS2D	DQ834193	1
RS2D	DQ834194	1
RS2D	DQ834195	1
RS2D	DQ834196	3
RS2D	DQ834197	1
RS2D	DQ834198	1
RS2D	DQ834199	1
RS2D	DQ834200	1
RS2D	DQ834201	1
RS2D	DQ834202	1
RS2D	DQ834203	1
RS2D	DQ834204	1
RS2D	DQ834205	1
RS2D	DQ834206	1

RS2D	DQ834207	1
RS2F	DQ834231	1
RS2F	DQ834232	1
RS2F	DQ834233	1
RS2F	DQ834234	5
RS2F	DQ834235	1
RS2F	DQ834236	1
RS2F	DQ834237	1
RS2F	DQ834238	1
RS2F	DQ834239	11
RS2F	DQ834240	3
RS2F	DQ834241	1
RS2F	DQ834242	1
RS2F	DQ834243	1
RS2F	DQ834244	1
NGB-OSPA, NGB-OSPB, NGB-DWC, NGB-BEE	EF156615	18
NGB-OSPA, NGB-OSPB	EF156616	2
NGB-OSPA, NGB-OSPB	EF156617	4
NGB-OSPA, NGB-EG (Clone Group 3)	EF156618	2

APPENDIX TABLE AC.2. Primers utilized in this study for both RT-qPCR and agarose gels with melting temperatures and product length (bp).

Primer ID	Sequenc 5'-3'	Metlting Temp	Product length
SoxBF	TGGGGCGCTCTACTACTATG	58.0	
SoxBR	TGTTAGACCTGAACCCGAAG	57.8	202
SoxMF	CTTCGGTCCCATAAACACTG	58.1	
SoxMR	CCAAGTGAAGAGCGACATCT	58.0	202
FoxAF	CCAGGACGAAGAGTACTGGA	57.9	
FoxAR	GTGGGCTCAACATCTACCTG	58.2	201
FoxCF	GGAGTAGCCTATGGTGCTGA	57.9	
FoxCR	CACTGTTGTGTGCCCTGATA	58.1	202
FoxGF	CCTGTCCACACGACAACATA	58.0	
FoxGR	GGTACCAGCAACTTGGAGAA	57.8	217
DoxB2F	GGCATGCTAGGCGTAATAGA	58.0	
DoxB2R	CCACTTTGCTCTAGGTTCCA	58.0	213
DoxBF	AAACCGAACAGATCCCTTTC	58.1	
DoxBR	TTTGTGACAGCTTTGTTCCA	57.9	218
SoxE1F	ACCTGCAGGCTACAGCATAG	58.2	
SoxE1R	ACTTCAGTGGCTGACTGACC	57.8	198
SoxE2F	TATCCATTGGCGGATGTAAC	58.3	
SoxE2R	ACACTCAACACCACCAAACC	58.3	212
TqodF	CTCTCAGGTTCGCTGTAGGA	58.2	
TqodR	GTAAGGAACGCTACGTCCAA	57.9	196
McoF	TGCAGGCTGGTACATAAACA	57.8	
McoR	AAGGACTTCCGAACTCTGGT	57.8	212
16SF	CCGTAAAGTCACCGTTTAAAGAC	59.2	
16SR	GTATCTAATCCCTTTTGCTACCC	57.4	206

SoxBF	TTACCTATCCCGCAAACAGC	55.1	
SoxBR	TACACCACTGGGTGACCGTA	57.7	580
SoxMF	CACCTTTCTTCGGTCCCATA	54.2	
SoxMR	GCTATCTCTCTGGCCACGTC	57.3	565
DoxBF	GCCATGTAAACCACAGCGTG	57.0	
DoxBR	GGTCTCAGGCGTACTTGTGT	56.9	600
DoxB2F	CATCAGTGCGGCTATCCTAGC	57.6	
DoxB2R	TCCTCCAGTTTCATACTCACCTCC	57.8	700
FoxAF	CTGGCCAACATATCCGTCTT	54.8	
FoxAR	CCGAATATCCAGCCTGTGTT	54.8	550
FoxBF	GAAGAACAGAGCTATTACAGTACC	52.7	
FoxBR	GGTACTGTAATAGCTCTGTTCTTC	52.7	520
FoxCF	ATCCTAATGAAGGCCCCAGT	55.8	
FoxCR	GGGGAGTGTAGGCAACTTGA	56.8	566
FoxDF	TGTTTCTTTAGTCTACGTTTTCG	51.1	
FoxDR	TGTCTTTTTTGTACTCTAACATCG	51.2	750
FoxEF	CCTGGCCATGGTGCTGGTGAC	63.3	
FoxER	TGGCAGGAGTTAAGTTCTCAAGG	56.7	520
FoxGF	GAGTGGGTGCACAGACTTCA	57.2	
FoxGR	AATAGGACGACACCGGTCAG	56.5	600
FoxJF	GGAAGATATTAACGCCAGTAAGGA	54.3	
FoxJR	TGTAGGATGGACCCTCATAATGC	56.3	710
SoxE1F	GACGGTGCAGATAACACTGG	55.7	
SoxE1R	CCACATTCCAGACTCAGCG	55.8	350
SoxE2F	CGAGAATCCAGTCGGGATGT	55.6	
SoxE2R	CAGCTGAGTCACAAGACTTCC	55.4	450
TqodF	CCTCTCAGGTTCGCTGTAGG	57.0	
TqodR	CCAGTAGGCTGGAGCGAAGC	60.5	250
McoF	CGCCTGGATTAATGAAAGTGA	52.9	
McoR	TTCCTGCCATCCCCATATTA	53.2	584

RcbfF	ATCCCAGCTGGATGTAAACG	54.8	
RcbfR	GGCCACATTTACATGGCTTT	53.9	460
CbsAF	GGTCGCAGCTCTCGTAATGG	58.0	
CbsAR	CCACTCGCGGGAGGATACAAC	59.9	300